

Dissertation
der Graduate School of Systemic Neurosciences
der Ludwig-Maximilians-Universität
München



Graduate School of
Systemic Neurosciences
LMU Munich

Functional imaging of the neural components of *Drosophila* motion detection

Submitted by

Matthew Maisak

13th of July 2017



Matthew Maisak: Functional Imaging of the Neural Components of *Drosophila* motion detection,
Dissertation
der Graduate School of Systemic Neurosciences
der Ludwig-Maximilians-Universität
München

WEBSITE:

<http://www.neuro.mpg.de/>

E-MAIL:

matt.maisak@gmail.com

First reviewer (supervisor)
Prof. Dr. Alexander Borst

Second reviewer
Prof. Dr. Hans Straka

Date of submission
2017, June, 27th

Date of defense
2018, November, 22nd

ABSTRACT

In order to safely move through the environment, visually-guided animals use several types of visual cues for orientation. Optic flow provides faithful information about ego-motion and can thus be used to maintain a straight course. Additionally, local motion cues or landmarks indicate potentially interesting targets or signal danger, triggering approach or avoidance, respectively. The visual system must reliably and quickly evaluate these cues and integrate this information in order to orchestrate behavior. The underlying neuronal computations for this remain largely inaccessible in higher organisms, such as in humans, but can be studied experimentally in more simple model species. The fly *Drosophila*, for example, relies heavily on such visual cues during its impressive flight maneuvers. Additionally, it is genetically and physiologically accessible. Therefore, it is regarded as an ideal model organism for exploring neuronal computations underlying visual processing.

During my PhD-thesis, I characterized neurons presynaptic to direction selective lobula plate tangential cells by exploiting the genetic toolbox of the fruit fly in combination with *in-vivo* imaging. The use of genetically encoded calcium indicators and two-photon microscopy allowed me to directly investigate response properties of small columnar neurons upstream of lobula plate wide field neurons. In the highly collaborative environment of our lab my imaging experiments were complemented by several other approaches, including electrophysiological and behavioral experiments, along with modeling which resulted in the publications that comprise this cumulative dissertation.

Measuring calcium signals in T4 and T5 cells in the first study, established that both populations of neurons exhibit direction selective response properties. Furthermore, T4 cells only respond to moving bright edges, whereas T5 cells encode exclusively dark edge motion. Silencing the synaptic output of T4 and T5 separately, we were able to determine that both lobula plate tangential cell responses as well as the turning behavior of walking flies were impaired only to bright or dark edges, respectively. We thus proposed that the detection of the direction of visual motion must happen either presynaptic to, or on the dendrites of T4 and T5 neurons, and that this computation takes place in-

dependently for brightness increments and decrements.

The second paper published in 2014 was motivated by an anatomical study that found an asymmetric wiring between L2 and L4 cells with the dendrites of Tm2 in the distal medulla. Using two-photon calcium imaging and neuronal silencing combined with postsynaptic electrophysiological recordings, we probed the contribution of L4 and Tm2 in the OFF pathway of *Drosophila* motion vision. We found that while Tm2 have small, isotropic, laterally inhibited receptive fields, L4 cells respond to both, small and large field darkening. Blocking the output of both cell types resulted in a strong impairment of OFF motion vision. In contrast to the anatomical prediction, we did not observe any directional effects for either of the cells.

ZUSAMMENFASSUNG

Visuell gesteuerte Tiere nutzen verschiedene visuelle Signale, um sicher in ihrer Umwelt zu bewegen. Der optische Fluss gibt Aufschluss über Eigenbewegungen und kann daher zur Kurskontrolle genutzt werden. Darüber hinaus lassen lokale Bewegungsreize auf potentiell interessante Ziele schließen oder signalisieren Gefahr und provozieren somit ein annäherndes bzw. vermeidendes Verhalten. Das visuelle System muss diese Reize verlässlich und schnell auswerten und integrieren, um Verhaltensweisen zu steuern. Zugrunde liegende neuronale Rechenleistungen sind in höheren Organismen, z.B. Menschen, nicht gut greifbar, sie können aber in experimentell besser zugänglichen Modellorganismen untersucht werden. Die Fliege *Drosophila* beispielsweise baut in ihren beeindruckenden Flugmanövern in hohem Maße auf derartige visuelle Reize. Zudem ist sie genetisch und physiologisch gut zugänglich. Sie wird daher als idealer Modellorganismus für die Untersuchung neuronaler Rechenleistungen für visuelles Verhalten gesehen.

In meiner PhD Arbeit charakterisierte ich Neurone, die richtungsensitiven Lobulaplatten Tangentialzellen vorgeschaltet sind, unter Ausnutzung genetischer Werkzeuge in Kombination mit in vivo optischer Bildgebung. Mit genetisch kodierte Kalziumindikatoren und 2-Photonenmikroskopie konnte ich direkt die Antworteigenschaften kleiner kolumnarer Neurone untersuchen, die den Weitfeldneuronen der Lobulaplatte vorgeschaltet sind. In der hochkollaborativen Umgebung unseres Labors wurden meine Bildgebungsexperimente durch Verhaltensexperimente und Modellierung ergänzt, was zu den in dieser kumulativen Dissertation enthaltenen Publikationen führte.

In unserer ersten Veröffentlichung beschäftigten wir uns mit zwei Zelltypen, T4-Zellen, die Medulla und Lobula-Platte miteinander verbinden und T5-Zellen, welche Verzweigungen sowohl in der Lobula, als auch in der Lobula-Platte vorweisen. Durch das Messen von Kalzium Signalen konnten wir zeigen, dass sowohl T4-, als auch T5-Zellen spezifisch auf visuelle Bewegungsreize in eine bestimmte Richtung reagieren. Zusätzlich stellte sich heraus, dass T4-Zellen ausschließlich auf positive Helligkeitsunterschiede (Licht an, ON) und T5-Zellen nur auf dunkle Reize (Licht aus, OFF) antworteten. Somit wurde bestätigt, dass

auch auf der Ebene der Lobula-Platten-Eingangsnuronen zwei getrennte Signalwege existieren. Indem wir diese bewegungs-sensitiven Elemente mit Hilfe genetischer Manipulationen aus dem Netzwerk entfernten und gleichzeitig entweder von nachgeschalteten Tangentialzellen ableiteten, oder das Laufverhalten von Fliegen beobachteten, gelang es uns zu beweisen, dass einerseits T₄-Zellen für die Wahrnehmung von ON-Signalen, andererseits T₅-Zellen für die Berechnung von OFF-Signalen von elementarer Bedeutung sind.

Der zweiten Arbeit war eine anatomische Studie vorangegangen, die herausgefunden hatte, dass L₂- und L₄-Zellen in der distalen Medulla asymmetrisch mit Tm₂-Dendriten verbunden sind. Mit Kalzium-Messungen mit einem Zwei-Photonen-Mikroskop und transgener Unterdrückung von synaptischer Signalweitergabe kombiniert mit elektrischen Ableitungen von Tangentialzellen untersuchten wir die Beteiligung von L₄- und Tm₂-Zellen im OFF-spezifischen Netzwerk des Bewegungsapparates des Fruchtfliege, d.h. die Zellen die für dunkler werdende Reize zuständig sind. Wir fanden, dass Tm₂-Zellen kleine, gleichförmige Rezeptive-Felder haben die durch laterale Hemmung geformt werden, während L₄-Zellen sowohl auf kleine als auch auf große negative Helligkeitsänderungen reagierten. Durch Ausschalten der synaptischen Weiterleitung in beiden Zelltypen konnten wir außerdem feststellen, dass beide für das Zustandekommen gerichteter, OFF-spezifischer Signale in Tangentialzellen benötigt werden, unabhängig der Bewegungsrichtung.

CONTENTS

1	INTRODUCTION	1
1.1	Sensory systems	1
1.2	Visual systems	2
1.3	Motion vision and the Hassenstein-Reichardt Detector	3
1.4	Tools in neuroscience	5
1.4.1	Physiology	6
1.4.2	<i>Drosophila</i> neurogenetics	8
1.4.3	Mapping neural circuits	10
1.5	Structure and Physiology of the Visual System	15
1.5.1	Retina	15
1.5.2	Motion vision circuit	19
1.6	Concluding remarks	21
2	PUBLICATIONS	23
2.1	A directional tuning map of <i>Drosophila</i> elementary motion detectors	23
2.2	Neural circuit components of the <i>Drosophila</i> OFF motion vision pathway	35
3	DISCUSSION	49
3.1	T4 and T5 Input	49
3.2	The Null Direction: Encoded in T4 and T5?	53
3.3	The Behavioral Relevance of the T4 T5 Motion Circuit	53
3.3.1	Optomotor Response	54
3.3.2	Landing and Avoidance Response	54
3.3.3	Fixation Response	56
3.4	Comparing Motion Detection in Mice and <i>Drosophila</i>	57
3.4.1	The First Signs of Direction Selectivity	60
	BIBLIOGRAPHY	63
	INDEX	81

1

INTRODUCTION

1.1 SENSORY SYSTEMS

Successful interaction with our environment requires rapid and precise computations transforming the various sensory input from the outside world into a meaningful internal representation.

Relevant changes must be reliably detected, processed and the appropriate actions must be initiated. Sensory organs distributed over the body constantly provide our brain with vital multimodal information. These sensory receptors, triggered by external stimuli, are the beginning of an electrochemical cascade of neuronal processing from the periphery to the central nervous system. Before we even actively perceive a sensation like a smell or a taste, the original signals have undergone impressive amounts of neural computation and filtering. In the case of vision, photons enter the eye and stimulate the photoreceptors in the retina. These in turn, stimulate the neural networks of the retina and the visual cortex. This leads to certain neurons or clusters of neurons to respond specifically to potentially complex features ranging from global motion patterns to the orientation, shape, or speed of an object.

Sensory systems are the most well studied parts of the brain in neurobiology for several reasons. One common feature shared by all sensory systems is relative experimental accessibility due to their localization at the periphery of the nervous system. The peripheral localization makes it comparatively easy to apply precise artificial stimuli and thereby intentionally elicit neural responses under controlled conditions in a laboratory. Furthermore, even though the computational performance is very elaborate, compared to networks in higher brain areas, like the cerebral cortex, the anatomical complexity of sensory circuits is fairly moderate. Thus, it is not surprising that the field of sensory neurobiology is a rather well studied discipline within neuroscience.

1.2 VISUAL SYSTEMS

The ability to see is one of the foundations of the human experience and is thus of great interest to scientists around the world. Vision is, across many animal species including humans, the primary sensory modality for the execution of diverse behavioral tasks such as orientation in complex environments, social interactions, predator or rival avoidance and food source localization. Sensory receptors extracting visual information are generally located in the eyes. The eye has evolved in several ways leading to an incredible diversity across the animal kingdom. Eyes can be classified in two groups; compound eyes, as found in crustaceans (e.g. shrimps, lobsters) and insects (e.g. flies, mosquitoes, beetles), and camera eyes that have evolved in parallel in arachnids (e.g. spiders, scorpions, mites), cephalopods (e.g. squids, octopuses) and vertebrates (e.g. fish, birds, mammals) ([Land and Nilsson, 2012](#)). One of the main challenges for visual systems is the projection of a 3D world onto a 2D array of photoreceptor cells. The neural networks in the mammalian eye accomplish this task through a highly complex parallel organization. The first stage of visual processing takes place in the retina, where light that hits the photoreceptors triggers a biochemical reaction altering their membrane voltage, resulting in a change of transmitter release that can be detected by postsynaptic neurons. In the downstream networks, generally two motifs are found; a parallel, retinotopic arrangement starting with photoreceptor cells that diverge onto approximately ten types of bipolar cells. The bipolar cells ultimately connect to retinal ganglion cells that form the optical nerve linking the retina to higher brain areas. In addition to this parallel organization, lateral interactions are introduced at two stages: horizontal cells shape the responses of photoreceptor and bipolar cells, and amacrine cells act on bipolar cell - ganglion cell connection (for review, see [Masland, 2001](#); [Gollisch and Meister, 2010](#)). The ganglion cell signals are subsequently conveyed to higher brain structures, where neuronal ensembles or sometimes single cells extract information about color, texture, or motion of an object ([Hadjikhani et al., 1998](#); [Kastner et al., 2000](#); [Hubel and Wiesel, 1968](#)), or even highly complex patterns like faces ([Quian Quiroga et al., 2005](#)). These neurons can then signal other neuronal networks to initiate appropriate behavioral actions.

Mammalian Eyes

However, the human brain with its 10^{11} neurons, intricate connectivity and extensive neural plasticity is far too complex to exhaustively study at this point. Instead, visual processing can be studied in simpler organisms like arthropods. Insects for in-

stance exhibit a number of interesting behaviors triggered by specific visual signals (Hassenstein, 1951; Reichardt and Wenking, 1969a; Borst, 1986; Bahl et al., 2013). Additionally, neural networks underlying visual feature extraction can be assessed in intact, living animals with fixed eyes, enabling precise stimulus presentation. Moreover, morphologically and genetically identified cell types allow for the specific manipulation of circuit elements.

1.3 MOTION VISION AND THE HASSENSTEIN-REICHARDT DETECTOR

It is clear that vision is an incredibly complex yet vital task for nearly all animals, including *Drosophila*. However, the exact mechanism of computation remained elusive. The neural pathways and computations that lie between the photoreceptor, which respond to motion in a non-direction selective manner and the behavioral output were a black box. However, motion vision in flies has been extensively studied by the application and elaboration of a mathematical model called Hassenstein-Reichardt detector. I will start with a brief summary of this model, in order to provide a context for the description of what is currently known about the circuitry that implements local motion detection.

The Hassenstein-Reichardt detector was originally developed based on studying the turning tendency of a beetle, *Chlorophanus*, which was tethered to a holder and walked on a spherical Y-maze made from straw. A periodic, moving pattern surrounded the beetle, and at each bifurcation of the maze it could turn left or right (Hassenstein and Reichardt, 1956). Bernard Hassensteins and Werner Reichardts model for elementary motion detection describes the behavior of the beetle in a quantitative way and accounts for their observations in remarkable detail. In its simplest form, it consists of two mirror-symmetrical subunits. Each subunit (or half-detector) processes luminance changes at two adjacent points in space. These values are multiplied, after one of them has been delayed by a low-pass filter. The outputs of the two half-detectors are finally subtracted (Reichardt and Wenking, 1969b) (Figure 1). A half detector generates a signal if the spatial arrangement of its delay and its direct line matches the direction of motion of an object passing by, that is, if the delayed signal coincides with the subsequently elicited direct signal at the multiplication stage. The signal is largest if the

spacing between the two sampling points (the ‘sampling base’) relative to the time delay introduced by the low pass filter just compensates the velocity of the object. The detector as a whole will give a positive output for its preferred and a negative output for its non-preferred direction after subtraction of the output of the two half-detectors.

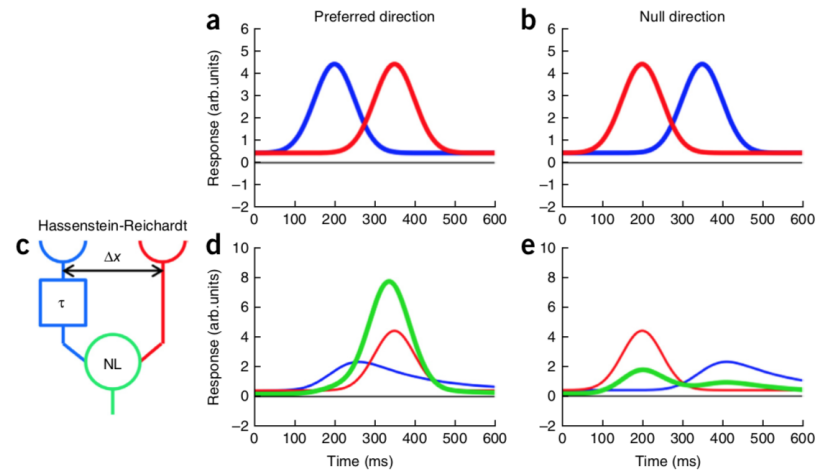


Figure 1. Motion Detection Schematic. (a,b) Sequences of activation of two neighboring photoreceptors (left, blue; right, red) at a distance Δx for light stimuli moving in the preferred direction (left to right) (a) and null direction (right to left) (b). (c) Schematic of the half-detector in the Hassenstein-Reichardt model. The signal from the left photoreceptor (blue) is delayed by a temporal filter (τ) and fed, together with the instantaneous signal from the right photoreceptor (red), into an excitatory nonlinearity (NL, green). (d,e) Input (blue and red lines) and output (heavy green line) signals for motion in the preferred (d) and null (e) directions. A multiplication was used as the nonlinear operation. Figure and caption taken with permission from [Borst and Helmstaedter \(2015\)](#).

In principle, four different detector subtypes are conceivable. A luminance increment or ON-signal at one point in space could be correlated with either a luminance increment or decrement (OFF signal) at a neighboring point. The four possible combinations are thus ON-ON, OFF-OFF, ON-OFF, OFF-ON. However, experiments using apparent motion stimuli (i.e., consecutive luminance increments or decrements at separate points in space that convey the illusion of a continuously moving object) indicated that only two of the four possible channels exist, one correlating luminance increments (ON-ON) and the other one correlating luminance decrements (OFF-OFF) ([Riehle and Franceschini, 1984](#); [Eichner and Borst, 2011](#)). This makes sense from a

biological standpoint since the movement of real objects will always lead to correlated ON or OFF signals at neighboring points in space. Still, one may wonder why there are two separate detectors, doubling wiring costs, and why not one single detector could implement the sign rule of multiplication, with the signal being positive when two positive as well as two negative brightness steps are correlated. However, it is hard to conceive how this could be implemented biophysically. Half-wave rectification of the input signal and splitting into an ON and OFF channel simplifies the problem considerably.

The Hassenstein-Reichardt detector model makes several predictions, which could be experimentally verified. Some of them even eluded its inventors, and have been studied much later (for review, see [Borst, 2014b](#)). For example, fed with a moving sine wave grating, a Hassenstein-Reichardt motion detector produces an output that is not just linearly dependent on the pattern velocity, like a simple speedometer. Instead, its output increases as a function of image angular velocity, up to a maximum after which the response declines again. This maximum increases linearly as a function of the pattern wavelength. The ratio of pattern wavelength and velocity, i.e., the temporal frequency of a pattern that elicits the maximal response, therefore remains constant. This dependency of the detector on the properties of the pattern has been confirmed experimentally by electrophysiological recordings of large lobula plate neurons in both blowflies ([Haag and Borst, 2004](#)) and fruit flies ([Joesch et al., 2008](#); [Schnell et al., 2010](#)). Moreover, the Hassenstein-Reichardt model makes specific predictions regarding the transient response to grating motion, and it exhibits gain control, a property that was not noticed until fairly recently (for review, see [Borst, 2010](#)). The close fit between these predictions and the behavioral and electrophysiological observations make it very likely that a Hassenstein-Reichardt-type algorithm underlies motion detection in flies. While the range of plausible model parameters could be confined experimentally, its actual neuronal and biophysical implementation is still largely uncovered.

1.4 TOOLS IN NEUROSCIENCE

Research on *Drosophila melanogaster* began in the early 1900s when Thomas Hunt Morgan identified – without knowledge of genes – the white gene that is responsible for the production of the typical red pigment in the fly eye ([Morgan, 1910](#)). This finding opened the gates for modern genetics and established

Drosophila as a model organism for genetics, behavior, learning and for studying neuronal networks in labs around the world.

The use of *Drosophila* as a model system offers several distinct advantages. They are small, easy to breed, and have a short generation time of approximately 10 days. In addition, they don't raise the ethical concerns associated with common mammalian model organisms. Their brains are relatively small with 300,000 neurons with mostly genetically hard wired development (Simpson, 2009). Nevertheless, *Drosophila* displays various complex behaviors (Borst, 2013; Dickson, 2008). Over the past hundred years of *Drosophila* research a variety of tools have been developed which have equipped researchers with a powerful armory to tackle the complex problems of circuit neuroscience.

1.4.1 Physiology

Electrophysiology

For a very long time, properties of nerves, brain regions and single neurons have been investigated using electrophysiological recordings of membrane voltage (Hodgkin and Huxley, 1952). In the blow fly *Calliphora* many cell types were characterized using intracellular and extracellular recordings with sharp electrodes (Hausen, 1976; Strausfeld and Lee, 1991). Recordings from two or more cells simultaneously enabled the description of connectivity between cells or connections of neurons with downstream nerves (Haag and Borst, 2001; Haag et al., 2004; Kauer et al., 2015). While these approaches worked well for the large nerve cells in the blow fly, recordings with sharp electrodes proved to be difficult at the small scale of *Drosophila* neurons. The whole-cell patch-clamp approach (Sakmann and Neher, 1984) was better suited for this task. Here, a glass electrode with a very fine opening is brought into close vicinity of a neuron under application of a small positive pressure. Once the electrode touches the cell membrane, the pressure is released and minute negative pressure is applied. This causes the cell membrane to become sucked slightly into the opening of the pipette. A so called "giga-Ohm seal" is formed, where the seal between glass capillary and cell membrane strongly increases the electrical resistance. In the next step, a short pulse of negative pressure leads to the detachment of a small patch of membrane into the electrode. The resistance drops and the remaining cell membrane now forms a continuum with the recording electrode, allowing the precise measurement of intracellular voltage or current. This technique permitted electrophysiological experiments in some larger cells of the fruit fly's brain (Wilson et al., 2004; Joesch et al., 2008).

Two-Photon Imaging

Most of the cells in the optic lobe of *Drosophila* are too small

to record from electrophysiologically. I therefore used 2-photon imaging (Denk et al., 1990), which offers several advantages over other imaging techniques for in-vivo imaging. The key advantage is that excitation quadratically depends on light intensity, and light intensity decreases dramatically outside of the focused laser beam. Therefore, excitation occurs almost exclusively in the focal volume, and practically all collected photons originate from the focal volume, scattered or unscattered. This improves the signal to noise ratio, especially for highly scattering tissues or when imaging deeper in the tissue. As a consequence, the effective spatial resolution of a 2-photon microscope can be 20x superior to that of a confocal microscope, although roughly twice the excitation wavelength is used, and one would expect a spatial resolution of 2-photon imaging that is worse by about a factor of two compared to confocal imaging. However, this would only be true theoretically, for an infinitely small pinhole. In practice, there is a trade-off in the size of the pinhole between the achieved spatial resolution and the amount of collected photons (Zipfel et al., 2003). Furthermore, using longer wavelengths for 2-photon excitation provides several other advantages that can be even more important when imaging in vivo: (1) reduced autofluorescence, which again improves the signal to noise ratio and reduces phototoxicity, (2) far less photobleaching of the fluorescent dye outside of the focal volume, which is critical for long in-vivo experiments at different depths in the tissue, (3) no interference with the visual system, since the excitation wavelengths used are outside of the absorption spectra of the fly photoreceptors, and (4) superior depth penetration (Zipfel et al., 2003; Svoboda and Yasuda, 2006).

Another technical innovation, namely the invention and improvement of electron microscopy, has had an enormous impact on neuroscience. Using electrons instead of photons to probe tissues allowed for pushing the resolution limit far beyond what was possible with optical microscopes (Knoll and Ruska, 1932; Denk and Horstmann, 2004). This innovation promoted the emergence of a new field of neuroscience: connectomics, where neural circuits are described based on dense reconstructions of brain areas (Kim et al., 2014; Takemura et al., 2013; Helmstaedter et al., 2013). In recent years, electron-microscopic studies have provided a new level of insight into the wiring of neuronal circuits. However, information about the connectivity of neurons is by far not enough to understand even primitive neural circuits. The whole neural system of the roundworm *Caenorhabditis elegans* with its 302 neurons was completely reconstructed 30 years ago (White et al., 1986), the function of the circuitry, how-

Connectomics

ever, is still subject to investigation. It is therefore indispensable to also probe nervous systems functionally, thus the continued need for the functional imaging and electrophysiological experiments done in this thesis.

1.4.2 *Drosophila* neurogenetics

At the turn of the century *Drosophila* was established as a model organism and scientists immediately got to work developing large numbers of mutant flies. In the beginning of *Drosophila* research, scientists used x-rays and chemicals to manipulate its DNA (Muller, 1928; Alderson, 1965) and screened for behavioral phenotypes (Benzer, 1967). However, these methods were not very controlled and resulted in random, unpredictable mutations. In order to gain insight into functional principles underlying neuronal circuits it is essential to study the building blocks of the circuitry, single neurons or cell types (for review see Luo et al., 2008). Random mutagenesis is unreliable and unspecific in affecting functions of single cells or defined classes of neurons. The biggest leap towards more targeted circuit manipulation came with the ability to specifically insert pieces of exogenous DNA into the fly's germline. In a pioneering study, Rubin and Spradling (1982) were able to stably insert a new gene into the DNA of a fly. They used mutant flies lacking *rosy*, a gene determining wildtype *Drosophila* eye color. When they injected a vector that contained a transposable element (P-element) carrying the intact *rosy* gene into *Drosophila* embryos, they could rescue the loss-of-function phenotype not only in the injected flies, but also in subsequent generations. This indicates a successful integration of the exogenous gene into the fly's germ-line. While this revolutionary technique broke new ground it also had several major drawbacks. Since the integration of the P-element happens in random positions of the host DNA, it is possible that it is inserted into encoding areas of the fly's genome which can cause malfunctions of important genes, that may result in off target effects. Moreover the promoters that determine the expression of the downstream genes can not be selected and therefore the cells in which the inserted gene will be expressed cannot be targeted. The biggest disadvantage of this method is that every effector protein has to be inserted *de novo* into the genome.

Gal4-UAS

In order to circumvent these issues scientists developed a new binary expression tool, Gal4-UAS, in the early 1990s (Figure 2a, Brand and Perrimon, 1993). The Gal4-UAS system combines two separate strategies to target the expression of any gene of interest to a specific subset of neurons. The yeast transcription

factor Gal4, expressed under the control of an endogenous promoter, drives the expression of any protein of interest controlled by the upstream-activation-sequence (UAS). Hence, UAS determines 'what' – which effector – is expressed, and the driver Gal4 defines 'where' this protein is supposed to be present. More recently, the efficiency in creating new fly strains has been considerably improved with the development of a new technique, the so-called ϕ C31 integrase system, that allows for the site-specific insertion of transgenes in the fly genome. Here, an attB donor plasmid containing the transgene is injected into an embryo of a *Drosophila* strain containing an attP-site (Fish et al., 2007; Bischof et al., 2007). This method helped to overcome the issues of random insertion and variable expression level and has supported enormous projects screening for cell type specific Gal4 lines that ultimately resulted in a database containing several thousand publicly available driver lines (Lindsley and Zimm, 1992; Jenett et al., 2012, see also **Bloomington stock collection**). Being able to search for distinct strains from a seemingly infinite pool of genetically modified flies created a whole new level of experimental accessibility. A second binary expression method, based on the bacterial DNA-binding protein-operator LexA-op and controlled by the expression of LexA works similarly (Lai and Lee, 2006). With complementary strategies that combine both systems one can target two cell populations independently with two different effectors.

The specificity of Gal4 or LexA driver lines is in some instances not sufficiently high to exclusively target certain subpopulations of neurons or single cell types. Two main intersectional tools help to constrain the expression patterns of driver lines. In the split-Gal4 system (Luan et al., 2006) the Gal4 is separated into two functional subunits, the DNA-binding (DBD) and the transcription-activation (AD) domains, each of which can be expressed under the control of a specific promoter. Neither domain can activate the transcription of a functional Gal4 protein on its own. Only in cells where both are expressed the AD and DBD domains heterodimerize and become transcriptionally competent. Hence, a transgene will only be expressed at the intersection of the expression patterns of both promoters. For example, the combination of driver line A containing populations 1 and 2, and driver line B containing populations 1 and 3 will result in a split-Gal4 line specific for cell population 1. Besides "A and B" strategies, expression patterns of driver lines can also be refined using "A not B" approaches. The combination of Gal4 and the yeast Gal4-inhibitor Gal80 under the control of two different promoters results in transgene expression in cells that

*Intersectional
strategies*

only contain Gal4 but not Gal80 (Lee and Luo, 1999; Suster et al., 2004). To profit from these novel transgenic techniques and the large amount of specific driver lines, a number of genetically encoded proteins that specifically manipulate functional properties of neurons in which they are expressed have been engineered.

1.4.3 Mapping neural circuits

In order to characterize neuronal circuits, the functional principles of single elements in these networks need to be understood. The discovery and synthesis of the green fluorescent protein (GFP, Figure 2b, Shimomura et al., 1962; Chalfie et al., 1994; Heim et al., 1994) enabled scientists to transgenetically label single cells *in vivo* without prior fixation and immunostaining. Using the Gal4-UAS system one can visualize subclasses of neurons in the optic lobe of the fruit fly brain (Figure 2b) and thus probe the specificity of driver lines.

Calcium indicators

Due to their small size, neurons in the brain of *Drosophila* are often inaccessible for electrophysiological recordings. Using light microscopy to observe intracellular calcium levels, a proxy for neuronal activity, can overcome this limitation (Fig. 2c). When a cell is depolarized, calcium enters the cytosol through voltage-gated calcium channels and calcium influx at the presynapse triggers the fusion of vesicles with the cell membrane which ultimately results in the release of neurotransmitters into the synaptic cleft (Hille, 2001; Grienberger and Konnerth, 2012). Different approaches to engineer genetically encoded calcium indicators have been followed. They are all based on fluorescent proteins equipped with calcium binding domains (Miyawaki et al., 1997). In general, there are two families: ratiometric indicators that consist of two fluorescent proteins linked by a domain, that changes its configuration upon calcium binding. This leads to a fluorescent resonance energy transfer (FRET) between the two fluorophores. Ultimately, the calcium level is read out through a change in the ratio between the emitted light from fluorophore A and fluorophore B (Mank et al., 2006, 2008; Broussard et al., 2014). The second class of calcium indicators are called single wavelength probes where the binding of calcium causes a conformational change in the fluorophore, leading to an increase in photon emission. Consequently, the read-out is the brightness of the indicator (Baird et al., 1999). Today, the most widely used calcium indicators are from the family of single wavelength probes GCaMP (Ohkura et al., 2005; Chen et al., 2013). In order to obtain high spatial resolution, with low tissue damage and acceptable temporal resolution, calcium imaging is often used in

combination with two-photon microscopy (Reiff and Borst, 2008; Reiff et al., 2010).

Carefully measuring the response characteristics of neurons can teach us a lot about their physiological contribution to neural networks. However, being able to specifically manipulate their functional properties would dramatically increase the number of experiments and could enhance our understanding of whole circuits. For centuries, the importance of regions of the human brain could only be determined through functional impairments occurring in individuals with localized damage from surgery or accidents (e.g. Broca, 1888). Using pharmacology it has been possible to manipulate predetermined brain areas and sometimes even identified subsets of neurons, with the disadvantage of limited temporal and spatial precision. Changing the membrane voltage of neurons with a recording electrode increases temporal accuracy, however, only to a spatially limited extent; i.e. only single or at the best a few cells can be targeted at the same time. Exploiting genetic techniques can overcome both of these issues, enabling the alteration of genetically defined sets of cells, if necessary with high temporal precision.

The genetic accessibility of many model systems has initiated the development of tools that allow interference with the function of nerve cells. One way to characterize the role of a network element is by investigating the effect of removing it from the circuit. There are several tools that allow for a removal of elements from a neural circuit. First, neurons can be killed by expressing apoptotic genes like *reaper* or *hid* (Grether et al., 1995) or by preventing protein synthesis using *ricin A* (Moffat et al., 1992). Second, their output can be permanently blocked by interrupting synaptic communication between neurons (tetanus toxin, Sweeney et al., 1995). Third, the expression of an inwardly rectified potassium channel (Kir2.1, Johns et al., 1999) causes neurons to hyperpolarize, resulting in suppressed excitability. While these tools provide effective and reliable control over the functionality of the targeted cells, the precise timing of activation cannot be determined and their expression is irreversible. In some circumstances, however, it is preferable to reversibly attenuate the activity or the synaptic output of a circuit element for a certain period of time. A dominant-negative version of the gene *shibire*, that encodes an important protein at the presynapse - *dynamin* - can be induced via temperature (Figure 2c). At a permissive temperature ($\sim 25^{\circ}\text{C}$) the reuptake of vesicles from the synaptic cleft, mediated by the GTPase *dynamin*, is still functional. When the ambient temperature is shifted by only a few degrees to a restrictive level of about 31°C the fusion of

Silencing neurons

vesicles with the presynaptic membrane is interrupted, preventing, within a few seconds to minutes, synaptic release, and ultimately silencing the neuron without changing its endogenous properties (Kitamoto, 2001). Lowering the temperature back to permissive levels releases the block effect. Interestingly, in *Drosophila* it has been shown that by exposing flies expressing *shibire^{ts}* to a persistent heat-shock for one hour at an elevated temperature (37°C), the effect becomes long-lasting and the output of the affected cells is suppressed for several hours (Joesch et al., 2010). While this experimental procedure increases the temporal extent of neuronal silencing, it does so at the cost of losing reversibility.

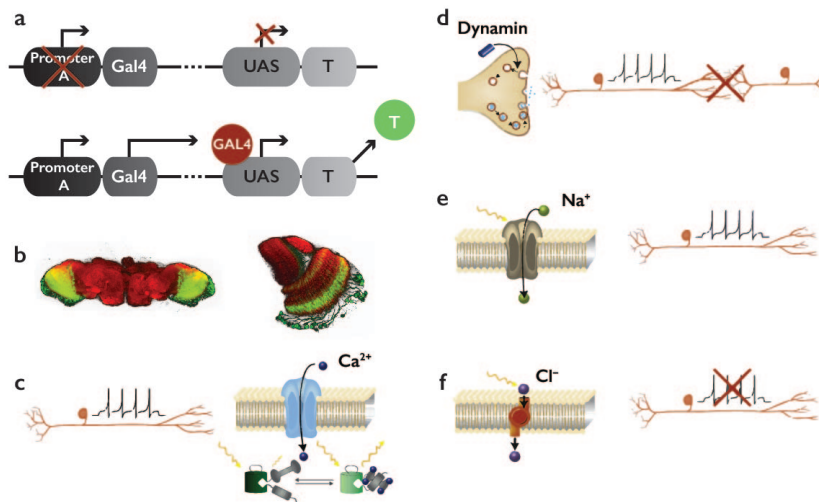


Figure 2. Genetic tools for manipulations in *Drosophila*. (a) The Gal4-UAS system is used to target genetically engineered effectors (UAS) to specific subsets of neurons (Gal4). (b) Transgenic expression of the green fluorescent protein (GFP) enables the visualization of single neurons or cell-types in living animals. E.g. in the optic lobe of the fly brain. (c-f) Genetically encoded effectors. (c) Calcium indicators are used to visualize neuronal activity based on their calcium dynamics. (d) The temperature dependent neuronal silencer *shibire^{ts}* prevents the fusion of synaptic vesicles with the presynaptic membrane and thereby interrupts synaptic communication. (e,f) Optogenetic tools. Light can be used to activate neurons, through channel proteins (e, Channelrhodopsin) or inactivate them via chloride pumps (f, Halorhodopsin). 2b from the Borst lab collection. Figure and caption taken and modified with permission from Borst (2009b) and Broussard et al. (2014).

Activating neurons

A second approach to probe the connectivity between neural elements in a network is their activation. Classically, connections between neurons have been interrogated using paired recordings from two or more potentially interconnected cells. By injecting current into one cell and recording from another, one can pre-

cisely characterize their connection strength and direction. Due to size limitations, unfavorable location or for reasons of efficiency this method is often not feasible. Stimulating or suppressing neurons by other, less invasive and more widespread mechanisms was necessary to improve the circuit mapping. Using temperature, neurons can not only be silenced but also activated. The transient receptor potential cation channel TrpA1 (Hamada et al., 2008; Pulver et al., 2009; Berni et al., 2010) naturally occurs in wild-type flies and is thought to be implicated in temperature sensing (Hamada et al., 2008). Transgenically expressing this channel in the membrane of neurons – for instance using the Gal4-UAS system – allows for temperature mediated excitation. Furthermore, transgenic activators can also be susceptible to chemicals. P2X₂, a cation channel that is activated upon the binding of ATP is used to selectively stimulate genetically identified neurons by application of ATP (Lima and Miesenböck, 2005).

All the tools described above permit the alteration of functional properties of nerve cells in a spatially confined pattern defined by the driver lines used. Nevertheless, the lack of temporal precision in stimulation excludes them for certain applications. The transgenic expression of light-activatable microbial opsins in eucaryotic cells has revolutionized modern neuroscience. The fundamental structure of rhodopsins is largely conserved for all subclasses; they consist of two sub-structures, a light absorbing retinal that is linked to a seven-transmembrane opsin protein. Upon contact with a photon, retinal undergoes isomerization which triggers a conformational change in the connected opsin. In type I rhodopsins found in prokaryotic organisms the photoisomerization of retinal results in the opening of a ion channel, whereas type II rhodopsins from eukaryotes functions as G-protein coupled receptors controlling second-messenger cascades (for review see Fenno et al., 2011). In 2005, the microbial channel-rhodopsin (ChR, Figure 2e) was expressed in hippocampal neurons for the first time enabling the activation of nerve cells with millisecond precision, by simply presenting brief flashes of blue light to the tissue (Boyden et al., 2005). Ever since, the field of optogenetics has developed numerous tools for the activation of neurons; improving photo-efficiency (Nagel et al., 2005), increasing speed (Gunaydin et al., 2010), and shifting excitation wavelengths (Lin et al., 2013). One particularly important alteration has been introduced by engineering a version of channelrhodopsin that can be switched on with a short pulse of light (sim10ms) instead of persistent illumination (Berndt et al., 2009). The slow decay time constant of the channel retains excitation for

Optogenetics

several seconds, allowing for the presentation of visual stimuli during optogenetic activation without interference of the excitation light with the visual system. Besides excitation, neurons can also be hyperpolarized. Using halorhodopsin (NpHR), a light activated chloride pump derived from *Natromonas pharaonis* (Figure 2f, [Schobert and Lanyi, 1982](#); [Zhang et al., 2007](#)), allows for the inhibition of neurons with light at high temporal resolution. Together, channelrhodopsin and halorhodopsin with their variants provide a toolset for the minimal invasive interrogation of neural circuits in living animals. Generally, optogenetic experiments can be applied with two different goals in mind; first, connectivity between cells can be probed in a similar way to classic paired electrophysiological recordings. Activating for instance a subset of neurons expressing channelrhodopsin and measuring resulting changes calcium levels in a second cell type expressing a genetically encoded calcium indicator can provide insight into their connectivity (e.g. [Guo et al., 2009](#); [Chuhma et al., 2011](#)). A second application can test the necessity or sufficiency of neural elements for certain behaviors or circuit functions (e.g. [Gordon and Scott, 2009](#); [Haikala et al., 2013](#)).

In the 20th century, classical techniques like electrophysiology, neuroanatomy and pharmacology laid the foundation for modern neuroscience. Deciphering the functional principles of neurons, the building blocks of the nervous system and the brain, describing coarse connections between brain regions, and synaptic communication. Recently, an immense number of new techniques have entered the game, dramatically changing large parts of neuroscience. Enormous amounts of data are generated with high throughput, semi-automated image acquisition at modern electron microscopes ([Kleinfeld et al., 2011](#); [Helmstaedter et al., 2013](#); [Lichtman et al., 2014](#)), transgenic engineering has opened the door to a whole new world of possibilities to interfere with neuronal networks, and new imaging and stimulation methods allow the observation and manipulation of live and even behaving animals. The fly visual system has been subject to intensive investigation for many years, but only with the genetic toolbox introduced in *Drosophila melanogaster* could a huge step be taken towards fully understanding an entire neural circuit.

1.5 STRUCTURE AND PHYSIOLOGY OF THE VISUAL SYSTEM

Drosophila's central nervous system can be divided into two major parts, the head and the thoracic ganglion. The thoracic ganglion is dedicated to motor control while the head ganglion is involved in sensory processing. The head ganglion or brain is further divided into three parts: the central brain and two optic lobes. The optic lobes process visual information and then pass it to the central brain and the thoracic ganglion thus controlling visually guided behaviors.

The visual system of the fly brain is called the 'optic lobe' consisting of 60,000 (Hofbauer and Campos-Ortega, 1990) neurons and is divided into several structures: the retina, the lamina, the medulla and the lobula complex, comprised of the lobula and lobula plate (Figure 4a). In 1915, Cajal and Sánchez (1915), used Golgi-stainings to describe the various cell types in the fly optic lobe. Later a complete catalog of the various cell types in the fly's optic lobe was provided (Fischbach and Dittrich, 1989).

1.5.1 Retina

Drosophila's compound eye is made up of 750 hexagonal ommatidia which compose an evenly spaced mosaic with an interommatidial angle of 5 degrees (Land, 1997). Amazingly, it samples nearly the entire visual hemisphere excluding only an area of approximately 20 degrees in the back of the fly (Buchner, 1976). Each ommatidium in the eye contains eight unfused rhabdomeres, R1-R8. R1-R6 are arranged in a hexagonal structure underneath the lens of each facet, while R7 and R8 are stacked on top of each other in the center of the hexagon. Central photoreceptors exist in two subtypes depending on the expression of one of two different light sensitive rhodopsins (Rh), pale (35%) and yellow (65%) (Franceschini et al., 1981). In pale ommatidia, R7 cells contain the UV-absorbing pigment Rhodopsin-3 (Rh3) and R8 cells contain a blue sensitive pigment Rhodopsin-5 (Rh5). In yellow-type ommatidia, photoreceptors R7 contain another type of UV-absorbing pigment, Rhodopsin-4 (Rh4) and photoreceptors R8 contain the green sensitive Rhodopsin-6 (Rh6). Both ommatidial subtypes are distributed stochastically across the retina. R7 and R8 are mainly involved in color discrimination (Schnaitmann et al., 2013), while R1-R6 are responsible for encoding spatial information crucial to motion vision.

Photoreceptors

The visual pigments are located in the rhabdomere, a densely

Phototransduction

packed structure of microvilli where light is converted into an electrical signal by an intricate biochemical cascade (Hardie and Raghu, 2001). Upon illumination, rhodopsin is photoisomerized into metarhodopsin. This leads to the dissociation of the alpha subunit from the heterotrimeric G-protein. Next phospholipase C (PLC) hydrolyzes PIP^2 to produce DAG and $InsP^3$ resulting in an activation of cation permeable channels and depolarization of the photoreceptor (Fig. 3). Phototransduction in flies is extremely fast; after a short light pulse depolarization is already detectable after a few milliseconds and quickly decays back to resting levels (Hardie, 1991), which accounts for the amazing temporal flicker resolution of the fly eye at values larger than 200Hz (Autrum, 1950). All photoreceptors use histamine as a neurotransmitter and hence provide an inhibitory signal to their postsynaptic targets (Hardie, 1989).

Neural Superposition

The photoreceptors within an ommatidium are spatially separated and point in different directions. Therefore, a simple convergence of their outputs onto the following lamina cartridge would result in drastically decreased spatial acuity. Nature has solved this problem by using the principle of neuronal superposition, which maintains resolution and increases sensitivity at the same time (Braitenberg, 1967). Photoreceptors R1-R6 from within one ommatidium project into distinct neighboring cartridges of the lamina such that the photoreceptors with the same optical axis project to the same lamina cartridge. The functional unit for processing light, therefore, is not the ommatidium but rather the lamina cartridge, also known as the neuro-ommatidium. R7 and R8, on the other hand, project directly through the next cartridge of the lamina and synapse onto medulla neurons. However, both R7 and R8 form gap junctions with R6 within the same cartridge at the level of the lamina (Shaw, 1989; Wardill et al., 2012)

Lamina

The first neural processing stage of the optic lobes is called lamina. The lamina is made up of 6000 neurons organized into repetitive units, called cartridges (Hofbauer and Campos-Ortega, 1990). Due to the principle of neural superposition each cartridge represents a single point in space and is therefore also referred to as a neuro-ommatidium. The photoreceptors R1-R6 project to the lamina cartridges in a retinotopic manner synapsing onto the five lamina monopolar cells L1-L5. Morphological investigations have shown, that L1, L2, and L3 cells receive the majority of their input from photoreceptors R1-R6, while L4

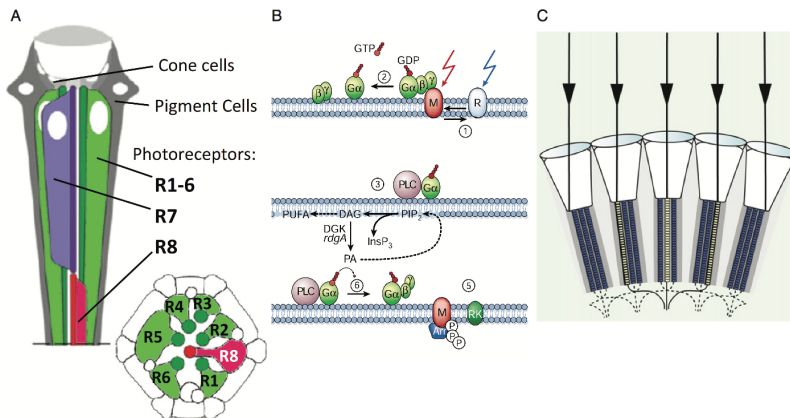


Figure 3. *Drosophila* Retina. (a) Schematic overview of an ommatidium (from (Wernet et al., 2015)). (b) Illustration of the phototransduction cascade (modified from (Hardie and Raghu, 2001)). (c) Schematic of the organization of a neural superposition eye. Figure and caption taken and modified with permission from Borst (2009a).

forms reciprocal connections with L2 and only shares a small number of synapses with R6 (Rivera-Alba et al., 2011). L5 has been shown to receive input from L2, L4 and several lamina interneurons such as an amacrine cell. Additionally, the lamina houses centrifugal, wide-field, and tangential neurons: C2, C3, T1, Lai, Lat, Lawf1 (Fischbach and Dittrich, 1989). All five classes of lamina monopolar cells send axonal arbors into distal layers of the subsequent processing stage, the medulla. The other lamina cell types have their axons in the lamina with their dendrites either in the medulla or in the lamina itself.

Medulla

The second and largest neuropil involved in early visual processing is the medulla. The medulla is extremely dense with 60 columnar neuron types forming a neural network of 40,000 neurons (Hofbauer and Campos-Ortega, 1990). The medulla is divided into ten layers (M1-M10) where lamina neurons synapse onto medulla neurons. Nearly all of the medulla neurons receive their input here and are grouped according to their shape and projections patterns. Broadly, there are two main classes of columnar interneurons: about 10 types of medulla intrinsic (Mi) cells and almost 30 subclasses of transmedullary (Tm) neurons (Fischbach and Dittrich, 1989). Mi cells have their dendrites in distal layers of the medulla and send their axons to the proximal medulla. Tm cells receive input from lamina monopolar cells and photoreceptors R7 and R8 in the distal medulla layers

Cell Types

1-5 and project onto neurons in the lobula. On the other hand trans medulla Y-cells bifurcate and synapse onto cells in both the lobula and the lobula plate. In addition to these two types of neurons, TmY cells, connecting medulla, lobula and lobula plate as well as numerous types of amacrine and wide-field neurons have been described. Another group of cells is formed by the bushy T-cells (T2, T3, T4, T5) which target different layers of the lobula (T2, T3) and the lobula plate (T4, T5). T2-T4 neurons receive input from within the medulla but T5 get input from the lobula. Both T4 and T5 are further divided in to subtypes a-d based on which layer of the lobula plate they project to ([Bausenwein and Fischbach, 1992](#)).

Connectivity

This jungle of interconnected nerve cells has proven very hard to disentangle. Nevertheless, recent advances in electron microscopy have lead to the creation of detailed connectivity maps, which revealed clusters of connectivity within the medulla network ([Shinomiya et al., 2014](#); [Takemura et al., 2011](#)). Three main clusters were found: one between L1, Mi1, Tm3, and T4, another between L2, L4, Tm1, Tm2, Tm4, and T5 cells and finally between L3, R7, R8, Tm9, and T5 neurons. It has been established in this work and others that the T4 and T5 clusters correspond to the ON and OFF motion pathways, respectively. It is thought that the Tm9 path is involved in color vision.

Lobula complex

The lobula complex, the final stage of neural processing in the optic lobes, is where large-field neurons integrate columnar input from the from the medulla. The lobula complex consists of two neuropils, the lobula and the lobula plate.

Lobula plate

The lobula plate is the most well studied neuropil in the fly brain ([Hausen, 1976](#); [Hengstenberg et al., 1982](#); [Haag and Borst, 1998, 2004](#)). Relatively easy access and the large size of the lobula plate tangential cells allowed for a thorough investigation of the lobula plate network (for review, see ([Borst and Haag, 2002](#))). Perpendicular to its columnar organization, the lobula plate is comprised of four structurally distinct layers. Each layer contains a number of wide-field tangential cells with their characteristic dendritic trees spanning much of the lobula plate. They respond to motion in their preferred direction with a depolarization and to motion in the opposite direction, the null direction, by hyperpolarization. They are tuned to different directions of motions and form groups of vertical system cells and horizontal system cells.

Lobula

In contrast to the lobula plate, the second part of the third neu-

ropil, the lobula is significantly less well studied on a functional level. In general it is comprised of both small columnar neurons as well as large field cells (Fischbach and Dittrich, 1989) that receive their major input through Tm and TmY cells from the medulla. The lobula constitutes an interesting morphological difference between the two input lines to the lobula plate. While T4 cells connect the medulla directly to the four layers of the lobula plate, the second parallel stream takes a detour to the lobula, where T5 cell dendrites reside. While this anatomical peculiarity has been known for a long time, its functional significance is to date unknown.

1.5.2 Motion vision circuit

Lobula plate tangential cells are thought to be involved in the initiation of turning behaviors (e.g. Heisenberg et al., 1978). Even though morphologically well described, physiological studies in *Drosophila* remained challenging due to its small size. Deoxyglucose mapping revealed a functional organization which was previously described in their bigger relatives, showing that the four layers of the lobula plate were active during visual stimulation in the four cardinal directions, respectively (Buchner et al., 1984). Only much later it became possible in *Drosophila* to record from tangential cells. Here, two major groups of lobula plate tangential cells have been described; cells of the horizontal system (HS) that respond preferentially to visual stimuli with horizontal orientations (Schnell et al., 2010), and vertical system (VS) cells that detect vertical motion (Joesch et al., 2008). Both classes of neurons are fully opponent (Figure 4c), i.e. they respond to motion in their preferred direction (PD) with an increase in membrane potential and hyperpolarize when stimulated in the opposite, their anti preferred or null direction (ND). The three HS cells reside in the first layer of the lobula plate and prefer front-to-back motion, while the number of VS cells, that have their dendritic arbors in the fourth layer and are excited by downward motion, has not been finally determined. Unlike in bigger flies like *Calliphora*, where tangential cells in layers 2 and 3 tuned to opposite directions are well characterized (Hausen, 1976; Wertz et al., 2008), descriptions of these neurons are missing in fruit flies. The response characteristics of VS and HS cells are well described by algorithmic models (for review see Borst et al., 2010). The cellular implementation of the necessary computations however is still subject to intense investigation. Anatomical studies proposed the existence of two parallel processing streams via T4 and T5 cells, based on neural connectivity patterns (Bausenwein

and Fischbach, 1992). Blocking the synaptic output of both cell types simultaneously rendered lobula plate tangential cells entirely motion insensitive (Schnell et al., 2010). Hence, these two classes of neurons are part of the circuitry responsible for the direction-selective properties of lobula plate tangential cells. Investigating their roles and contributions is part of the content of this dissertation.

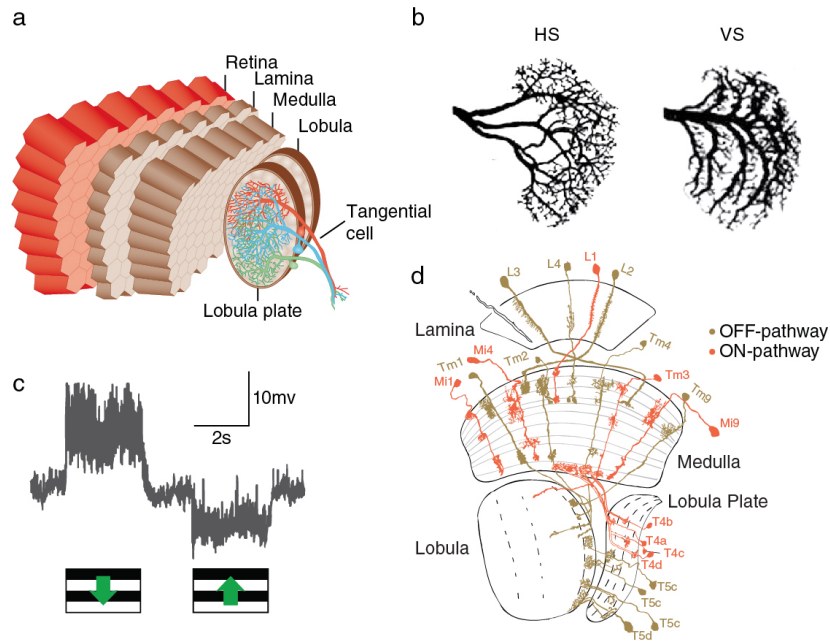


Figure 4. The Fly Visual System (a) Schematic overview of the nervous system of the fruit fly *Drosophila melanogaster*. (a) Illustration of the optic lobe of a fly. (b) Lobula plate tangential cells of the horizontal (HS) and vertical (VS) system. (c) Electrophysiological recordings from a direction-selective vertical system tangential cell. VS cells depolarize to downward motion (PD) and hyperpolarize to visual stimulation in the opposite direction (ND). (d) Horizontal section through the visual system of *Drosophila*. Presumed OFF pathway elements are depicted in brown, ON pathway candidates in red. Figure and caption taken and modified with permission from Rajashekar and Shamprasad (2004) and Borst (2014a) and Fischbach and Dittrich (1989) and Joesch et al. (2008).

Already at an earlier stage of neural processing, in the lamina, the computation of visual motion is implemented, similar to the vertebrate visual system, in two parallel streams for brightness increments and decrements, respectively (Joesch et al., 2010). When blocking the output of lamina monopolar cells L1 and simultaneously recording from downstream direction-selective tangential cells, only responses to bright stimuli (ON edges) were abolished, while dark edge processing was still in-

tact. The exact opposite effect was found when genetically silencing L2 cells, tangential cells still depolarized when stimulated in their preferred direction with bright edges, but exhibited no response to OFF edges. In a morphological study, [Bausenwein and Fischbach \(1992\)](#) hypothesized that L1 could be connected to T4 via Mi1 cells, while L2 contact T5 via Tm1. In the L2 pathway, Tm1 and Tm2 cells have been shown later by electron microscopy to receive synaptic input from L2 ([Takemura et al., 2011](#)). Furthermore an asymmetric connection between L2, L4 and Tm2 cells in the outer medulla could be identified. Tm2 receives input from L2 in its home-column, while L4 connects to two "walking-legs", dendritic proliferations extending posteriorly into neighboring columns. This morphological feature suggested a distinct, potentially directionality-specific role of the L4-Tm2 connection ([Takemura et al., 2011](#)). Subsequent investigations revealed two more cell types that are likely to be involved in the computation of moving dark-edges; Tm4 and Tm9 ([Shinomiya et al., 2014](#)). Other than Tm1, Tm2 and Tm4, Tm9 cells are not postsynaptic to L2 or L4, but receive the majority of their input from L3 cells. For the ON-selective pathway, Mi1 and Tm3 have been proposed to play major roles due to their synaptic connectivity to L1 and T4 ([Takemura et al., 2013](#)). Later, Mi4 and Mi9 cells have been added to the potential candidates for the ON pathway of motion vision (Figure 4d, see also [Janelia EM reconstructions](#)). However, without functional studies, the implication in motion detection remains hypothetical.

1.6 CONCLUDING REMARKS

The visual system of the fruit fly is particularly well suited for studying the underlying principles of neural network computation. The combination of anatomy and physiology, theoretical models and the availability of genetic tools makes this small insect particularly useful. In the course of my PhD thesis, I investigated the neural correlate of an elementary motion detector in the visual system of *Drosophila*. I used two-photon calcium imaging of various interneurons upstream of the large lobula plate tangential cells to better understand and characterize their response properties and role in elementary motion detection. In the highly collaborative environment of our lab my imaging experiments were complemented by several other approaches, including electrophysiologic and behavioral experiments, along with modeling which resulted in the publications that comprise this cumulative dissertation.

2 | PUBLICATIONS

2.1 A DIRECTIONAL TUNING MAP OF *drosophila* ELEMENTARY MOTION DETECTORS

This paper ([Maisak et al., 2013](#)) describes response properties of T4 and T5 cells and characterizes their role in *Drosophila* motion vision. It was published in *Nature* in August 2013.

Bushy T4 cells connect the medulla to the four layers of the lobula plate, while T5 cells provide input from the lobula. Measuring changes in calcium levels in response to moving gratings revealed that each subtype of T4 and T5 cells is tuned selectively to one of four cardinal directions (down, up, left, and right). Moreover, polarity specific stimulation provided evidence that T4 cells are activated only by moving brightness increments (ON edges), whereas T5 cells are susceptible for brightness decrements (OFF edges). Blocking the synaptic output of T4 and T5 cells separately, specifically rendered downstream lobula plate tangential cells insensitive for moving bright and dark edges, respectively. Similar phenotypes could be observed when monitoring the turning behavior of T4 and T5 block flies presented with moving ON and OFF edges. From these experiments we concluded that T4 and T5 cells are motion detectors that process visual information from two parallel pathways.

Summary

The following authors contributed to this work:

Matthew S. Maisak, Jürgen Haag, Georg Ammer, Etienne Serbe, Matthias Meier, Aljoscha Leonhardt, Tabea Schilling, Armin Bahl, Gerald M. Rubin, Aljoscha Nern, Barry J. Dickson, Dierk F. Reiff, Elisabeth Hopp, and Alexander Borst

Matthew S. Maisak and Jürgen Haag jointly performed and, together with Alexander Borst, evaluated all calcium imaging experiments. Georg Ammer, Etienne Serbe and Matthias Meier recorded from tangential cells. Aljoscha Leonhardt, Tabea Schilling and Armin Bahl performed the behavioral experiments. Gerald Rubin, Barry J. Dickson and Aljoscha Nern generated the driver lines and characterized their expression pattern. Dierk F. Reiff performed preliminary imaging experiments. Elisabeth Hopp

Author contribution

helped with programming and developed the PMT shielding for the two-photon microscope. Alexander Borst designed the study and wrote the manuscript with the help of all authors.

This article was highlighted in a number of journals ([Flight, 2013](#); [Gilbert, 2013](#); [Masland, 2013](#); [Yonehara and Roska, 2013](#)).

A directional tuning map of *Drosophila* elementary motion detectors

Matthew S. Maisak^{1*}, Juergen Haag^{1*}, Georg Ammer¹, Etienne Serbe¹, Matthias Meier¹, Aljoscha Leonhardt¹, Tabea Schilling¹, Armin Bahl¹, Gerald M. Rubin², Aljoscha Nern², Barry J. Dickson³, Dierk F. Reiff[†], Elisabeth Hopp¹ & Alexander Borst¹

The extraction of directional motion information from changing retinal images is one of the earliest and most important processing steps in any visual system. In the fly optic lobe, two parallel processing streams have been anatomically described, leading from two first-order interneurons, L1 and L2, via T4 and T5 cells onto large, wide-field motion-sensitive interneurons of the lobula plate¹. Therefore, T4 and T5 cells are thought to have a pivotal role in motion processing; however, owing to their small size, it is difficult to obtain electrical recordings of T4 and T5 cells, leaving their visual response properties largely unknown. We circumvent this problem by means of optical recording from these cells in *Drosophila*, using the genetically encoded calcium indicator GCaMP5 (ref. 2). Here we find that specific subpopulations of T4 and T5 cells are directionally tuned to one of the four cardinal directions; that is, front-to-back, back-to-front, upwards and downwards. Depending on their preferred direction, T4 and T5 cells terminate in specific sublayers of the lobula plate. T4 and T5 functionally segregate with respect to contrast polarity: whereas T4 cells selectively respond to moving brightness increments (ON edges), T5 cells only respond to moving brightness decrements (OFF edges). When the output from T4 or T5 cells is blocked, the responses of postsynaptic lobula plate neurons to moving ON (T4 block) or OFF edges (T5 block) are selectively compromised. The same effects are seen in turning responses of tethered walking flies. Thus, starting with L1 and L2, the visual input is split into separate ON and OFF pathways, and motion along all four cardinal directions is computed separately within each pathway. The output of these eight different motion detectors is then sorted such that ON (T4) and OFF (T5) motion detectors with the same directional tuning converge in the same layer of the lobula plate, jointly providing the input to downstream circuits and motion-driven behaviours.

Most of the neurons in the fly brain are dedicated to image processing. The respective part of the head ganglion, called the optic lobe, consists of several layers of neuropile called lamina, medulla, lobula and lobula plate, all built from repetitive columns arranged in a retinotopic way (Fig. 1a). Each column houses a set of identified neurons that, on the basis of Golgi staining, have been described anatomically in great detail^{3–5}. Owing to their small size, however, most of these columnar neurons have never been recorded from electrophysiologically. Therefore, their specific functional role in visual processing is still largely unknown. This fact is contrasted by rather detailed functional models about visual processing inferred from behavioural studies and recordings from the large, electrophysiologically accessible output neurons of the fly lobula plate (tangential cells). As the most prominent example of such models, the Reichardt detector derives directional motion information from primary sensory signals by multiplying the output from adjacent photoreceptors after asymmetric temporal filtering⁶. This model makes a number of rather counter-intuitive predictions all of which have been confirmed experimentally (for review, see ref. 7). Yet, the neurons corresponding to most

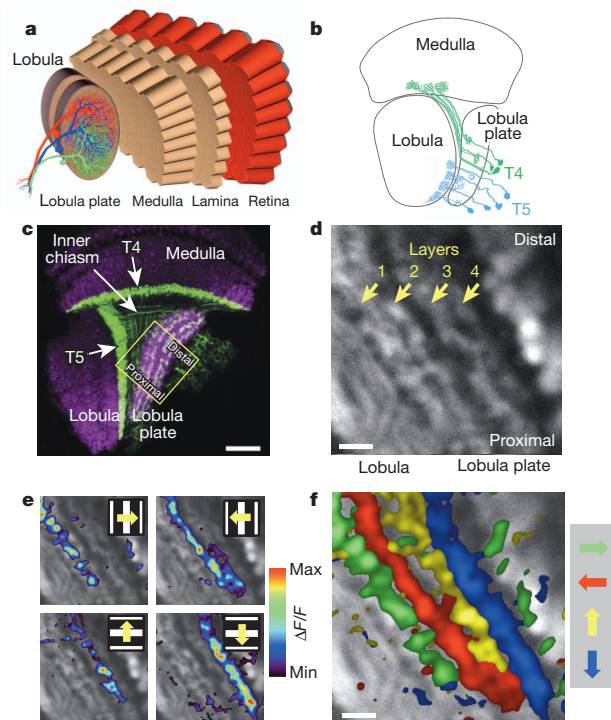


Figure 1 | Directional tuning and layer-specific projection of T4 and T5 cells. **a**, Schematic diagram of the fly optic lobe. In the lobula plate, motion-sensitive tangential cells extend their large dendrites over many hundreds of columns. Shown are the reconstructions of the three cells of the horizontal system²². **b**, Anatomy of T4 and T5 cells, as drawn from Golgi-impregnated material (from ref. 5). **c**, Confocal image of the Gal4-driver line R42F06, shown in a horizontal cross-section (from ref. 10). Neurons are marked in green (Kir2.1-EGFP labelled), whereas the neuropile is stained in purple by an antibody against the postsynaptic protein Dlg. Scale bar, 20 μm . **d**, Two-photon image of the lobula plate of a fly expressing GCaMP5 under the control of the same driver line R42F06. Scale bar, 5 μm . The size and orientation of the image approximately corresponds to the yellow square in **c**. **e**, Relative fluorescence changes ($\Delta F/F$) obtained during 4-s grating motion along the four cardinal directions, overlaid on the greyscale image. Each motion direction leads to activity in a different layer. Minimum and maximum $\Delta F/F$ values were 0.3 and 1.0 (horizontal motion), and 0.15 and 0.6 (vertical motion). **f**, Compound representation of the results obtained from the same set of experiments. Scale bar, 5 μm . Results in **e** and **f** represent the data obtained from a single fly averaged over four stimulus repetitions. Similar results were obtained from six other flies.

¹Max Planck Institute of Neurobiology, 82152 Martinsried, Germany. ²Janelia Farm Research Campus, Ashburn, Virginia 20147, USA. ³Institute of Molecular Pathology, 1030 Vienna, Austria. [†]Present address: Institute Biology 1, Albert-Ludwigs University, 79085 Freiburg, Germany.

*These authors contributed equally to this work.

of the circuit elements of the Reichardt detector have not been identified so far. Here, we focus on a set of neurons called T4 and T5 cells (Fig. 1b) which, on the basis of circumstantial evidence, have long been speculated to be involved in motion detection^{1,8–10}. However, it is unclear to what extent T4 and T5 cells are directionally selective or whether direction selectivity is computed or enhanced within the dendrites of the tangential cells. Another important question concerns the functional separation between T4 and T5 cells; that is, whether they carry equivalent signals, maybe one being excitatory and the other inhibitory on the tangential cells, or whether they segregate into directional- and non-directional pathways¹¹ or into separate ON- and OFF-motion channels^{12,13}.

To answer these questions, we combined Gal4-driver lines specific for T4 and T5 cells¹⁴ with GCaMP5 (ref. 2) and optically recorded the visual response properties using two-photon fluorescence microscopy¹⁵. In a first series of experiments, we used a driver line labelling both T4 and T5 cells. A confocal image (Fig. 1c, modified from ref. 10) revealed clear labelling (in green) in the medulla (T4 cell dendrites), in the lobula (T5 cell dendrites), as well as in four distinct layers of the lobula plate, representing the terminal arborizations of the four subpopulations of both T4 and T5 cells. These four layers of the lobula plate can also be seen in the two-photon microscope when the calcium indicator GCaMP5 is expressed (Fig. 1d). After stimulation of the fly with grating motion along four cardinal directions (front-to-back, back-to-front, upwards and downwards), activity is confined to mostly one of the four layers, depending on the direction in which the grating is moving (Fig. 1e). The outcome of all four stimulus conditions can be combined into a single image by assigning a particular colour to each pixel depending on the stimulus direction to which it responded most strongly (Fig. 1f). From these experiments it is clear that the four subpopulations of T4 and T5 cells produce selective calcium signals depending on the stimulus direction, in agreement with previous deoxyglucose labelling⁸. Sudden changes of the overall luminance evokes no responses in any of the layers (field flicker; $n = 4$ experiments, data not shown). However, gratings flickering in counter-phase lead to layer-specific responses, depending on the orientation of the grating (Supplementary Fig. 1).

The retinotopic arrangement of this input to the lobula plate is demonstrated by experiments where a dark edge was moved within a small area of the visual field only. Depending on the position of this area, activity of T4 and T5 cells is confined to different positions within the lobula plate (Fig. 2a). Consequently, when moving a bright vertical edge horizontally from back to front, activity of T4 and T5 cells is elicited sequentially in layer 2 of the lobula plate (Fig. 2b). These two experiments also demonstrate that T4 and T5 cells indeed signal motion locally. We next investigated the question of where direction selectivity of T4 and T5 cells arises; that is, whether it is already present in the dendrite, or whether it is generated by synaptic interactions within the lobula plate. This question is hard to answer, as the dendrites of both T4 and T5 cells form a dense mesh within the proximal layer of the medulla (T4) and the lobula (T5), respectively. However, signals within the inner chiasm where individual processes of T4 and T5 cells can be resolved in some preparations show a clear selectivity for motion in one over the other directions (Fig. 2c). Such signals are as directionally selective as the ones measured within the lobula plate, demonstrating that the signals delivered from the dendrites of T4 and T5 cells are already directionally selective.

To assess the particular contribution of T4 and T5 cells to the signals observed in the above experiments, we used driver lines specific for T4 and T5 cells, respectively. Applying the same stimulus protocol and data evaluation as in Fig. 1, identical results were obtained as before for both the T4- as well as the T5-specific driver line (Fig. 3a, b). We conclude that T4 and T5 cells each provide directionally selective signals to the lobula plate, in contrast to previous reports¹¹. Thus, both T4 and T5 cells can be grouped, according to their preferred direction, into four subclasses covering all four cardinal directions, reminiscent of ON-OFF ganglion cells of the rabbit retina¹⁶.

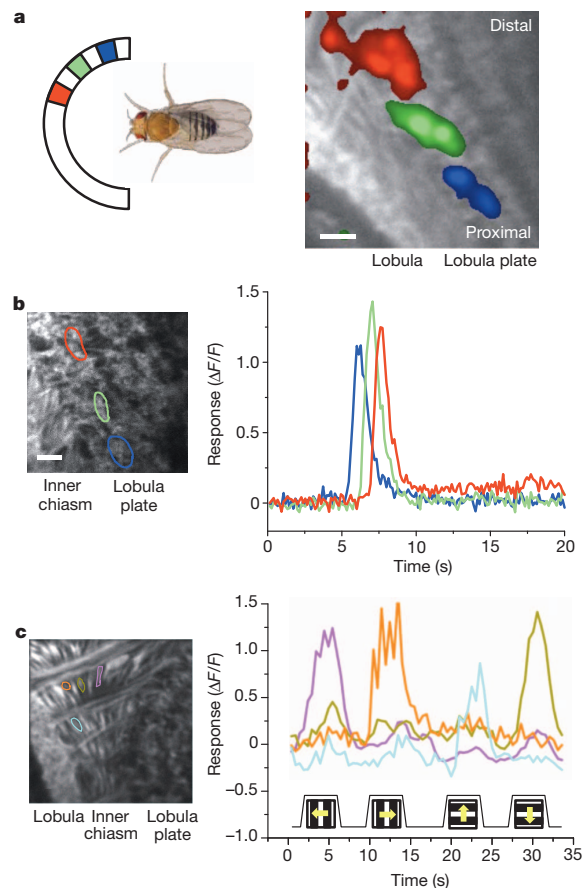


Figure 2 | Local signals of T4 and T5 cells. **a**, Retinotopic arrangement of T4 and T5 cells. A dark edge was moving repeatedly from front-to-back within a 15° wide area at different azimuthal positions (left). This leads to relative fluorescence changes at different positions along the proximal–distal axis within layer 1 of the lobula plate (right). Scale bar, $5 \mu\text{m}$. Similar results have been obtained in four other flies. **b**, Sequential activation of T4 and T5 cells. A bright edge was moving from back-to-front at 15° s^{-1} . Scale bar, $5 \mu\text{m}$. Similar results have been obtained in six other flies. **c**, Signals recorded from individual fibres within the inner chiasm (left) reveal a high degree of direction selectivity (right). Scale bar, $5 \mu\text{m}$. Similar results were obtained from four other flies, including both lines specific for T4 and T5 cells. Response traces in **b** and **c** are derived from the region of interest encircled in the image with the same colour.

We next addressed whether T4 cells respond differently to T5 cells. To answer this question, we used, instead of gratings, moving edges with either positive (ON edge, brightness increment) or negative (OFF edge, brightness decrement) contrast polarity as visual stimuli. We found that T4 cells strongly responded to moving ON edges, but showed little or no response to moving OFF edges (Fig. 3c). This is true for T4 cells terminating in each of the four layers. We found the opposite for T5 cells. T5 cells selectively responded to moving OFF edges and mostly failed to respond to moving ON edges (Fig. 3d). Again, we found this for T5 cells in each of the four layers. We next addressed whether there are any other differences in the response properties between T4 and T5 cells by testing the velocity tuning of both cell populations by means of stimulating flies with grating motion along the horizontal axis from the front to the back at various velocities covering two orders of magnitude. T4 cells revealed a maximum response at a stimulus velocity of 30° s^{-1} , corresponding to a temporal frequency of 1 Hz (Fig. 3e). T5 cell responses showed a similar dependency on stimulus velocity, again with a peak at a temporal frequency of

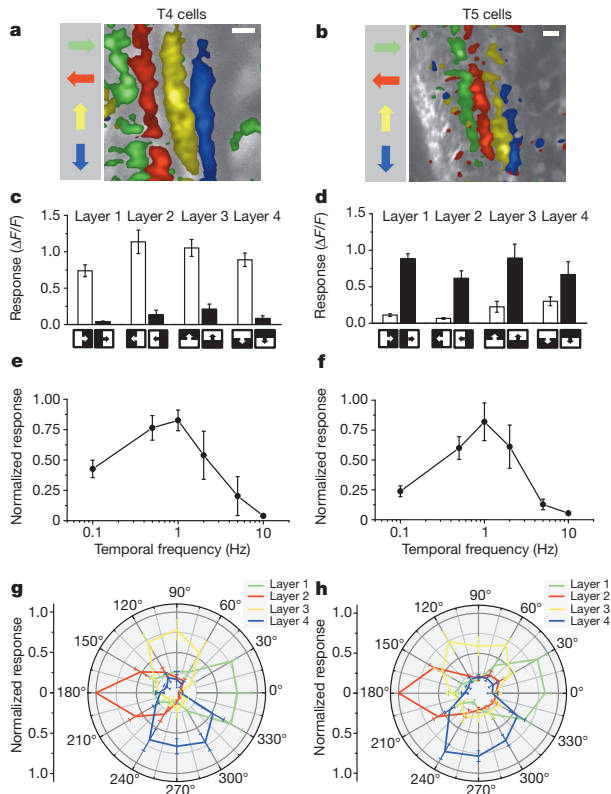


Figure 3 | Comparison of visual response properties between T4 and T5 cells. **a, b**, Relative fluorescence changes ($\Delta F/F$) of the lobula plate terminals of T4 (**a**) and T5 (**b**) cells obtained during grating motion along the four cardinal directions. Results represent the data obtained from a single fly each, averaged over two stimulus repetitions. Scale bars, 5 μm . Similar results have been obtained in ten other flies. **c, d**, Responses of T4 (**c**) and T5 (**d**) cells to ON and OFF edges moving along all four cardinal directions. ON (white) and OFF (black) responses within each layer are significantly different from each other, with $P < 0.005$ except for layers 3 and 4 in T5 cells, where $P < 0.05$. **e, f**, Responses of T4 (**e**) and T5 (**f**) cells to gratings moving horizontally at different temporal frequencies. Relative fluorescence changes were evaluated from layer 1 of the lobula plate and normalized to the maximum response before averaging. **g, h**, Responses of T4 (**g**) and T5 (**h**) cells to gratings moving in 12 different directions. Relative fluorescence changes were evaluated from all four layers of the lobula plate normalized to the maximum response before averaging. Data represent the mean \pm s.e.m. of the results obtained in $n = 8$ (**c**), $n = 7$ (**d**), $n = 6$ (**e**), $n = 7$ (**f**), $n = 6$ (**g**) and $n = 5$ (**h**) different flies. Significances indicated are based on two-sample *t*-test.

1 Hz (Fig. 3f). Thus, there is no obvious difference in the velocity tuning between T4 and T5 cells. As another possibility, T4 cells might functionally differ from T5 cells with respect to their directional tuning width. To test this, we stimulated flies with gratings moving into 12 different directions and evaluated the relative change of fluorescence in all four layers of the lobula plate. Using the T4-specific driver line, we found an approximate half width of 60–90° of the tuning curve, with the peak responses in each layer shifted by 90° (Fig. 3g). No decrease of calcium was detectable for grating motion opposite to the preferred direction of the respective layer. When we repeated the experiments using the T5-specific driver line, we found a similar dependence of the relative change of fluorescence on the stimulus direction (Fig. 3h). We conclude that T4 cells have the same velocity and orientation tuning as T5 cells. The only functional difference we were able to detect remains their selectivity for contrast polarity.

Our finding about the different preference of T4 and T5 cells for the polarity of a moving contrast makes the strong prediction that selective

blockade of T4 or T5 cells should selectively compromise the responses of downstream lobula plate tangential cells to either ON or OFF edges. To test this prediction, we blocked the output of either T4 or T5 cells via expression of the light chain of tetanus toxin¹⁷ and recorded the responses of tangential cells via somatic whole-cell patch to moving ON and OFF edges. In response to moving ON edges, control flies, strong and reliable directional responses were observed in all control flies (Fig. 4a). However, T4-block flies showed a strongly reduced response to ON edges, whereas the responses of T5-block flies were at the level of control flies (Fig. 4b, c). When we used moving OFF edges, control flies again responded with a large amplitude (Fig. 4d). However, the responses of T4-block flies were at the level of control flies, whereas the responses of T5-block flies were strongly reduced (Fig. 4e, f). These findings are reminiscent of the phenotypes obtained from blocking lamina cells L1 and L2 (ref. 13) and demonstrate that T4 and T5 cells are indeed the motion-coding intermediaries for these contrast polarities on their way to the tangential cells of the lobula plate. Whether the residual responses to ON edges in T4-block flies and to OFF edges in T5-block flies are due to an incomplete signal separation between the two pathways or due to an incomplete genetic block in both fly lines is currently unclear.

To address the question of whether T4 and T5 cells are the only motion detectors of the fly visual system, or whether they represent one cell class, in parallel to other motion-sensitive elements, we used tethered flies walking on an air-suspended sphere¹⁸ and stimulated them by ON and OFF edges moving in opposite directions¹⁹. As in the previous experiments, we blocked T4 and T5 cells specifically by selective expression of the light chain of tetanus toxin. During balanced motion, control flies did not show significant turning responses to either side (Fig. 4g). T4-block flies, however, strongly followed the direction of the moving OFF edges, whereas T5-block flies followed the direction of the moving ON edges (Fig. 4h, i). In summary, the selective preference of T4-block flies for OFF edges and of T5-block flies for ON edges not only corroborates our findings about the selective preference of T4 and T5 cells for different contrast polarities, but also demonstrates that the signals of T4 and T5 cells are indeed the major, if not exclusive, inputs to downstream circuits and motion-driven behaviours.

Almost a hundred years after T4 and T5 cells have been anatomically described³, this study reports their functional properties in a systematic way. Using calcium as a proxy for membrane voltage²⁰, we found that both T4 and T5 cells respond to visual motion in a directionally selective manner and provide these signals to each of the four layers of the lobula plate, depending on their preferred direction. Both cell types show identical velocity and orientation tuning which matches the one of the tangential cells^{21,22}. The strong direction selectivity of both T4 and T5 cells is unexpected, as previous studies had concluded that the high degree of direction selectivity of tangential cells is due to a push–pull configuration of weakly directional input with opposite preferred direction^{23,24}. Furthermore, as the preferred direction of T4 and T5 cells matches the preferred direction of the tangential cells branching within corresponding layers, it is currently unclear which neurons are responsible for the null-direction response of the tangential cells. As for the functional separation between T4 and T5 cells, we found that T4 cells selectively respond to brightness increments, whereas T5 cells exclusively respond to moving brightness decrements. Interestingly, parallel ON and OFF motion pathways had been previously postulated on the basis of selective silencing of lamina neurons L1 and L2 (ref. 13). Studies using apparent motion stimuli to probe the underlying computational structure arrived at controversial conclusions: whereas some studies concluded that there was a separate handling of ON and OFF events by motion detectors^{12,25,26}, others did not favour such a strict separation^{19,27}. The present study directly demonstrates the existence of separate ON and OFF motion detectors, as represented by T4 and T5 cells, respectively. Furthermore, our results anatomically confine the essential processing steps of elementary

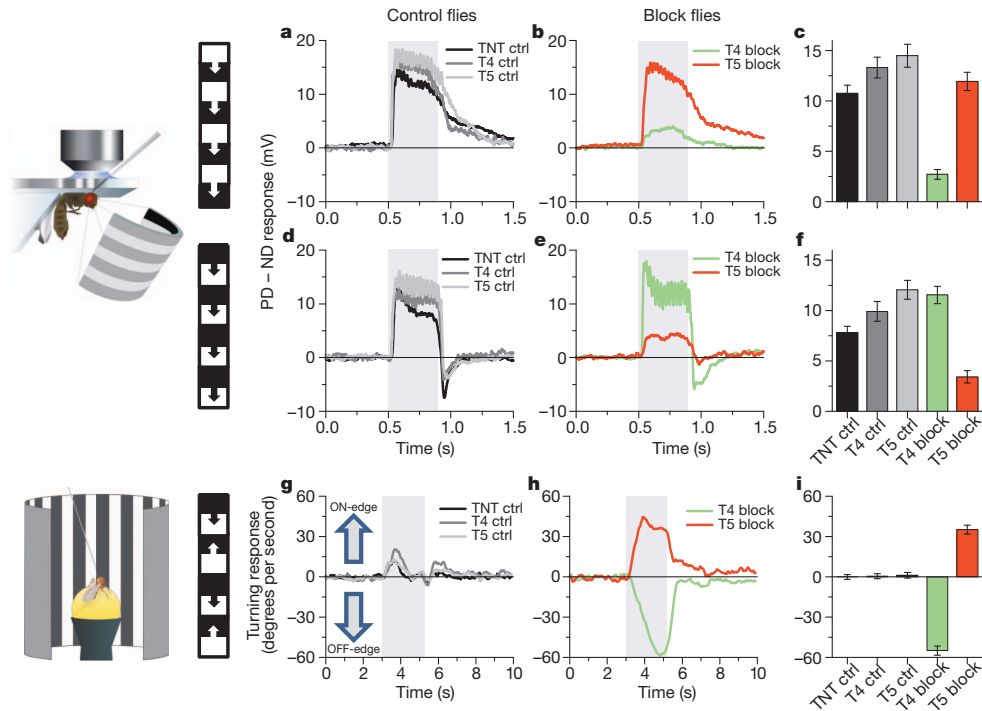


Figure 4 | Voltage responses of lobula plate tangential cells and turning responses of walking flies to moving ON and OFF edges. **a, d,** Average time course of the membrane potential in response to preferred direction motion minus the response to null direction motion (PD – ND response) as recorded in three types of control flies (stimulation period indicated by shaded area). **b, e,** Same as in **a, d**, but recorded in T4-block flies (green) and T5-block flies (red). The stimulus pattern, shown to the left, consisted of multiple ON- (a) or OFF-edges (d). **c, f,** Mean voltage responses (PD – ND) of tangential cells in the five groups of flies. Recordings were done from cells of the vertical²¹ and the horizontal²² system. Because no difference was detected between them, data were pooled. Data comprise recordings from $n = 20$ (TNT control), $n = 12$ (T4 control), $n = 16$ (T5 control), $n = 17$ (T4 block) and $n = 18$ (T5 block) cells. In both T4 and T5-block flies, ON and OFF responses are significantly different

from each other with $P < 0.001$. In T4-block flies, ON responses are significantly reduced compared to all three types of control flies, whereas in T5-block flies, OFF responses are significantly reduced, both with $P < 0.001$. **g,** Average time course of the turning response of three types of control flies to ON and OFF edges moving simultaneously to opposite directions (stimulation period indicated by shaded area). **h,** Same as in **g**, but recorded from T4-block flies (green) and T5-block flies (red). **i,** Mean turning tendency (\pm s.e.m.) during the last second of the stimulation period averaged across all flies within each group. Data comprise average values obtained in $n = 12$ (TNT controls), $n = 11$ (T4 controls), $n = 11$ (T5 controls), $n = 13$ (T4 block) and $n = 12$ (T5 block) flies. Values of T4 and T5-block flies are highly significantly different from zero with $P < 0.001$. Significances indicated are based on two-sample t -test.

motion detection—that is, asymmetric temporal filtering and non-linear interaction—to the neuropile between the axon terminals of lamina neurons L1 and L2 (ref. 28) and the dendrites of directionally selective T4 and T5 cells (Supplementary Fig. 2). The dendrites of T4 and T5 cells might well be the place where signals from neighbouring columns interact in a nonlinear way, similar to the dendrites of starburst amacrine cells of the vertebrate retina²⁹.

METHODS SUMMARY

Flies. Flies used in calcium imaging experiments (Figs 1–3) had the following genotypes: T4/T5 line (w^- ; +/+; *UAS-GCaMP5,R42F06-GAL4/UAS-GCaMP5,R42F06-GAL4*), T4 line (w^- ; +/+; *UAS-GCaMP5,R54A03-GAL4/UAS-GCaMP5,R54A03-GAL4*), T5 line (w^- ; +/+; *UAS-GCaMP5,R42H07-GAL4/UAS-GCaMP5,R42H07-GAL4*). Flies used in electrophysiological and behavioural experiments (Fig. 4) had identical genotypes of the following kind: TNT control flies (w^+/w^+ ; *UAS-TNT-E/UAS-TNT-E*; +/+), T4 control flies (w^+/w^- ; +/+; *VT37588-GAL4/+*), T5 control flies (w^+/w^- ; +/+; *R42H07-GAL4/+*), T4-block flies (w^+/w^- ; *UAS-TNT-E/+*; *VT37588-GAL4/+*), T5-block flies (w^+/w^- ; *UAS-TNT-E/+*; *R42H07-GAL4/+*).

Two-photon microscopy. We used a custom-built two-photon laser scanning microscope²⁹ equipped with a $\times 40$ water immersion objective and a mode locked Ti:sapphire laser. To shield the photomultipliers from the stimulus light, two separate barriers were used: the first was placed directly over the LEDs, the second extended from the fly holder over the arena. Images were acquired at a resolution of 256×256 pixels and a frame rate of 1.87 Hz, except where indicated, using ScanImage software³⁰.

Electrophysiology. Recordings were established under visual control using a Zeiss Microscope and a $\times 40$ water immersion objective.

Behavioural analysis. The locomotion recorder was custom-designed according to ref. 18. It consisted of an air-suspended sphere floating in a bowl-shaped sphere holder. Motion of the sphere was recorded by two optical tracking sensors.

Visual stimulation. For calcium imaging and electrophysiological experiments, we used a custom-built LED arena covering 180° and 90° of the visual field along the horizontal and the vertical axis, respectively, at 1.5° resolution. For the behavioural experiments, three 120-Hz LCD screens formed a U-shaped visual arena with the fly in the centre, covering 270° and 114° of the visual field along the horizontal and the vertical axes, respectively, at 0.1° resolution.

Data evaluation. Data were evaluated off-line using custom-written software (Matlab and IDL).

Full Methods and any associated references are available in the online version of the paper.

Received 16 April; accepted 20 May 2013.

- Bausenwein, B., Dittrich, A. P. M. & Fischbach, K. F. The optic lobe of *Drosophila melanogaster* II. Sorting of retinotopic pathways in the medulla. *Cell Tissue Res.* **267**, 17–28 (1992).
- Akerboom, J. *et al.* Optimization of a GCaMP calcium indicator for neural activity imaging. *J. Neurosci.* **32**, 13819–13840 (2012).
- Cajal, S. R. & Sanchez, D. *Contribucion al conocimiento de los centros nerviosos de los insectos* (Imprenta de Hijos de Nicholas Moja, 1915).
- Strausfeld, N. J. *Atlas of an Insect Brain* (Springer, 1976).
- Fischbach, K. F. & Dittrich, A. P. M. The optic lobe of *Drosophila melanogaster*. I. A Golgi analysis of wild-type structure. *Cell Tissue Res.* **258**, 441–475 (1989).

6. Reichardt, W. Autocorrelation, a principle for the evaluation of sensory information by the central nervous system. In *Sensory Communication* (ed. Rosenblith, W. A.) 303–317 (MIT Press and John Wiley & Sons, 1961).
7. Borst, A., Haag, J. & Reiff, D. F. Fly motion vision. *Annu. Rev. Neurosci.* **33**, 49–70 (2010).
8. Buchner, E., Buchner, S. & Buelthoff, I. Deoxyglucose mapping of nervous activity induced in *Drosophila* brain by visual movement. 1. Wildtype. *J. Comp. Physiol. A* **155**, 471–483 (1984).
9. Strausfeld, N. J. & Lee, J. K. Neuronal basis for parallel visual processing in the fly. *Vis. Neurosci.* **7**, 13–33 (1991).
10. Schnell, B., Raghu, V. S., Nern, A. & Borst, A. Columnar cells necessary for motion responses of wide-field visual interneurons in *Drosophila*. *J. Comp. Physiol. A* **198**, 389–395 (2012).
11. Douglass, J. K. & Strausfeld, N. J. Visual motion-detection circuits in flies: Parallel direction- and non-direction-sensitive pathways between the medulla and lobula plate. *J. Neurosci.* **16**, 4551–4562 (1996).
12. Franceschini, N., Riehle, A. & Le Nestour, A. Directionally selective motion detection by insect neurons. In *Facets of Vision* (ed. Stavenha, H.) 360–390 (Springer, 1989).
13. Joesch, M., Schnell, B., Raghu, S. V., Reiff, D. F. & Borst, A. ON and OFF pathways in *Drosophila* motion vision. *Nature* **468**, 300–304 (2010).
14. Pfeiffer, B. D. *et al.* Tools for neuroanatomy and neurogenetics in *Drosophila*. *Proc. Natl Acad. Sci. USA* **105**, 9715–9720 (2008).
15. Denk, W., Strickler, J. H. & Webb, W. W. Two-photon laser scanning fluorescence microscopy. *Science* **248**, 73–76 (1990).
16. Oyster, C. W. & Barlow, H. B. Direction-selective units in rabbit retina: distribution of preferred directions. *Science* **155**, 841–842 (1967).
17. Sweeney, S. T., Broadie, K., Keane, J., Niemann, H. & O’Kane, C. J. Targeted expression of tetanus toxin light chain in *Drosophila* specifically eliminates synaptic transmission and causes behavioral defects. *Neuron* **14**, 341–351 (1995).
18. Seelig, J. D. *et al.* Two-photon calcium imaging from head-fixed *Drosophila* during optomotor walking behavior. *Nature Methods* **7**, 535–540 (2010).
19. Clark, D. A., Bursztyn, L., Horowitz, M. A., Schnitzer, M. J. & Clandinin, T. R. Defining the computational structure of the motion detector in *Drosophila*. *Neuron* **70**, 1165–1177 (2011).
20. Egelhaaf, M. & Borst, A. Calcium accumulation in visual interneurons of the fly: Stimulus dependence and relationship to membrane potential. *J. Neurophysiol.* **73**, 2540–2552 (1995).
21. Joesch, M., Plett, J., Borst, A. & Reiff, D. F. Response properties of motion-sensitive visual interneurons in the lobula plate of *Drosophila melanogaster*. *Curr. Biol.* **18**, 368–374 (2008).
22. Schnell, B. *et al.* Processing of horizontal optic flow in three visual interneurons of the *Drosophila* brain. *J. Neurophysiol.* **103**, 1646–1657 (2010).
23. Borst, A. & Egelhaaf, M. Direction selectivity of fly motion-sensitive neurons is computed in a two-stage process. *Proc. Natl Acad. Sci. USA* **87**, 9363–9367 (1990).
24. Single, S., Haag, J. & Borst, A. Dendritic computation of direction selectivity and gain control in visual interneurons. *J. Neurosci.* **17**, 6023–6030 (1997).
25. Eichner, H., Joesch, M., Schnell, B., Reiff, D. F. & Borst, A. Internal structure of the fly elementary motion detector. *Neuron* **70**, 1155–1164 (2011).
26. Joesch, M., Weber, F., Eichner, H. & Borst, A. Functional specialization of parallel motion detection circuits in the fly. *J. Neurosci.* **33**, 902–905 (2013).
27. Egelhaaf, M. & Borst, A. Are there separate ON and OFF channels in fly motion vision? *Vis. Neurosci.* **8**, 151–164 (1992).
28. Takemura, S. Y., Lu, Z. & Meinertzhagen, I. A. Synaptic circuits of the *Drosophila* optic lobe: the input terminals to the medulla. *J. Comp. Neurol.* **509**, 493–513 (2008).
29. Euler, T., Detwiler, P. B. & Denk, W. Directionally selective calcium signals in dendrites of starburst amacrine cells. *Nature* **418**, 845–852 (2002).
30. Pologruto, T. A., Sabatini, B. L. & Svoboda, K. ScanImage: Flexible software for operating laser scanning microscopes. *Biomed. Eng. Online* **2**, 13 (2003).

Supplementary Information is available in the online version of the paper.

Acknowledgements We thank L. Looger, J. Simpson, V. Jayaraman and the Janelia GECI team for making and providing us with the GCaMP5 flies before publication; J. Plett for designing and engineering the LED arena; C. Theile, W. Essbauer and M. Sauter for fly work; and A. Mauss, F. Gabbiani and T. Bonhoeffer for critically reading the manuscript. This work was in part supported by the Deutsche Forschungsgemeinschaft (SFB 870). M.S.M., G.A., E.S., M.M., A.L., A.Ba and A.Bo are members of the Graduate School of Systemic Neurosciences.

Author Contributions M.S.M. and J.H. jointly performed and, together with A.Bo., evaluated all calcium imaging experiments. G.A., E.S. and M.M. recorded from tangential cells. A.L., T.S. and A.Ba. performed the behavioural experiments. G.R., B.D. and A.N. generated the driver lines and characterized their expression pattern. D.F.R. performed preliminary imaging experiments. E.H. helped with programming and developed the PMT shielding for the two-photon microscope. A.Bo. designed the study and wrote the manuscript with the help of all authors.

Author Information Reprints and permissions information is available at www.nature.com/reprints. The authors declare no competing financial interests. Readers are welcome to comment on the online version of the paper. Correspondence and requests for materials should be addressed to A.Bo. (borst@neuro.mpg.de).

METHODS

Flies. Flies were raised on standard cornmeal-agar medium at 25 °C and 60% humidity throughout development on a 12 h light/12 h dark cycle. For calcium imaging, we used the genetically encoded single-wavelength indicator GCaMP5, variant G, with the following mutations: T302L, R303P and D380Y (ref. 2). Expression of GCaMP5 was directed by three different Gal4 lines, all from the Janelia Farm collection¹⁴. Flies used in calcium imaging experiments (Figs 1–3) had the following genotypes: T4/T5 line ($w^-/+;$ $UAS-GCaMP5,R42F06-GAL4/UAS-GCaMP5,R42F06-GAL4$), T4 line ($w^-/+;$ $UAS-GCaMP5,R54A03-GAL4/UAS-GCaMP5,R54A03-GAL4$), T5 line ($w^-/+;$ $UAS-GCaMP5,R42H07-GAL4/UAS-GCaMP5,R42H07-GAL4$). All driver lines were generated by the methods described in ref. 14 and were identified by screening a database of imaged lines, followed by reimaging of selected lines³¹. As homozygous for both the Gal4-driver and the $UAS-GCaMP5$ genes, T4 flies also showed some residual expression in T5 cells, and T5 flies also in T4 cells. This unspecific expression, however, was in general less than 25% of the expression in the specific cells. Flies used in electrophysiological and behavioural experiments (Fig. 4) had identical genotypes of the following kind: TNT control flies ($w^+/w^+;$ $UAS-TNT-E/UAS-TNT-E$; $+/+$), T4 control flies ($w^+/w^+;$ $+/+$; $VT37588-GAL4/+$), T5 control flies ($w^+/w^+;$ $+/+$; $R42H07-GAL4/+$), T4-block flies ($w^+/w^+;$ $UAS-TNT-E/+;$ $VT37588-GAL4/+$), T5-block flies ($w^+/w^+;$ $UAS-TNT-E/+;$ $R42H07-GAL4/+$). $UAS-TNT-E$ flies were derived from the Bloomington Stock Center (stock no. 28837) and $VT37588-GAL4$ flies were derived from the VDRC (stock no. 205893). Before electrophysiological experiments, flies were anaesthetized on ice and waxed on a Plexiglas holder using bees wax. The dissection of the fly cuticle and exposure of the lobula plate were performed as described previously (for imaging experiments, see ref. 32; for electrophysiology, see ref. 21). Flies used in behavioural experiments were taken from 18 °C just before the experiment and immediately cold-anaesthetized. The head, the thorax and the wings were glued to a needle using near-ultraviolet bonding glue (Sinfony Opaque Dentin) and strong blue LED light (440 nm, dental curing-light, New Woodpecker).

Two-photon microscopy. We used a custom-built two-photon laser scanning microscope³³ equipped with a $\times 40$ water immersion objective (0.80 NA, IR-Achroplan; Zeiss). Fluorescence was excited by a mode locked Ti:sapphire laser (<100 fs, 80 MHz, 700–1,020 nm; pumped by a 10 W CW laser; both Mai Tai; Spectraphysics) with a DeepSee accessory module attached for dispersion compensation control resulting in better pulse compression and fluorescence at the target sample. Laser power was adjusted to 10–20 mW at the sample, and an excitation wavelength of 910 nm was used. The photomultiplier tube (H10770PB-40, Hamamatsu) was equipped with a dichroic band-pass mirror (520/35, Brightline). Images were acquired at a resolution of 256×256 pixels and a frame rate of 1.87 Hz, except in Fig. 2 (7.5 Hz), using the ScanImage software³⁰.

Electrophysiology. Recordings were established under visual control using a $\times 40$ water immersion objective (LumplanF, Olympus), a Zeiss microscope (Axiotech vario 100, Zeiss), and illumination (100 W fluorescence lamp, hot mirror, neutral density filter OD 0.3; all from Zeiss). To enhance tissue contrast, we used two polarization filters, one located as an excitation filter and the other as an emission filter, with slight deviation on their polarization plane. For eye protection, we additionally used a 420-nm LP filter on the light path.

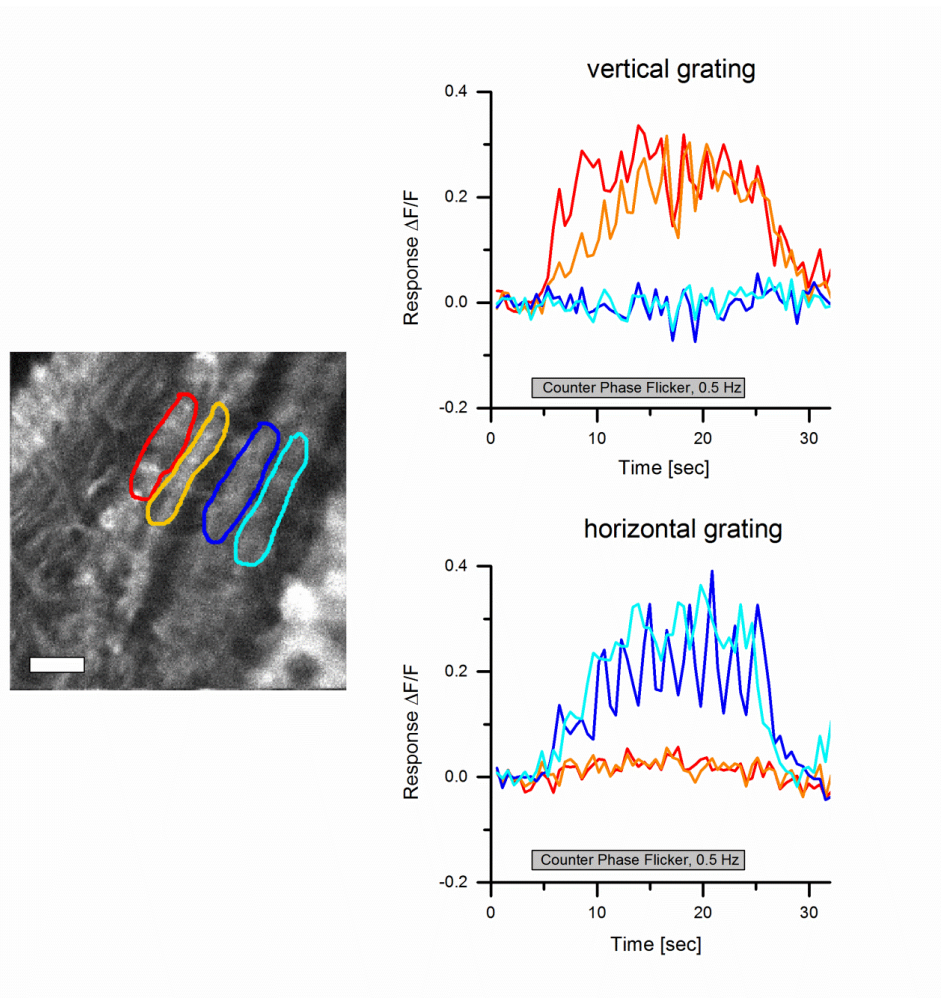
Behavioural analysis. The locomotion recorder was custom-designed according to ref. 18. Briefly, it consists of an air-suspended sphere floating in a bowl-shaped sphere holder. A high-power infrared LED (800 nm, JET series, 90 mW, Roithner Electronics) is located in the back to illuminate the fly and the sphere surface. Two optical tracking sensors are equipped with lens and aperture systems to focus on the sphere behind the fly. The tracking data are processed at 4 kHz internally, read out via a USB interface and processed by a computer at ≈ 200 Hz. This allows real-time calculation of the instantaneous rotation axis of the sphere. A third camera (GRAS-20S4M-C, Point Grey Research) is located in the back which is essential for proper positioning of the fly and allows real-time observation and video recording of the fly during experiments.

Visual stimulation. For calcium imaging and electrophysiological experiments, we used a custom-built LED arena that allowed refresh rates of up to 550 Hz and 16 intensity levels. It covered 180° (1.5° resolution) and 90° (1.5° resolution) of the visual field along the horizontal and the vertical axis, respectively. The LED arena was engineered and modified based upon ref. 34. The LED array consists of 7×4 individual TA08-81GWA dot-matrix displays (Kingbright), each harbouring 8×8 individual green (568 nm) LEDs. Each dot-matrix display is controlled by an ATmega168 microcontroller (Atmel) combined with a ULN2804 line driver (Toshiba America) acting as a current sink. All panels are in turn controlled via an I2C interface by an ATmega128 (Atmel)-based main controller board, which reads in pattern information from a compact flash (CF) memory card. Matlab was used for programming and generation of the patterns as well as for sending the serial command sequences via RS-232 to the main controller board. The

luminance range of the stimuli was $0.5\text{--}33\text{ cd m}^{-2}$. For the calcium imaging experiments, two separate barriers were used to shield the photomultipliers from the stimulus light coming from the LED arena. The first was a spectral filter with transparency to wavelengths >540 nm placed directly over the LEDs (ASF SFG 10, Microchemicals). The second was a layer of black PVC extending from the fly holder over the arena. Square wave gratings had a spatial wavelength of 30° of visual angle and a contrast of 88%. Unless otherwise stated, they were moving at 30° s^{-1} . Edges had the same contrast and were also moving at 30° s^{-1} . For the experiments shown in Figs 1, 2b and 3, each grating or edge motion was shown twice within a single sweep, resulting in a total of eight stimulation periods. Each stimulus period lasted 4 s, and subsequent stimuli were preceded by a 3-s pause. In the experiment shown in Fig. 2a, a dark edge of 88% contrast was moved for 1 s at 15° s^{-1} from the front to the back at three different positions (22° , 44° , 66° , from frontal to lateral). At each position, edge motion was repeated 15 times. For the experiment shown in Fig. 2b, a bright edge of 88% contrast was moving at 15° s^{-1} from the back to the front, and images were acquired at a frame rate of 7.5 Hz. For the experiments shown in Figs 3e, f, all six stimulus velocities were presented once within one sweep, with the stimulus lasting 4 s, and different stimuli being separated by 2 s. In the experiments shown in Figs 3g, h, a single sweep contained all 12 grating orientations with the same stimulus and pause length as above. For the electrophysiology experiments (Fig. 4a–f), multiple edges were used as stimuli moving simultaneously at 50° s^{-1} . To stimulate cells of horizontal system (HS cells), a vertical, stationary square-wave grating with 45° spatial wavelength was presented. For ON-edge motion, the right (preferred direction, PD) or the left edge (null direction, ND) of each light bar started moving until it merged with the neighbouring bar. For OFF-edge motion, the right or the left edge of each dark bar was moving. To stimulate cells of the vertical system (VS cells), the pattern was rotated by 90° clockwise. For the behavioural experiments (Fig. 4g–i), three 120-Hz LCD screens (Samsung 2233 RZ) were vertically arranged to form a U-shaped visual arena ($w = 31\text{ cm} \times d = 31\text{ cm} \times h = 47\text{ cm}$) with the fly in the centre. The luminance ranged from 0 to 131 cd m^{-2} and covered large parts of the flies' visual field (horizontal, $\pm 135^\circ$; vertical, $\pm 57^\circ$; resolution, $<0.1^\circ$). The three LCD screens were controlled via NVIDIA 3D Vision Surround Technology on Windows 7 64-bit allowing a synchronized update of the screens at 120 frames per second. Visual stimuli were created using Panda3D, an open-source gaming engine, and Python 2.7, which simultaneously controlled the frame rendering in Panda3D, read out the tracking data and temperature and streamed data to the hard disk. The balanced motion stimulus consisted of a square-wave grating with 45° spatial wavelength and a contrast of 63%. Upon stimulation onset, dark and bright edges moved into opposite directions at 10° s^{-1} for 2.25 s. This stimulation was performed for both possible edge directions and two initial grating positions shifted by half a wavelength, yielding a total of four stimulus conditions.

Data evaluation. Data were evaluated off-line using custom-written software (Matlab and IDL). For the images shown in Figs 1e, f, 2a and 3a, b, the raw image series was converted into four images representing the relative fluorescence change during each direction of grating motion: $(\Delta F/F)_{\text{stim}} = (F_{\text{stim}} - F_{\text{ref}})/F_{\text{ref}}$. The image representing the stimulus fluorescence (F_{stim}) was obtained by averaging all images during stimulation; the image representing the reference fluorescence (F_{ref}) was obtained by averaging three images before stimulation. Both images were smoothed using a Gaussian filter of 10 pixel half-width. For the images shown in Figs 1f and 3a, b, $\Delta F/F$ images were normalized by their maximum value. Then, a particular colour was assigned to each pixel according to the stimulus direction during which it reached maximum value, provided it passed a threshold of 25%. Otherwise, it was assigned to background. The response strength of each pixel was coded as the saturation of that particular colour. For the data shown in Figs 2b, c and 3c–h, the raw image series was first converted into a $\Delta F/F$ series by using the first three images as reference. Then, a region was defined within a raw image, and average $\Delta F/F$ values were determined within that region for each image, resulting in a $\Delta F/F$ signal over time. Responses were defined as the maximum $\Delta F/F$ value reached during each stimulus presentation minus the average $\Delta F/F$ value during the two images preceding the stimulus. For the bar graphs shown in Fig. 4c, f, the average voltage responses during edge motion (0.45 s) along the cell's preferred (PD) and null direction (ND) were calculated. For each recorded tangential cell, the difference between the PD and the ND response was determined, and these values were averaged across all recorded cells. The data shown in Fig. 4g, h were obtained from the four stimulus conditions by averaging the turning responses for the two starting positions of the grating and calculating the mean difference between the turning responses for the two edge directions. For the bar graph shown in Fig. 4i, the average turning response of each fly during the last second of balanced motion stimulation was calculated. These values were averaged across all recorded flies within each genotype.

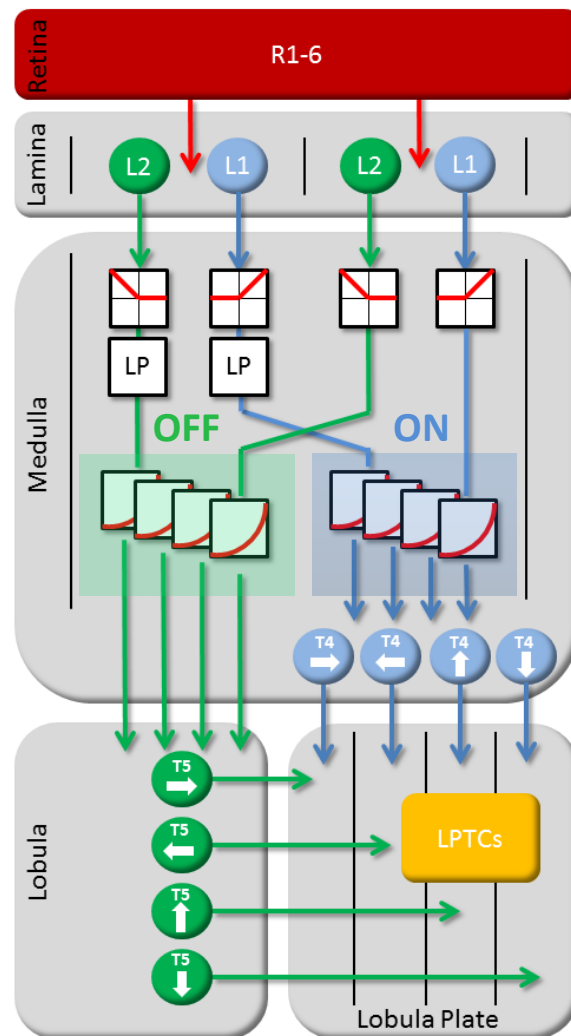
31. Jenett, A. *et al.* A Gal4-driver line resource for *Drosophila* neurobiology. *Cell Rep.* **2**, 991–1001 (2012).
32. Reiff, D. F., Plett, J., Mank, M., Griesbeck, O. & Borst, A. Visualizing retinotopic half-wave rectified input to the motion detection circuitry of *Drosophila*. *Nature Neurosci.* **13**, 973–978 (2010).
33. Euler, T. *et al.* Eyecup scope—optical recording of light stimulus-evoked fluorescence signals in the retina. *Pflüger Arch.* **457**, 1393–1414 (2009).
34. Reiser, M. B. & Dickinson, M. H. A modular display system for insect behavioral neuroscience. *J. Neurosci. Methods* **167**, 127–139 (2008).



Supplemental Fig.1 Responses of T4 and T5 cells to counter-phase flicker. Square-wave gratings (15 deg spatial wavelength and 88% contrast) with vertical (top) and horizontal (bottom) orientation were phase-shifted every second by 180 deg for 20 seconds. Response traces are derived from the region of interest encircled in the image to the left with the same color from a single stimulation period. T4 and T5 cells in layers 1 and 2 only respond to the vertical grating, cells in layers 3 and 4 selectively respond to the horizontal grating. Similar results were obtained in n=4 flies. Scale bar = 5 μ m. Together with the missing response of T4 and T5 cells to full-field flicker, these findings suggest that T4 and T5 cells receive input signals from neurons with different orientation tuning, depending on whether they respond to motion along the horizontal (layers 1 and 2) or the vertical (layers 3 and 4) axis^{1,2}.

1 Pick, B. & Buchner, E. Visual movement detection under light- and dark-adaptation in the fly, *Musca domestica*. *J. Comp. Physiol.* **134**, 45-54 (1979).

2 Srinivasan, M.V. & Dvorak, D.R. Spatial processing of visual information in the movement-detecting pathway of the fly. *J. Comp. Physiol.* **140**, 1-23 (1980).



Supplemental Fig.2 Circuit diagram of the fly elementary motion detector. Visual input from photoreceptors R1-6 is split into parallel pathways, L1 and L2, at the level of the lamina. Two neighboring columns are shown. The outputs from both L1 and L2 are half-wave rectified, such that downstream elements carry information about ON (L1-pathway) and OFF (L2-pathway) signals separately. After temporal low-pass filtering ('LP') the signals from one column, they interact in a supra-linear way with the instantaneous signals derived from the other column. This interaction takes place, separately in both pathways, along all four cardinal directions. Directionally selective signals are carried via T4 and T5 cells to the four layers of the lobula plate where T4 and T5 cells with the same preferred direction converge again on the dendrites of the tangential cells ('LPTCs').

2.2 NEURAL CIRCUIT COMPONENTS OF THE *drosophila* OFF MOTION VISION PATH- WAY

In this publication ([Meier et al., 2014](#)) we examined the response properties and functional roles of two columnar cell types in the lamina and the medulla. It appeared in *Current Biology* in February 2014.

Based on morphological evidence, a direction specific role for lamina neurons L4 and transmedullary neurons Tm2 had been proposed. Using two-photon calcium imaging, we probed the functional characteristics of these two cell types. Presenting shifting gratings and edges of either polarity we found that both cell types are excited by brightness decrements moving in any direction. Moreover, while their spatial receptive fields were similar, L4 appeared to integrate dark signals over large areas, whereas Tm2 seemed to be subject to lateral inhibition. Investigating their temporal properties revealed fast, transient kinetics for Tm2 and slower, more sustained responses for L4. We then tested their necessity for the processing of visual motion by recording from motion sensitive lobula plate tangential cells while blocking the synaptic output of either L4 or Tm2. Here, we observed that responses to OFF edges were selectively reduced in both genotypes. From these data we concluded that both L4 and Tm2 cells were crucially involved in the detection of moving dark edges and that they contribute different spatial and temporal filters to this computation.

Summary

The following people contributed to this work:

Matthias Meier¹, Etienne Serbe¹, **Matthew S. Maisak**, Jürgen Haag, Barry J. Dickson, and Alexander Borst

Matthias Meier, Etienne Serbe and Alexander Borst designed the study. Matthias Meier and Etienne Serbe performed electrophysiological recordings. Matthias Meier, Etienne Serbe, **Matthew S. Maisak**, and Jürgen Haag performed calcium imaging experiments. Barry J. Dickson provided unpublished Gal4-lines. Matthias Meier, Etienne Serbe and Alexander Borst wrote the paper

Author contribution

with help of the other authors.

¹ equal contribution

Neural Circuit Components of the *Drosophila* OFF Motion Vision Pathway

Matthias Meier,^{1,3} Etienne Serbe,^{1,3} Matthew S. Maisak,¹ Jürgen Haag,¹ Barry J. Dickson,^{2,4} and Alexander Borst^{1,*}

¹Department of Circuits-Computation-Models, Max Planck Institute of Neurobiology, Am Klopferspitz 18, 82152 Martinsried, Germany

²Research Institute of Molecular Pathology, Dr. Bohr-Gasse 7, 1030 Vienna, Austria

Summary

Background: Detecting the direction of visual motion is an essential task of the early visual system. The Reichardt detector has been proven to be a faithful description of the underlying computation in insects. A series of recent studies addressed the neural implementation of the Reichardt detector in *Drosophila* revealing the overall layout in parallel ON and OFF channels, its input neurons from the lamina (L1 → ON, and L2 → OFF), and the respective output neurons to the lobula plate (ON → T4, and OFF → T5). While anatomical studies showed that T4 cells receive input from L1 via Mi1 and Tm3 cells, the neurons connecting L2 to T5 cells have not been identified so far. It is, however, known that L2 contacts, among others, two neurons, called Tm2 and L4, which show a pronounced directionality in their wiring.

Results: We characterized the visual response properties of both Tm2 and L4 neurons via Ca²⁺ imaging. We found that Tm2 and L4 cells respond with an increase in activity to moving OFF edges in a direction-unselective manner. To investigate their participation in motion vision, we blocked their output while recording from downstream tangential cells in the lobula plate. Silencing of Tm2 and L4 completely abolishes the response to moving OFF edges.

Conclusions: Our results demonstrate that both cell types are essential components of the *Drosophila* OFF motion vision pathway, prior to the computation of directionality in the dendrites of T5 cells.

Introduction

The computation of motion is imperative for fundamental behaviors such as mate or prey detection, predator avoidance, and visual navigation. In the fruit fly *Drosophila*, motion cues are processed in the optic lobe, a brain area comprised of the lamina, medulla, lobula, and lobula plate, each arranged in a columnar, retinotopic fashion. Whereas photoreceptors respond to motion in a nondirectional way, wide-field tangential cells of the lobula plate depolarize to motion in their preferred direction (PD) and hyperpolarize to motion in the opposite or null direction (ND) [1, 2]. These direction-selective responses are well characterized by a mathematical model, the so-called Reichardt detector. In this model, signals from neighboring photoreceptors are multiplied after asymmetric

temporal filtering [3–5]. Due to the anatomical complexity and miniscule size of the columnar neurons of the optic lobe, identification of the neural elements of the motion detection circuit has long proven difficult.

In agreement with previous suggestions based on costratification of Golgi-stained columnar cells [6, 7] and cell-unspecific activity labeling using the deoxyglucose method [8], recent studies identified two parallel motion processing streams, one leading from lamina neuron L1 via T4 cells and the other from lamina neuron L2 via T5 onto the dendrites of the tangential cells [9, 10]. Within each pathway, four subpopulations of T4 and T5 cells are tuned to one of the four cardinal directions (front to back, back to front, upward, or downward), providing direction-selective signals to four different sublayers of the lobula plate [11, 12]. Here, they become spatially integrated on the dendrites of tangential cells [12, 13]. The two pathways are functionally segregated with regard to their selectivity for contrast polarity: the L1 pathway is selectively responsive to the motion of brightness increments (ON pathway), while the L2 pathway responds selectively to the motion of brightness decrements (OFF pathway) [10, 12, 14–16]. These findings suggest that important processing steps of motion computation take place between the axon terminals of L1/L2 and the output regions of T4/T5.

For the ON pathway, a recent connectomic EM study of the fly medulla [17] not only identified two neurons, Mi1 and Tm3, as the most prominent postsynaptic targets of L1, but also showed that these cells make up for more than 90% of all input synapses on the dendrites of T4 cells. Most interestingly, the innervation of Tm3 and Mi1 on a single T4 cell is asymmetric, consistent with the preferred direction of the T4 cell, i.e., the lobula plate layer where it terminates. Because connectomic analysis has not yet reached the lobula, where the dendrites of T5 cells reside [6], the connectivity for the OFF pathway is known only within the lamina and the medulla [17–22]. Here, several cell types have been found to be postsynaptic to L2 [17, 18], i.e., L4, Tm1, and Tm2. Tm1 and Tm2 both receive synaptic input from L2 in the second layer of the medulla [17, 18] projecting to the first layer of the lobula. Within the lamina, L4 sends its processes into three neighboring columns, one into its “home” column and two into the two neighboring posterior columns [19, 20]. Within each of these columns, L4 forms reciprocal connections with L2 and with the processes of those L4s originating from other columns [19–22]. In its home column, L4 receives additional synaptic input from a lamina amacrine cell, as well as from photoreceptor R6 [21, 22], which might explain why blocking synaptic output from L2 leaves the visual responses of L4 intact [23]. Within the medulla, L4 synapses onto three Tm2 cells, one located in the home column and two in the adjacent columns located posterior in visual space [17, 18] (Figure 1A; for illustration purposes, only two neighboring columns are depicted). Based on their connectivity and anatomical layout, there are two plausible hypotheses for these cells’ role in the motion detection circuit. First, Tm2 could exhibit a directional tuning for OFF motion from the front to the back, as suggested by the asymmetrical wiring between L4 and Tm2 [18]. Alternatively, Tm2 could act as one of the two input arms of the elementary OFF motion detector. In this case, Tm2 would reveal a preference for moving

³These authors contributed equally to this work

⁴Present address: Janelia Farm Research Campus, 19700 Helix Drive, Ashburn, VA 20147, USA

*Correspondence: borst@neuro.mpg.de



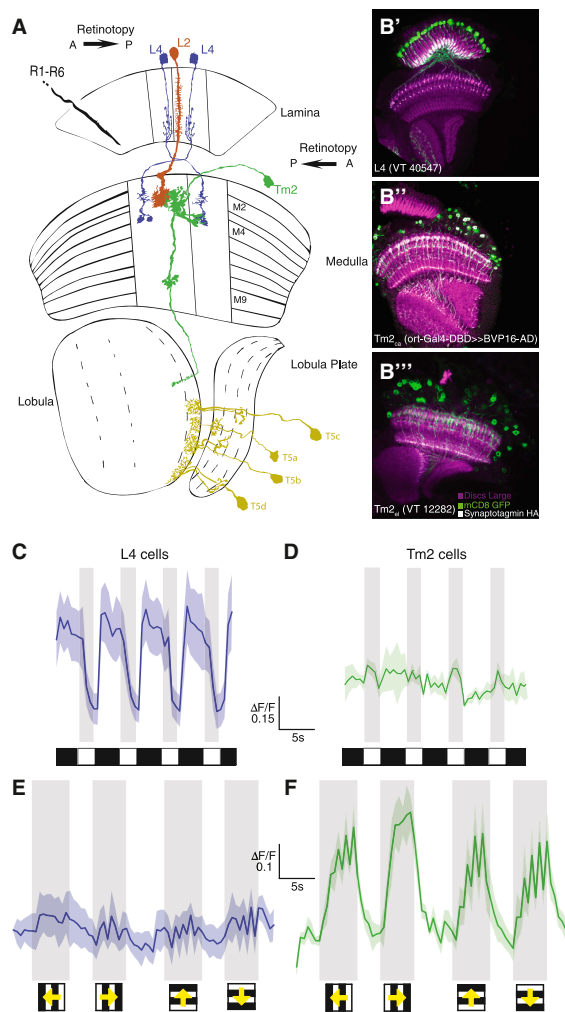


Figure 1. Wiring Diagram and Basic Response Properties of L4 and Tm2
 (A) Photoreceptors (R1–R6) synapse onto the lamina monopolar cells L2 (red) and L4 (blue). These two cell types are connected in an intercolumnar and reciprocal manner in the lamina. Both give input to the transmedulla neuron Tm2 (green) in their home column. Additionally, two L4 cells from posterior columns are presynaptic to Tm2, with axonal output regions coinciding with T5 dendrites in the lobula. Adapted and modified from [6, 18].
 (B) Confocal images of the Gal4-driver lines used in this study, shown in horizontal cross-sections. Neurons are marked in green (mCD8-GFP expression), neuropils in magenta (antibody against Dlg), and synaptic output regions in white (antibody against HA, bound to synaptotagmin). L4 (B') and Tm2_{ca} (B'') lines were used for Ca²⁺ imaging. L4 (B') and Tm2_{el} (B''') lines were used for blocking experiments.
 (C and D) Average relative change of fluorescence in response to four full-field flicker stimuli in L4 (C; n = 7) and Tm2 (D; n = 5) terminals (±SEM).
 (E and F) Mean responses of L4 (E; n = 7) and Tm2 (F; n = 8) to square-wave gratings moving in all four cardinal directions at 30° s⁻¹.
 (C–F) Grey-shaded areas indicate the stimulation period. For Tm2, responses to vertical motion are slightly but significantly smaller than to horizontal motion (p < 0.015).

OFF edges, but its responses would be nondirectional; direction selectivity would only arise after a multiplicative interaction of the two input signals on the dendrites of T5 cells.

Functional analysis using behavioral readouts during selective blockade of L4 arrived at controversial conclusions: while one study found no impairment of motion-dependent behavior after silencing of L4 [23], another study observed a specific deficit in L4 block flies to detect motion from the front to the back, consistent with the first of the above hypotheses, as well as to detect moving OFF edges, consistent with the second hypothesis [24].

To probe these cells' specificity for OFF motion and their potential direction selectivity, we analyzed the visual response properties of Tm2 and L4 using Ca²⁺ imaging. Both Tm2 and L4 are excited exclusively by moving OFF edges, albeit in a non-directional way. Both cells have a bell-shaped receptive field with a half width of approximately 5°. While L4 exhibits rather linear spatial integration properties and responds to changes in full-field luminance, Tm2 becomes inhibited by stimuli of increasing size. To investigate the participation of L4 and Tm2 in motion processing, we recorded the motion responses from wide-field tangential cells, instead of using a behavioral readout. When synaptic output from either Tm2 or L4 was blocked, responses of LPTCs to moving OFF edges are eliminated, demonstrating their crucial role in the OFF pathway of *Drosophila* motion vision.

Results

To investigate the visual response properties of L4 and Tm2, we used cell-specific Gal4 driver lines. To verify these lines' specificity, we drove the expression of membrane-bound GFP and the hemagglutinin (HA)-tagged presynaptic marker protein synaptotagmin. We then antibody stained against GFP and HA, allowing us to compare the labeling with the branching as known from Golgi studies (GFP), as well as to determine the synaptic output layers (synaptotagmin). The L4 line shows specific expression of GFP within the optic lobe that is characteristic for this cell. Synaptotagmin staining of the line indicates synaptic output in the distal portion of the lamina and the second and fourth layer of the medulla, which is in agreement with previous Golgi and electron microscopy studies (Figure 1B') [6, 17, 18]. Both of our Tm2 driver lines showed a specific, Tm2-characteristic expression within the optic lobe and similar synaptotagmin staining, labeling the ninth layer of the medulla and the first layer of the lobula (Figures 1B'' and B'''). The strong synaptotagmin staining in the first layer of the lobula suggests that this is also an output region of Tm2 where it could provide input to T5.

Visual Response Properties of L4 and Tm2

To optically record from these cells using two-photon microscopy [25], we used the Tm2_{ca} and L4 driver lines and crossed them with UAS-GCaMP5. To investigate how whole-field brightness changes are encoded in the terminals of both L4 and Tm2, we presented four spatially uniform bright pulses of light, each lasting for 2 s, interleaved by 4 s, and measured the change in fluorescence of individual L4 terminals in the second layer of the medulla and Tm2 terminals in the first layer of the lobula. In L4, the activity follows the full-field luminance in an almost tonic way, such that the lowest brightness level leads to the strongest response (Figure 1C). In contrast to L4, Tm2 does not respond to full-field luminance changes (Figure 1D). In order to test whether direction selectivity is already

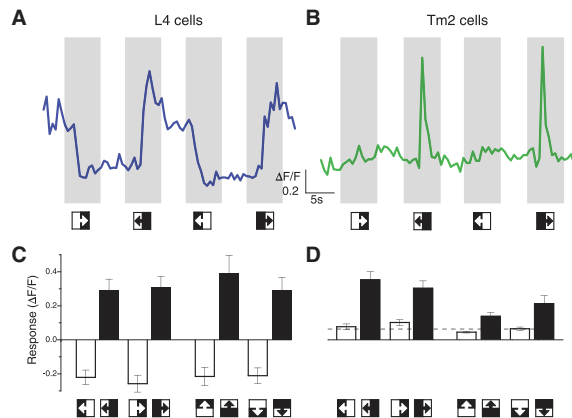


Figure 2. L4 and Tm2 Responses to Moving Edges
(A and B) Single-cell response traces of L4 (A) and Tm2 (B) to horizontally moving edges of either polarity. Stimulation period is indicated by the shaded area.
(C and D) Mean responses of L4 (C; $n = 10$) and Tm2 (D; $n = 12$) to ON (white bars) and OFF (black bars) edges moving at 30° s^{-1} . Chance response level is indicated by the dashed line (see the [Experimental Procedures](#)). Error bars indicate \pm SEM. For Tm2, responses to OFF edges moving in the vertical direction are significantly smaller than those for the horizontal direction ($p < 0.01$).
See also [Figure S3](#).

present at the level of Tm2 or L4, we presented square-wave gratings moving in the four cardinal directions (back to front, front to back, upward, and downward). L4 responds with only small modulations in activity to square-wave motion ([Figure 1E](#)). In striking difference to L4, Tm2 responds strongly to gratings moving in all directions. Contradicting the hypothesis based on the asymmetric wiring in the medulla [18], Tm2 shows no directional preference, responding to gratings moving in all directions in a similar way, albeit with a somewhat smaller amplitude to vertical than to horizontal motion ([Figure 1F](#)).

Anatomical evidence has implicated both Tm2 and L4 as being postsynaptic to L2 and, thus, as potential elements in the OFF motion pathway [17, 18]. Therefore, we tested their sensitivity to the contrast polarity of moving edges. We presented either bright or dark edges, each moving in all four cardinal directions. Interestingly, L4 and Tm2 respond with quite different dynamics, as exemplified in single-cell traces in response to horizontal edge motion ([Figures 2A and 2B](#)). In L4, when an OFF edge passes the fly's visual field, the activity transiently increases settling at a plateau level that persists until the subsequent ON edge arrives. The ON edge strongly reduces L4's activity. Hence, L4 encodes moving edges with a persistent DC component, which is superimposed by a small transitory peak ([Figure 2A](#)). In contrast to L4, Tm2 responds solely with a fast, transient increase in activity to moving OFF edges ([Figure 2B](#)). When probed with moving ON and OFF edges in all directions, L4 responds to moving OFF edges equally in all four directions, primarily with a persistent change in activity. If L4's activity is at an elevated level, it becomes reduced by an ON edge ([Figures 2A and 2C](#)). As does L4, Tm2 responds to OFF edges moving in all four directions. However, in contrast to L4, Tm2 responds to moving OFF edges with a pronounced transient increase in activity. Tm2 does not respond at all to moving ON edges ([Figures 2B and 2D](#)).

To measure the receptive fields of Tm2 and L4, we periodically presented a dark vertical bar of 4.5° width on a bright background at different azimuthal positions and measured the response of both cells as defined by the difference between the relative fluorescence during bar presentation and the response level before ([Figures 3A and 3B](#)). L4 responded most strongly when the bar was within a window of about $\pm 5^\circ$ around a position, leading to maximal response ([Figure 3A](#)). The average sensitivity profile, obtained after aligning the results from different cells with respect to their maximum, closely resembles a bell-shaped Gaussian with a half width of $\sim 5^\circ$. Tm2 responded to such stimuli in a similar way: again, maximum responses were elicited in a rather small window of about 10° widths, with no significant responses to stimulation outside this window ([Figure 3B](#)). In order to examine the spatial integration properties of L4 and Tm2, on a bright background, we presented a dark, vertical bar, increasing in size and centered at the position of a cell's maximum response. Based on L4's receptive field derived from the previous experiment and assuming linear spatial integration, we expected the responses to strongly increase with increasing bar width until approximately 10° and plateau thereafter. The response of L4 to small bar widths is consistent with this expectation; however, the response of L4 even increases when the bar width changes from 25° to 50° without any sign of saturation ([Figure 3C](#)). For Tm2, considering the data from the previous experiment ([Figure 3B](#)) and the fact that Tm2 doesn't respond to full-field flicker ([Figure 1D](#)), we expected a rather different spatial integration property. Indeed, Tm2 responses differ strongly from those of L4, displaying a maximum response to a bar of 4.5° and then decreasing rapidly as the bar becomes wider ([Figure 3D](#)). This implicates the existence of lateral inhibition, shaping the receptive field properties of Tm2.

In addition to the spatial response properties of these cells, their temporal dynamics are also of interest. Using the line-scan mode of the two-photon microscope, we measured single terminals of both cell types in response to flickering dark bars of 4.5° width at a temporal resolution of 480 Hz. As can be expected from their full-field flicker and edge responses, L4 and Tm2 responded with considerably different temporal dynamics. L4 reached its maximal response level approximately 100 ms after stimulus onset. At the end of the dark bar presentation, the fluorescence in L4 was still approximately 50% of the maximum response ([Figure 3E](#)). Tm2 responded with comparable rise times—reaching maximum response levels 100 ms after stimulus onset—but decayed much faster than L4. At the end of the bar presentation, Tm2 responses had decayed to 20% of their maximum value ([Figure 3F](#)). Note that all data obtained from Ca^{2+} imaging in layer 1 of the lobula are consistent with data from M9 (data not shown).

Motion Responses after Blocking L4 or Tm2

Our results from Ca^{2+} imaging of Tm2 and L4 cells revealed that none of these cells exhibit a preference for grating or edge motion in any direction. However, both cells become selectively excited by brightness decrease, as expected from being postsynaptic to L2. In order to assess their participation in motion processing, we blocked synaptic output of either Tm2 or L4 by expressing shibire [27] and recorded the responses of lobula plate tangential cells to moving ON and OFF edges (data from horizontal system [HS] and vertical system [VS] cells were pooled). Control flies of identical genotype but not subjected to a temperature shift showed strong and

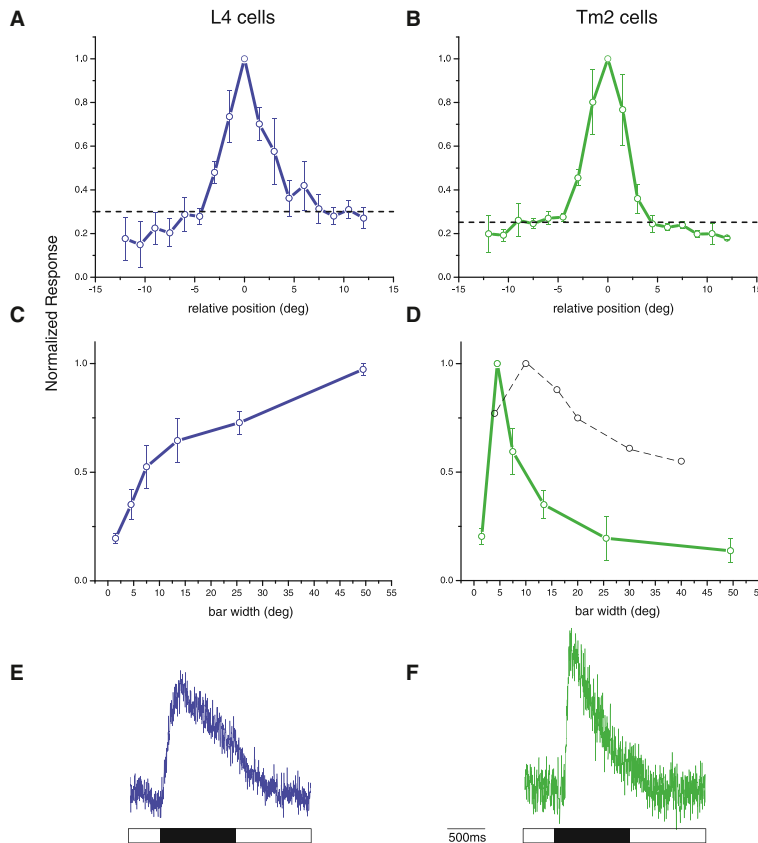


Figure 3. Response Characteristics of L4 and Tm2 Cells upon Stimulation with Flickering Bars

(A and B) Ca^{2+} response of L4 (A; $n = 5$) and Tm2 (B; $n = 5$) to 4.5°-wide, dark, vertical bars appearing and disappearing at various positions (shifted by 1.5°) on a bright background at a frequency of 0.5 Hz. Graphs were normalized to the position of the maximum response. Chance response level is indicated by the dashed line (see the [Experimental Procedures](#)). Error bars indicate \pm SEM.

(C and D) Normalized Ca^{2+} response of L4 (C; $n = 7$) and Tm2 (D; $n = 5$) cells to dark, vertical bars of increasing size (bar widths: 1.5°, 4.5°, 7.5°, 13.5°, 25.5°, and 49.5°). For comparison, L2 responses from [26] are indicated as a dashed line in (D).

(E and F) Ca^{2+} response of a single L4 (E; 50 sweeps) and Tm2 (F; ten sweeps) cell (in arbitrary units) stimulated by a 4.5°-wide dark bar for 1 s, recorded at 480 Hz. The duration of the stimulation is indicated by the black bar below.

See also [Figure S3](#).

responses between control and block flies is shown in [Figure S1](#) (available online). All of these findings are reminiscent on the results of previous studies in which either L2 or T5 cells were blocked, leading to a selective loss of tangential cell responses to OFF edges [10, 12].

We also tested the responses of L4 and Tm2 block flies to grating motion ([Figure S2](#)). As expected from the above results and the assumption that T4 and T5 cells contribute to the grating response with about equal weight, grating responses to horizontal and to vertical

reliable directional responses to both ON and OFF edges, depolarizing by about 8 mV during motion in the preferred direction and hyperpolarizing by about 5 mV during motion in the null direction of the tangential cells (black and gray traces in [Figures 4A–4D](#)). When L4 cells were blocked, the responses to ON edges moving along the preferred as well the null direction were almost indistinguishable from those in control flies (blue traces in [Figures 4A](#) and [4C](#)). However, the responses to OFF edges were severely reduced, both for preferred-direction and for null-direction motion (blue traces in [Figures 4B](#) and [4D](#)). When Tm2 was blocked, tangential cells responded strongly to ON edges moving along the preferred direction of the cells, but the response to null direction had less than half of the amplitude as compared to control flies (green traces in [Figures 4A](#) and [4C](#)). For OFF edge motion, a similar result was obtained as for L4 block flies: Again, the response to motion along both the preferred and the null directions was almost completely abolished (green traces in [Figures 4B](#) and [4D](#)). Using the time average of the difference between the preferred- and null-direction response as a measure, the results can be summarized as follows ([Figures 4E](#) and [4F](#)): blocking synaptic output from L4 cells leaves the ON edge responses unaffected, but strongly and highly significantly reduces the OFF edge response (blue bars, compared to black bars); and blocking synaptic output from Tm2 cells reduces the ON edge responses somewhat, but abolishes the OFF edge response completely (green bars, compared to gray bars). A detailed comparison of preferred- and null-direction

motion in L4 and Tm2 block flies are found to be at roughly half of the amplitude as in control flies. However, consistently in HS and VS cells, the null-direction response is compromised more strongly than is the preferred-direction response. While this might indicate a direction-specific contribution of L4 and Tm2 at first sight, it can be readily explained by a slightly elevated threshold of the inhibitory input to the tangential cells. We therefore conclude that both L4 and Tm2 cells represent essential, nondirectional components of the OFF motion pathway in *Drosophila*.

Discussion

Our results reveal that L4 and Tm2 cells are necessary components for the computation of OFF motion signals. In line with this notion, we find both L4 and Tm2 neurons being excited preferentially by moving OFF edges. Furthermore, we demonstrate that direction selectivity does not occur at the level of L4 or Tm2 cells, but is rather computed downstream of Tm2, presumably in the dendrites of T5 cells.

Contrast Polarity and Direction Sensitivity

Using full-field flicker and moving edges of single contrast polarity, we measured the basic response characteristics of both L4 and Tm2 cells. L4 cells receive their main input from L2 in the lamina, where they form reciprocal, cholinergic connections [18, 21]. In agreement with previous studies [23, 28], we observed a decrease in Ca^{2+} when stimulating

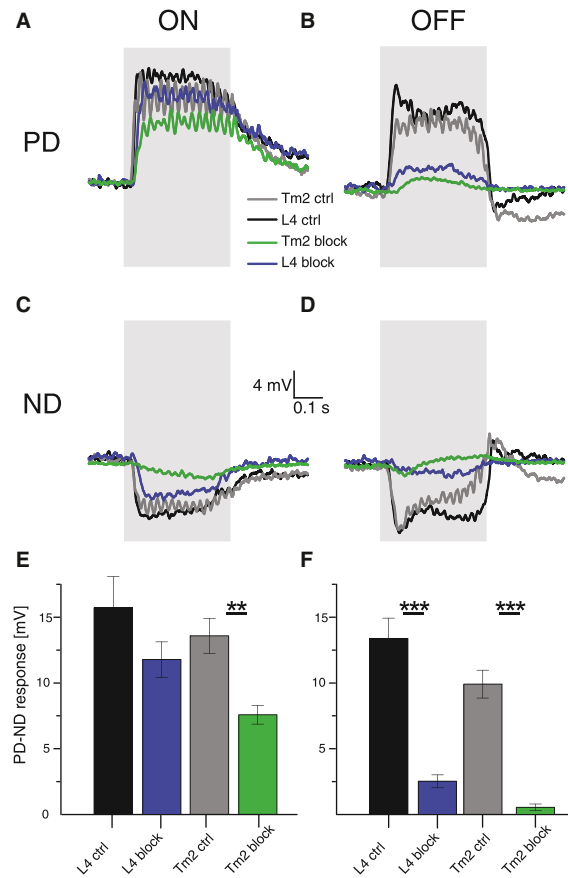


Figure 4. Voltage Responses of Lobula Plate Tangential Cells to Moving ON and OFF Edges

(A–D) Average time course of the membrane potential in response to ON (A and C) and OFF (B and D) edges moving along the preferred (PD; A and B) and null (ND; C and D) direction as recorded in two types of control flies (gray and black), as well as in flies in which synaptic output from L4 (blue) or Tm2 (green) cells was blocked. The stimulation period is indicated by the shaded area.

(E and F) Mean voltage responses (PD – ND) to ON (E) and OFF (F) edges of tangential cells in all four groups of flies. Recordings were done from HS [2] and VS [1] cells. HS cells have front to back as their PD and back to front as their ND; VS cells have downward as their PD and upward as their ND. Since no difference was detected between HS and VS cells, data from both cell types were pooled. L4 control data are from nine cells (four HS, five VS) in two flies, L4 block data are from ten cells (three HS, seven VS) in two flies, Tm2 control data are from 14 cells (six HS, eight VS) in eight flies, and Tm2 block data are from 11 cells (five HS, six VS) in five flies. In L4 block flies, ON responses are nonsignificantly different from control flies, whereas OFF responses are highly significantly reduced. In Tm2 block flies, ON responses are significantly different from control flies, and OFF responses are highly significantly reduced. * $p < 0.05$, ** $p < 0.001$, *** $p < 0.0001$, tested using two-tailed t tests against their controls. Error bars indicate \pm SEM. See also Figures S1–S3.

L4 with brightness increments and an increase of Ca^{2+} when presenting light decrements. Assuming an excitatory connection between L2 and L4, these results are consistent with data that have been described for L2 [23, 26, 29]. The temporal response characteristics of L4, however, differ substantially from those observed in L2 by the existence of a sustained

component in L4, which is not seen in L2. This discrepancy is in agreement with the finding that L4 receives input from photoreceptors, both directly from R6 and indirectly via the lamina amacrine cell, in addition to the input from L2 [22]. Tm2 receives its main input from L2. In agreement with this notion, we observed an increased Ca^{2+} signal in response to brightness decrements and no response to brightness increments. The transient nature of the signal and its selectivity for OFF edges parallels the reported findings for the Ca^{2+} signal in the terminal region of L2 [15, 29], suggesting that half-wave rectification in the L2 terminal represents the biophysical mechanism for OFF selectivity within the L2 pathway [29]. In contrast to L2, L4, and previous electrophysiological recordings in the calliphorid ortholog of Tm2 [28], Tm2 cells in *Drosophila* do not show any response to full-field luminance changes of either polarity. This finding indicates the existence of an inhibitory subregion of the receptive field. It also argues against the hypothesis that intercolumnar L4 connections onto Tm2 might implement a pooling of excitatory neighboring signals [18]. Furthermore, the observed nondirectional responses of both L4 and Tm2 allow us to rule out the hypothesis that the asymmetrical wiring between L4 and Tm2 could implement direction selectivity [18]. This passes the emergence of direction selectivity to the postsynaptic neurons—presumably T5—that have been shown to exhibit a precise directional tuning [12].

Receptive Field Properties

Stimulation with dark bars at different positions and increasing widths revealed the receptive field properties of L4 and Tm2 cells. We could demonstrate that the spatial sensitivity distribution for excitatory input to both cells exhibits comparable characteristics in the azimuthal extent when probed by small bars. However, it differs significantly in response to larger objects. Here, the response of L4 cells increases with the size of the visual stimulus, and thus varies distinctly from the center-surround receptive field described in L2 [26]. This is a further indication for a contribution of additional inputs to L4, e.g., via wide-field amacrine cells. As is shown by a linear receptive field model—an isotropic Gaussian inhibitory center with a half width σ of 2° and a spatially constant excitatory surround—even a minute excitatory surround contribution, undetectable by local stimulation, is sufficient to account for the increase in response with increasing stimulus size (Figure 5E). Tm2, in contrast, seems to be inhibited by large objects, since their response decreases dramatically when stimulated with bars wider than 4.5° . With Ca^{2+} as a proxy for membrane voltage, this inhibitory surround has not been detected by the stimulation with small bars at such lateral positions, either because intracellular Ca^{2+} does not decrease with membrane hyperpolarization or because the Ca^{2+} indicator does not report these low concentrations. Compared to L2 [26], surround inhibition seems to be much more pronounced in Tm2 (L2 responses from [26] are indicated as dashed line in Figure 3D). Tm2 cells lack every response to objects larger than 25° , indicating the existence of further lateral inhibition at the level of Tm2 that leads to a sharpening of their receptive field, probably via wide-field amacrine cells. In order to quantitatively reproduce Tm2 responses to bars of increasing width and moving gratings, we modeled the receptive field of Tm2 as the difference of two Gaussians with a half width σ of 2° horizontally and 4° vertically for the inhibitory center and of 10° horizontally and 20° vertically for the excitatory surround. This combination resulted in a maximum local surround excitation that amounted

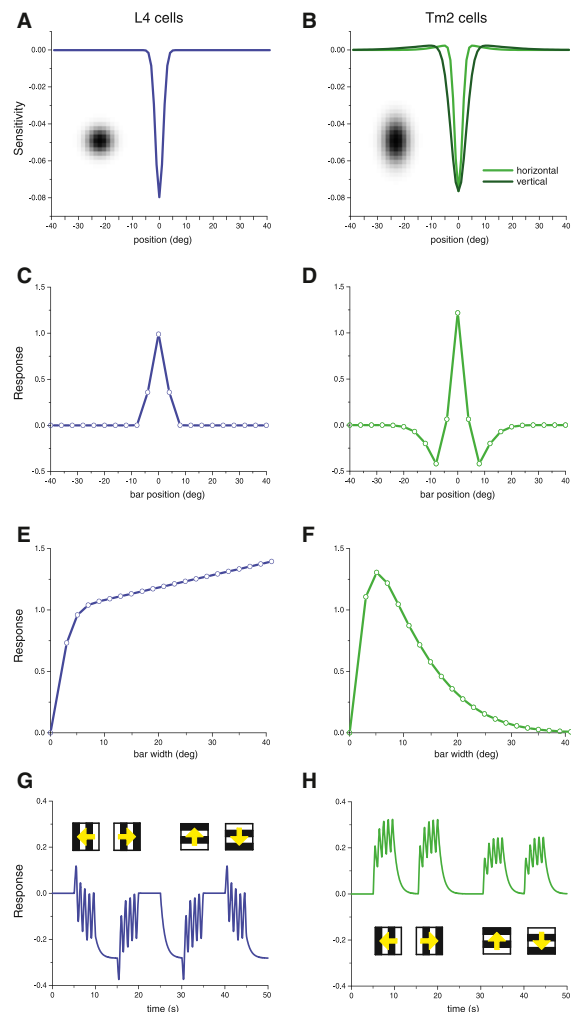


Figure 5. Model Simulations of L4 and Tm2 Receptive Fields
(A and B) Sensitivity profile across the receptive field of L4 (A) and Tm2 (B). The insets show a magnified view of the 2D receptive field, with each pixel corresponding to one $1^\circ \times 2^\circ$ of visual space.
(C and D) Responses of L4 (C) and Tm2 (D) to a 7° -wide bar as a function of bar position.
(E and F) Responses of L4 (E) and Tm2 (F) to a bar, centered in the receptive field, as a function of bar width.
(G and H) Responses of L4 (G) and Tm2 (H) to a grating (spatial wavelength = 20°) moving at a temporal frequency of 1 Hz along four orthogonal directions. Responses were obtained by low-pass filtering ($\tau = 1$ s) of original signals from L4 and half-wave rectifying signals from Tm2.
See also Figure S3.

to only 3% of the peak center inhibition, but nevertheless was able to fully reproduce the strong decrease of the response of Tm2 with increasing bar width seen in the experiments (Figures 5B and 5F). A further interesting difference between L4 and Tm2 appears in their responses to moving square wave gratings: while L4 responses remain at rest, at best being slightly modulated at the temporal frequency of the local luminance changes (Figure 1E), Tm2 responses build up during grating motion with temporal modulations riding on

top (Figure 1F). As shown by model simulations, these differences are readily explained by the half-wave rectified response property of Tm2, but not in L4, assuming a temporal integration of the membrane potential either by intracellular Ca^{2+} and/or the buffering of the indicator (Figures 5G and 5H). Furthermore, assuming a slight anisotropy of the receptive field of Tm2 as explained above (Figure 5B), similar to what has been reported for L2 [26], the simulation results for grating motion are consistent with the somewhat smaller response amplitude of Tm2 to vertical than to horizontal motion (Figure 5H). Note, however, that the anisotropy of the Tm2 receptive field was not directly measured.

L4 and Tm2 Are Crucial OFF Pathway Elements

To test the role of L4 and Tm2 in motion detection in *Drosophila*, we blocked their synaptic output and recorded from tangential cells of the lobula plate. Unlike a behavioral study by Silies and colleagues that shows only mild reductions in responses to OFF motion stimuli when blocking L4 [23], we observed a strong impairment of tangential cell responses for OFF motion. This difference might be explained by differing expression levels of Gal4 in L4 fly lines: in the same study, silencing L4 in two different fly lines caused significantly different effects of responses toward opposing edges [23]. In another study, Tuthill and colleagues tested the effect of blocking all lamina neurons individually on turning behavior of flying *Drosophila* [24]. In agreement with our results, blocking L4 resulted in a selective impairment of the turning responses to OFF versus ON edges. In response to grating motion from the front to the back, these flies also exhibited a response reduction to about 50% of control level, as is expected from our data (Figures 4, S1, and S2). However, the same flies reacted with the same amplitude as control flies to grating motion from the back to the front. Since the behavioral response to back-to-front motion is much smaller than that to front-to-back motion, the residual tangential cell response might be sufficient to generate normal behavioral output under these conditions. Our results show that L4 is necessary for OFF motion signals in tangential cells (Figure 4). The same effect was observed when Tm2 was blocked. Blocking and Ca^{2+} imaging experiments match, because no direction-specific defect could be detected. This speaks in favor of the hypothesis that blocking Tm2 corresponds to the disruption of one input element to the Reichardt detector. L4, on the other hand, as one of the major input elements to Tm2 [18], seems to be needed either for a proper functioning of L2, or in conjunction with L2 to successfully evoke signals in Tm2. Our data also show a reduction in the responses of tangential cells in Tm2 block flies to ON stimuli, especially in the cells' null direction (Figure 4). This decrease of the ON response could be caused by disruption of a potential tonic input of Tm2 to the ON pathway via L5 [17, 18] or via its arborization in medulla layer 9. Together with the spatiotemporal response properties of Tm2 reported above, the following conclusions can be drawn regarding motion processing in the OFF pathway: (1) The narrow receptive field of Tm2 (Figure 3B) with a half width of about 5° indicates input from only a single optical cartridge. This is significantly smaller than the "anatomical receptive field," as reported in Takemura et al. [17] for Tm3, one of the inputs to the T4 cells, and thus might represent an interesting difference between the ON and the OFF motion pathway. (2) The strong surround inhibition we see in Tm2 (Figure 3D) readily explains the missing responses to field flicker stimuli that was observed in T5 cells

[12]. (3) The rather transient response of Tm2 (Figures 2B and 3F) makes it a candidate for the fast (i.e., high-pass filtered) input to the motion detection mechanism in the postsynaptic dendrite of T5 cells. This is all the more true since the calcium indicator is expected to slow down the signal significantly: thus, the membrane potential response in Tm2 will certainly be even faster. As a caveat, however, no data on Tm1 neurons exist so far to compare with. (4) The fact that blocking Tm2 abolishes the OFF response in the tangential cells for all stimulus directions (Figures 4B, 4D, and 4F) suggests that Tm2 serves as input element for all four types of T5 cells tuned to the four cardinal directions.

In summary, we thus conclude that L4 and Tm2 are essential OFF motion processing elements in the fly visual system that are not directionally selective. Consequently, direction selectivity in the OFF pathway is likely to arise at the level of the T5 dendrites.

Experimental Procedures

Flies

Flies were raised on standard cornmeal-agar medium with 12 hr light/12 hr dark cycles, 25°C, and 60% humidity. For Ca²⁺ imaging, we used the genetically encoded indicator GCaMP5 [30] driven by two different Gal4 lines with the following genotypes: Tm2_{ca} line (*w⁻;ort-Gal4-DBD,N9A >> BVP16-AD;UAS-GCaMP5*), provided by Chi-Hon Lee [31], and L4 line (*w⁻;UAS-GCaMP5;VT40547-Gal4*, VDRC stock number 200265). Cell-specific block effects in electrophysiological experiments were accomplished using UAS-shibire^{ts} [27]. Fly lines with the following genotypes were used for electrophysiological recordings: L4 line (*shi^{ts}/+;+;shi^{ts}/VT40547-Gal4*, VDRC stock number 200265) and Tm2_{el} line (*shi^{ts}/+;+;shi^{ts}/VT12282-Gal4*, VDRC stock number 203097). Expression and specificity of driver lines were investigated using a combination of membrane tethered GFP and synaptotagmin-hemagglutinin (courtesy of Andreas Prokop) [32, 33]. Fly lines had the following genotypes: Tm2_{ca} line (*w⁻;UAS-SYT-HA,UAS-mCD8-GFP/ort-Gal4-DBD,N9A >> BVP16-AD;+*), Tm2_{el} line (*w⁻;UAS-SYT-HA,UAS-mCD8-GFP/+;VT12282-Gal4/+*), and L4 line (*w⁻;UAS-SYT-HA,UAS-mCD8-GFP/+;VT40547-Gal4/+*). The Tm2_{ca} line had a higher Gal4 expression level than did the Tm2_{el} line. The Tm2_{el} line, however, showed a more specific expression pattern. Detailed descriptions of preparation and experiments are found in [29] for Ca²⁺ imaging and in [1] for electrophysiology.

Immunohistochemistry and Confocal Imaging

Immunostainings were performed as described in [2]. As primary antibodies (1:200) we used mouse anti-discs large (DLG, Developmental Studies Hybridoma Bank), rabbit anti-GFP-Alexa488 conjugate (Molecular Probes), and rat anti-hemagglutinin (Roche). For visualization, we used the following secondary antibodies (1:200 in PBT): goat anti-mouse Alexa 568, goat anti-rat Alexa 568 (Molecular Probes), and goat anti-mouse Alexa 647 (Rockland Immunochemicals). Brains were mounted (IMM, Ibbidi) and optically sectioned in the horizontal plane with a Leica SP5 confocal microscope. For documentation, single sections were processed in ImageJ 1.46r (NIH).

Electrophysiology

The recording protocol was adapted from [1]. In addition, the glial sheet was digested locally by application of a stream of 0.5 mg/ml collagenase IV (GIBCO) through a cleaning micropipette (~5 µm opening) under polarized light contrast.

Two-Photon Microscopy and Visual Stimulation

Two-photon microscopy and visual stimulus presentation were performed as described in [12]. Square-wave gratings had a spatial wavelength of 30° of visual angle and a contrast of 88%, moving at either 30° s⁻¹ or 60° s⁻¹. Edges had the same contrast and were moving at 30° s⁻¹. For the experiments shown in Figures 1 and 2, each grating or edge motion was shown twice within a single sweep, each lasting 4 s. Subsequent stimuli were preceded by a 3 s pause. For the experiments shown in Figures 3A and 3B, we flickered 4.5°-wide vertical dark bars on a bright background at 0.5 Hz at 10 different positions. The position yielding maximum response was set to 0°. The responses were normalized and plotted depending on their distance to the peak response. For Figures 3C and 3D, vertical dark

bars, increasing in size, were flickered at the peak response position. The responses were normalized to the peak response. For Figures 3E and 3F, a 4.5° vertical dark bar was flickered for 1 s on a bright background (line scan, averaged trace, ten repetitions). For the experiments shown in Figure 4, multiple edges were used as stimuli moving simultaneously at 60° s⁻¹. For stimulation of HS cells, a vertical, stationary square-wave grating with 45° spatial wavelength was presented. For ON edge motion, the right (PD) or the left (ND) edge of each light bar started moving until it merged with the neighboring bar. For OFF edge motion, the right or the left edge of each dark bar was moving. For stimulation of VS cells, the pattern was rotated by 90°. A collection of all stimuli is presented as space-time plots in Figure S3.

Data Evaluation

Data were evaluated offline using custom written software (MATLAB) and Origin (OriginLab). For evaluation of the Ca²⁺ imaging data, the raw image series was first converted into a relative fluorescence change (ΔF/F) series using the first five images as reference. Then a region was defined within a raw image and average ΔF/F values were determined within that region for each image, resulting in a ΔF/F signal over time. The Ca²⁺ signal traces in Figures 1C–1F were obtained by calculation of the average ΔF/F signal over trials and flies, with shading indicating the SEM. For the bar graphs in Figure 2C, the average signals of three frames before stimulus onset were subtracted from the mean response within the three last images of edge motion. For Figure 2D, the average Ca²⁺ signal of three images prior to visual stimulation (reference value) was subtracted from the maximum response during each stimulus presentation. The dashed line was calculated by subtraction of the reference value from a maximum, obtained without visual stimulation (chance response level). The graphs in Figures 3A and 3B show the average signal (maximum – minimum of peaks, five presentations) to flickering bars normalized to the maximum response. Again, the dashed line represents chance level. The voltage traces in Figures 4A–4D were obtained by averaging of the responses of all cells upon visual stimulation with multiple edges of either polarity in the four cardinal directions. For the bar graphs in Figures 4E and 4F, the responses during edge motion (0.375 s) along the preferred and null direction were subtracted (PD – ND). The mean PD – ND responses were subsequently averaged across all cells, with error bars representing the SEM.

Supplemental Information

Supplemental Information includes three figures and can be found with this article online at <http://dx.doi.org/10.1016/j.cub.2014.01.006>.

Acknowledgments

We thank Chi-Hon Lee and Andreas Prokop for providing us with fly lines; David Soll for the DLG-antibody; Johannes Plett for designing and engineering the LED arena and for technical support; Christian Theile, Wolfgang Essbauer, and Michael Sauter for fly work; Romina Kutlesa for stainings; and Aljoscha Leonhardt, Elisabeth Hopp, and Georg Ammer for constructive discussions and help with programming.

Received: October 22, 2013
Revised: November 29, 2013
Accepted: January 3, 2014
Published: February 6, 2014

References

1. Joesch, M., Plett, J., Borst, A., and Reiff, D.F. (2008). Response properties of motion-sensitive visual interneurons in the lobula plate of *Drosophila melanogaster*. *Curr. Biol.* 18, 368–374.
2. Schnell, B., Joesch, M., Forstner, F., Raghu, S.V., Otsuna, H., Ito, K., Borst, A., and Reiff, D.F. (2010). Processing of horizontal optic flow in three visual interneurons of the *Drosophila* brain. *J. Neurophysiol.* 103, 1646–1657.
3. Hassenstein, B., and Reichardt, W. (1956). Systemtheoretische Analyse der Zeit-, Reihenfolgen- und Vorzeichenauswertung bei der Bewegungspertzeption des Rüsselkäfers *Chlorophanus*. *Z. Naturforsch.* B 11b, 513–524.
4. Reichardt, W. (1987). Computation of optical motion by movement detectors. *J. Comp. Physiol. A* 161, 533–547.

5. Borst, A., and Euler, T. (2011). Seeing things in motion: models, circuits, and mechanisms. *Neuron* 71, 974–994.
6. Fischbach, K., and Dittrich, A. (1989). The optic lobe of *Drosophila melanogaster*. I. A Golgi analysis of wild-type structure. *Cell Tissue Res.* 258, 441–475.
7. Bausenwein, B., Dittrich, A.P.M., and Fischbach, K.F. (1992). The optic lobe of *Drosophila melanogaster*. II. Sorting of retinotopic pathways in the medulla. *Cell Tissue Res.* 267, 17–28.
8. Bausenwein, B., and Fischbach, K.F. (1992). Activity labeling patterns in the medulla of *Drosophila melanogaster* caused by motion stimuli. *Cell Tissue Res.* 270, 25–35.
9. Rister, J., Pauls, D., Schnell, B., Ting, C.Y., Lee, C.H., Sinakevitch, I., Morante, J., Strausfeld, N.J., Ito, K., and Heisenberg, M. (2007). Dissection of the peripheral motion channel in the visual system of *Drosophila melanogaster*. *Neuron* 56, 155–170.
10. Joesch, M., Schnell, B., Raghu, S.V., Reiff, D.F., and Borst, A. (2010). ON and OFF pathways in *Drosophila* motion vision. *Nature* 468, 300–304.
11. Buchner, E., Buchner, S., and Bülthoff, I. (1984). Deoxyglucose mapping of nervous activity induced in *Drosophila* brain by visual movement. *J. Comp. Physiol.* 155, 471–483.
12. Maisak, M.S., Haag, J., Ammer, G., Serbe, E., Meier, M., Leonhardt, A., Schilling, T., Bahl, A., Rubin, G.M., Nern, A., et al. (2013). A directional tuning map of *Drosophila* elementary motion detectors. *Nature* 500, 212–216.
13. Schnell, B., Raghu, S.V., Nern, A., and Borst, A. (2012). Columnar cells necessary for motion responses of wide-field visual interneurons in *Drosophila*. *J. Comp. Physiol. A Neuroethol. Sens. Neural Behav. Physiol.* 198, 389–395.
14. Eichner, H., Joesch, M., Schnell, B., Reiff, D.F., and Borst, A. (2011). Internal structure of the fly elementary motion detector. *Neuron* 70, 1155–1164.
15. Clark, D.A., Bursztyn, L., Horowitz, M.A., Schnitzer, M.J., and Clandinin, T.R. (2011). Defining the computational structure of the motion detector in *Drosophila*. *Neuron* 70, 1165–1177.
16. Joesch, M., Weber, F., Eichner, H., and Borst, A. (2013). Functional specialization of parallel motion detection circuits in the fly. *J. Neurosci.* 33, 902–905.
17. Takemura, S.Y., Bharioke, A., Lu, Z., Nern, A., Vitaladevuni, S., Rivlin, P.K., Katz, W.T., Olbris, D.J., Plaza, S.M., Winston, P., et al. (2013). A visual motion detection circuit suggested by *Drosophila* connectomics. *Nature* 500, 175–181.
18. Takemura, S.Y., Karuppururai, T., Ting, C.-Y., Lu, Z., Lee, C.-H., and Meinertzhagen, I.A. (2011). Cholinergic circuits integrate neighboring visual signals in a *Drosophila* motion detection pathway. *Curr. Biol.* 21, 2077–2084.
19. Braitenberg, V., and Debbage, P. (1974). A regular net of reciprocal synapses in the visual system of the fly, *Musca domestica*. *J. Comp. Physiol.* 90, 25–31.
20. Strausfeld, N.J., and Campos-Ortega, J.A. (1973). The L4 monopolar neurone: a substrate for lateral interaction in the visual system of the fly *Musca domestica* (L.). *Brain Res.* 59, 97–117.
21. Meinertzhagen, I.A., and O’Neil, S.D. (1991). Synaptic organization of columnar elements in the lamina of the wild type in *Drosophila melanogaster*. *J. Comp. Neurol.* 305, 232–263.
22. Rivera-Alba, M., Vitaladevuni, S.N., Mishchenko, Y., Lu, Z., Takemura, S.Y., Scheffer, L., Meinertzhagen, I.A., Chklovskii, D.B., and de Polavieja, G.G. (2011). Wiring economy and volume exclusion determine neuronal placement in the *Drosophila* brain. *Curr. Biol.* 21, 2000–2005.
23. Silies, M., Gohl, D.M., Fisher, Y.E., Freifeld, L., Clark, D.A., and Clandinin, T.R. (2013). Modular use of peripheral input channels tunes motion-detecting circuitry. *Neuron* 79, 111–127.
24. Tuthill, J.C., Nern, A., Holtz, S.L., Rubin, G.M., and Reiser, M.B. (2013). Contributions of the 12 neuron classes in the fly lamina to motion vision. *Neuron* 79, 128–140.
25. Denk, W., Strickler, J.H., and Webb, W.W. (1990). Two-photon laser scanning fluorescence microscopy. *Science* 248, 73–76.
26. Freifeld, L., Clark, D.A., Schnitzer, M.J., Horowitz, M.A., and Clandinin, T.R. (2013). GABAergic lateral interactions tune the early stages of visual processing in *Drosophila*. *Neuron* 78, 1075–1089.
27. Kitamoto, T. (2001). Conditional modification of behavior in *Drosophila* by targeted expression of a temperature-sensitive shibire allele in defined neurons. *J. Neurobiol.* 47, 81–92.
28. Douglass, J.K., and Strausfeld, N.J. (1995). Visual motion detection circuits in flies: peripheral motion computation by identified small-field retinotopic neurons. *J. Neurosci.* 15, 5596–5611.
29. Reiff, D.F., Plett, J., Mank, M., Griesbeck, O., and Borst, A. (2010). Visualizing retinotopic half-wave rectified input to the motion detection circuitry of *Drosophila*. *Nat. Neurosci.* 13, 973–978.
30. Akerboom, J., Chen, T.-W., Wardill, T.J., Tian, L., Marvin, J.S., Mutlu, S., Calderón, N.C., Esposti, F., Borghuis, B.G., Sun, X.R., et al. (2012). Optimization of a GCaMP calcium indicator for neural activity imaging. *J. Neurosci.* 32, 13819–13840.
31. Ting, C.-Y., Gu, S., Guttikonda, S., Lin, T.-Y., White, B.H., and Lee, C.-H. (2011). Focusing transgene expression in *Drosophila* by coupling Gal4 with a novel split-LexA expression system. *Genetics* 188, 229–233.
32. Löhr, R., Godenschwege, T., Buchner, E., and Prokop, A. (2002). Compartmentalization of central neurons in *Drosophila*: a new strategy of mosaic analysis reveals localization of presynaptic sites to specific segments of neurites. *J. Neurosci.* 22, 10357–10367.
33. Robinson, I.M., Ranjan, R., and Schwarz, T.L. (2002). Synaptotagmins I and IV promote transmitter release independently of Ca(2+) binding in the C(2)A domain. *Nature* 418, 336–340.

Current Biology, Volume 24

Supplemental Information

Neural Circuit Components of the

***Drosophila* OFF Motion Vision Pathway**

Matthias Meier, Etienne Serbe, Matthew S. Maisak, Jürgen Haag, Barry J. Dickson, and Alexander Borst

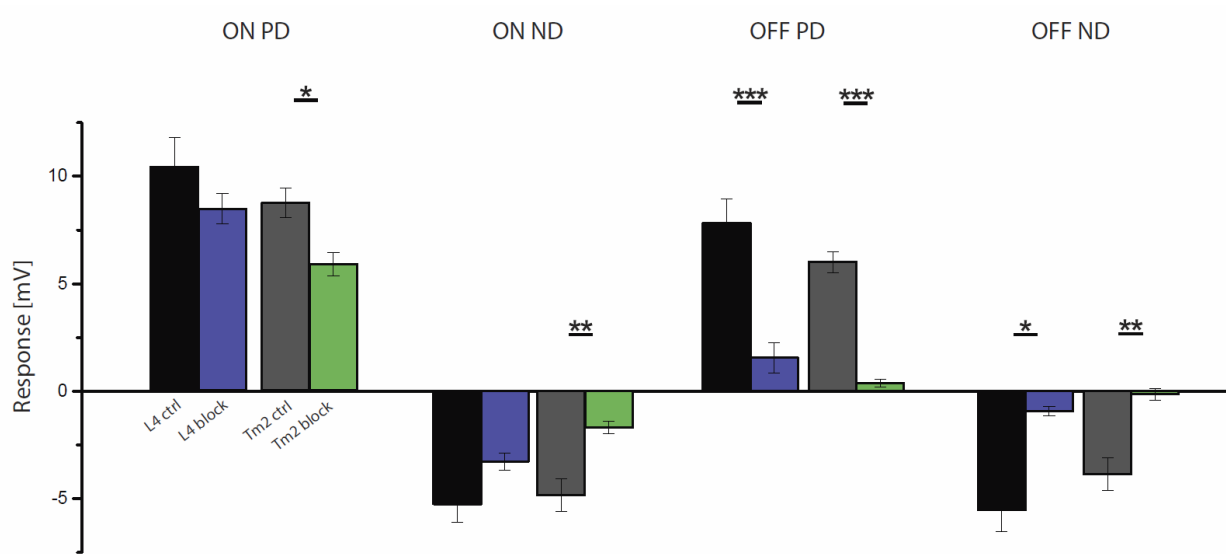


Figure S1: Detailed comparison of preferred (PD) and null (ND) direction responses to moving ON (left) and OFF (right) edges between L4 control and L4 block flies, and between Tm2 control and Tm2 block flies. As in Figure 4, data are pooled from HS and VS cells. L4 control data are from 9 cells (4 HS, 5 VS) in 2 flies, L4 block data from 10 cells (3 HS, 7 VS) in 2 flies, Tm2 control data from 14 cells (6 HS, 8 VS) in 8 flies, Tm2 block data from 11 cells (5 HS, 6 VS) in 5 flies. * $p < 0.05$, ** $p < 0.001$, *** $p < 0.0001$, tested using two-tailed t tests against their controls. Error bars denote \pm SEM. Related to Figure 4.

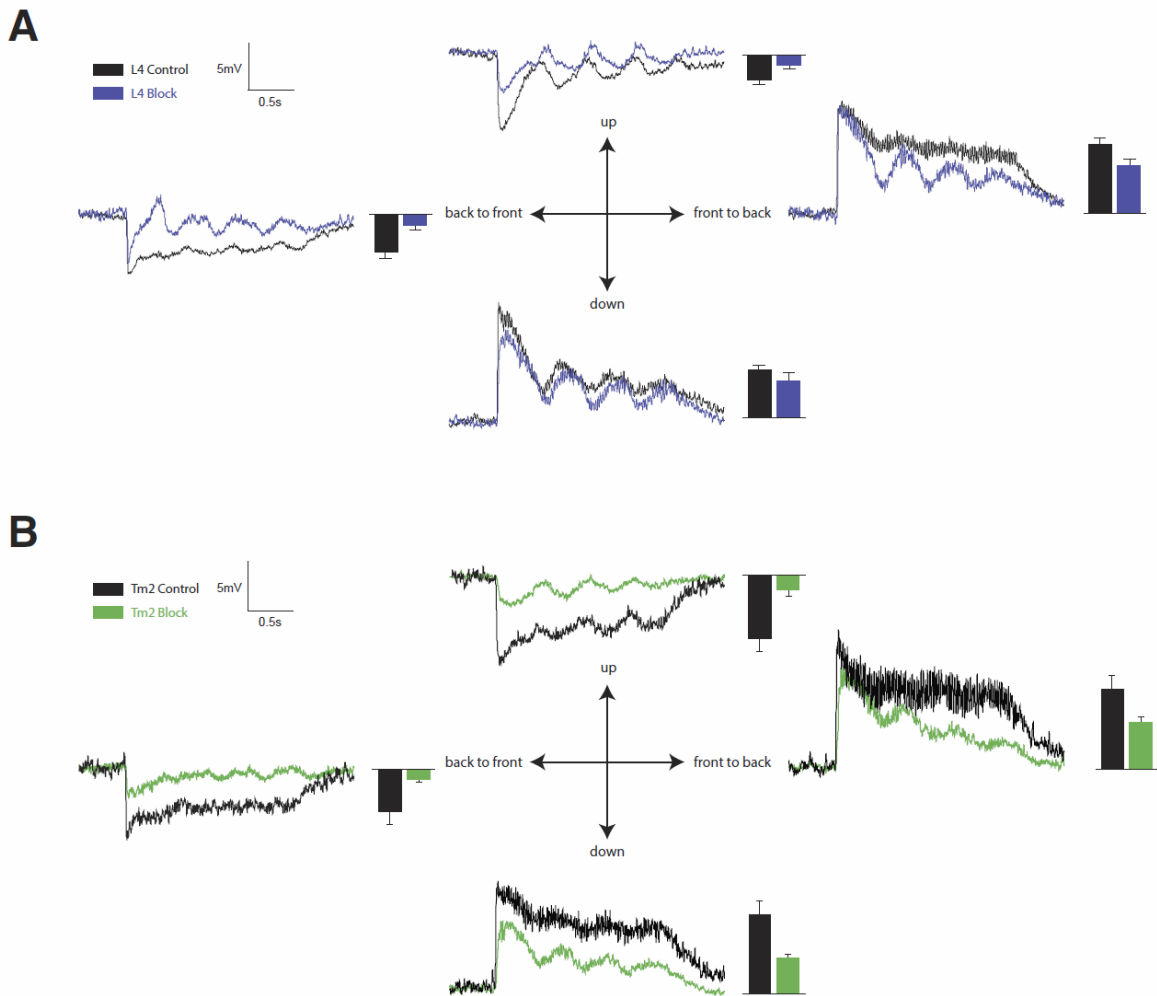


Figure S2: Responses to moving gratings of L4 control and L4 block flies **(A)** and of Tm2 control and Tm2 block flies **(B)**. Data for horizontal motion are from HS cells, for vertical motion from VS cells. L4 control data are from 40 cells (21 HS, 19 VS) in 15 flies, L4 block data from 31 cells (12 HS, 19 VS) in 12 flies. Tm2 control data are from 14 cells (6 HS, 8 VS) in 7 flies, Tm2 block data from 11 cells (6 VS, 5 HS) in 5 flies. Error bars denote \pm SEM. Gratings had a spatial wavelength of 30 deg and were moving at 60 deg/s resulting in a temporal frequency of 2 Hz. Related to Figure 4.

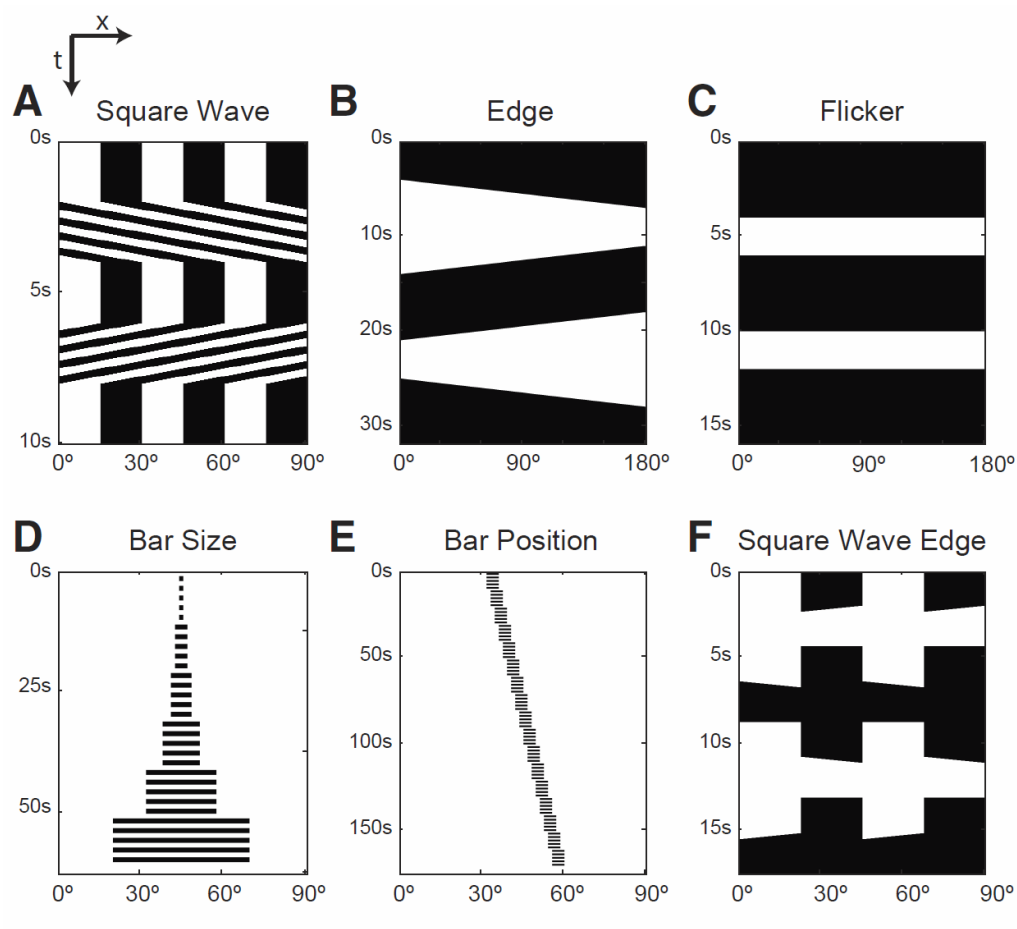


Figure S3: Space-time (xt) plots of all visual stimuli used in the study. Related to Figures 2-5.

3 | DISCUSSION

I investigated the neural network underlying the computation of direction selectivity in the visual system of the fruit fly *Drosophila melanogaster*. Here, algorithmic models, based on the differential temporal filtering of two signals originating from spatially offset inputs accurately describe the responses of both large field interneurons in the optic lobe of the brain, as well as the turning behavior of walking flies. Probing the nervous system with various physiological assays combined with transgenic manipulations of neurons resulted in a number of important findings.

My collaborators and I were able to determine that bushy T4 and T5 cells respond to local brightness increments and decrements, respectively, providing evidence that the separation into ON and OFF processing streams is conserved at the level of the lobula plate inputs. I could furthermore show that the four subclasses of T4 and T5 cells exhibit direction selective responses tuned to the four cardinal directions. When I then investigated presynaptic elements to OFF-selective T5 cells I found that four Tm cell types each contribute to the computation of direction selectivity and that they provide a variety of temporal filter properties.

3.1 T4 AND T5 INPUT

One possibility based on the results of the T4/T5 study is that direction selectivity could arise within the dendrites of the T4 and T5 cells respectively, due to the temporally offset signals from neighboring facets converging there. One study probed the anatomy of the T4 ON circuit using serial electron microscopy and found two interneurons, Mi1 and Tm3, represent both the major output at the L1 level and the major input to T4. Additionally, they observed a physical offset of the Mi1 and Tm3 inputs onto the T4 dendrites, which corresponds to the layer in which the T4 projects and thus the preferred direction of the individual cell (Fig.5). This leads to the obvious conclusion that Mi1 and Tm3 could represent the two arms of the Reichardt detector, one transmitting the low-pass, the other the high-pass signal (Take-mura, 2014). However, a recent study from the same lab, Take-

[mura et al. \(2017\)](#), using a novel EM technique with better Z-axis resolution was unable to confirm the spatial offset between Mi1 and Tm3. They were able to identify new inputs to T4: Mi4, Mi9, C3, and CT1, which are distributed in an asymmetric manner depending on the T4 subtype and its preferred direction. In the OFF pathway anatomy, things aren't as clear. Using a similar EM technique as in the ON pathway study, [Shinomiya et al. \(2014\)](#), showed that four different medulla neurons, Tm1, Tm2, Tm4, and Tm9 provide the major input onto the T5 dendrites. Part of this hypothesis is consistent with our finding that Tm2 is necessary for OFF responses of the lobula plate tangential cells; namely blocking Tm2 eliminated OFF responses in LPTCs while leaving ON responses intact.

While both of these anatomical studies are of great importance, it is still critical to probe the functional role of each of the interneurons in their respective circuits. From our studies, it would be assumed that the cells presynaptic to T4 respond to brightness increments with increased activity and that the cells presynaptic to T5 are activated by brightness decrements. The response properties of four of the interneurons have recently been investigated in a series of studies. Two different studies used genetically encoded calcium indicators and found that, in line with expectations, Mi1 is excited by brightness increments and Tm1 and Tm2 respond solely to brightness decrements ([Meier et al., 2014](#); [Strother et al., 2014](#)). In addition to these calcium imaging studies there is also a publication using electrophysiological techniques in which the authors successfully performed whole-cell patch clamping from several of the medulla interneurons ([Behnia and Desplan, 2015](#)). They showed that Mi1 and Tm3 depolarize exclusively in response to ON and Tm1 and Tm2 in response to OFF signals with only a slight hyperpolarization to stimuli with the opposite polarity. This and previous blocking studies ([Joesch et al., 2010](#)) prove that interneurons of the ON-OFF pathway respond in exact counterphase and exhibit half-wave rectification. A closer look at the temporal dynamics of these cells leads to more interesting observations; both cells exhibit a band-pass characteristic with a difference in the time constants between Mi1 and Tm3 and Tm1 and Tm2, respectively, of approximately 15ms ([Behnia et al., 2014](#)). Based on these time differences and the anatomical studies previously mentioned, the authors hypothesize that Mi1 and Tm3 might perform the critical delayed and non-delayed processing steps in the detection of moving bright edges.

In the OFF pathway Tm1 and Tm2 play similar roles ([Behnia et al., 2014](#)). An alternative explanation, proposed by [Shinomiya](#)

[et al. \(2014\)](#), posits that the delay could be implemented in the T4 or T5 dendrites through asymmetric distribution of different receptor types. RNAi profiling of T4 and T5 cells shows that each subtype expresses both nicotinic and muscarinic acetylcholine receptors that could mediate a fast ionotropic and a slow metabotropic signal ([Shinomiya et al., 2014](#)).

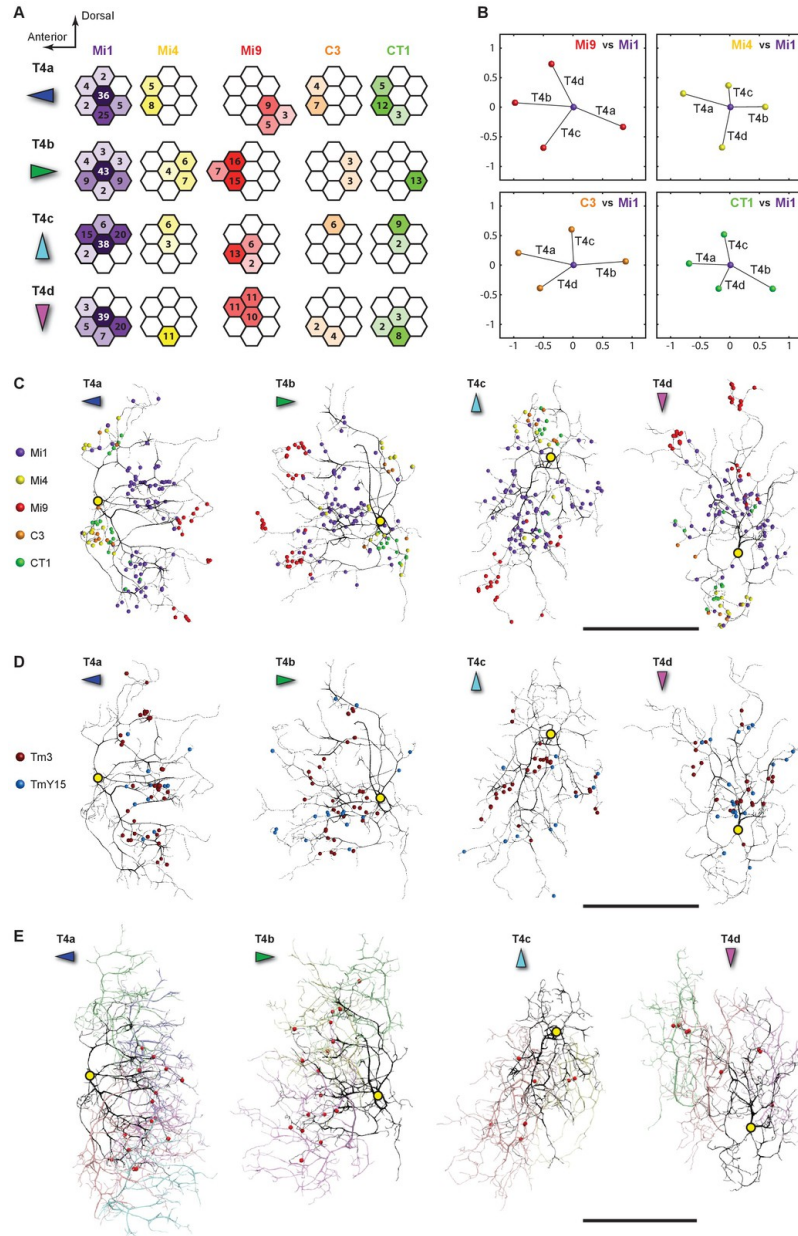


Figure 5. Motion Circuitry (A) Counts of synaptic inputs to T4s from each class of input neuron from neighbouring columns are shown in the corresponding hexagonal array. (B) Angular subtense between weighted anatomical subfield centres for Mi1 paired with four other medulla cell input neurons for the four T4 subtypes. Axes of X and Y show centre-to-centre distances between adjacent columns. The plots show considerable spatial displacements, in some cases more than an inter-ommatidial distance. (C) Distributions of synaptic inputs onto T4 dendrites. Colors of puncta correspond to presynaptic cell types. Yellow circles indicate the locations of the axonâs main trunk. (D) Distributions of synaptic inputs from Tm3 and TmY15. (E) Distributions of synaptic inputs from T4s in the surrounding columns. The T4 subtypes in the Home column (black) each receive input from other T4s (colours) that have the same dendritic branch orientation (i.e. the same preferred direction). Red puncta indicate the synaptic contacts from the neighbouring T4s onto the T4s. Figure and caption taken with permission from [Takemura et al. \(2017\)](#). Scale bar, 10 μ m(C – E).

Another important point in the characterization of these neurons is their receptive fields. Again, there are strong differences between the receptive field properties of these cells: Mi1 responds strongly to the full field flicker (brightness increments) (Strother et al., 2014) while Tm1 and Tm2 receive a pronounced surround inhibition reducing their responses to larger stimuli (Meier et al., 2014; Strother et al., 2014).

3.2 THE NULL DIRECTION: ENCODED IN T4 AND T5?

One of first, and most surprising phenomenon that we observed while imaging T4 and T5 was the fact that they exhibited no or very little null direction response: an increase in activity when stimulated in exactly the opposite direction as the preferred direction. As mentioned previously, the final processing stage of the Reichardt detector is the subtraction of oppositely tuned motion detectors, which when the two subunits are identical leads to the pronounced “fully opponent” response as observed in the LPTCs. The question arises how this response is implemented in biophysical terms. One hypothesis, which has been tossed around for quite some time, states that a population of cells morphologically identical to T4/T5 might exist which act as inhibitory neurons. This, however, seems unlikely because when blocking T4/T5 both null and preferred direction responses in the LPTCs are eliminated (Schnell et al., 2012). A study from the Borst Lab, Mauss et al. (2014), has suggested an alternative explanation where inhibition is transferred from excitatory T4/T5 signals from one layer of the lobula plate to the neighboring one via local inhibitory neurons, LPIs. They postulated this based on optogenetic experiments with T4 and T5: when T4 and T5 are activated, a fast excitatory postsynaptic potential is recorded from LPTCs followed by a delayed inhibitory postsynaptic potential.

3.3 THE BEHAVIORAL RELEVANCE OF THE T4 T5 MOTION CIRCUIT

As discussed previously visually guided behavior can be divided into three different categories: optomotor response, landing and avoidance response, and fixation response. A pertinent question, which needs to be addressed, is what role the T4/T5 circuitry and thus the Reichardt detector plays in each of these behaviors.

3.3.1 Optomotor Response

LPTCs have been thought to be responsible for the optomotor response since they were discovered in the 1970s. This assumption has been proved through decades of experimentation in both *Calliphora vicina* and *Drosophila melanogaster* (For review see: (Borst, 2014a)). We have shown that T4 and T5 are responsible for carrying the direction selective signal to the LPTCs and that either ON or OFF motion responses are eliminated in LPTCs when genetically blocking T4 or T5, respectively. We have also shown that blocking either T4 or T5 selectively eliminates optomotor responses to brightness increments or decrements.

3.3.2 Landing and Avoidance Response

Looming sensitive neurons in the lobula and lobula plate have been described in *D. melanogaster* (De Vries and Clandinin, 2012). Genetically blocking these cells reduces the avoidance response, thus implicating their necessity. Additionally, optogenetic activation of these cells in blind flies elicited the same response as in tethered wild type flies, namely take off and the beginnings of flight. These looming sensitive neurons have an interesting morphology with dendritic branches in both the lobula and the lobula plate (Wu et al., 2016), however the underlying mechanism of their responses still remains unclear. It is not unthinkable that T4 and T5 provide feed-forward input onto the looming sensitive neurons, especially within the lobula plate. Nevertheless this is pure speculation and the exact role of the T4/T5 circuitry in landing and avoidance responses remains unclear and unstudied.

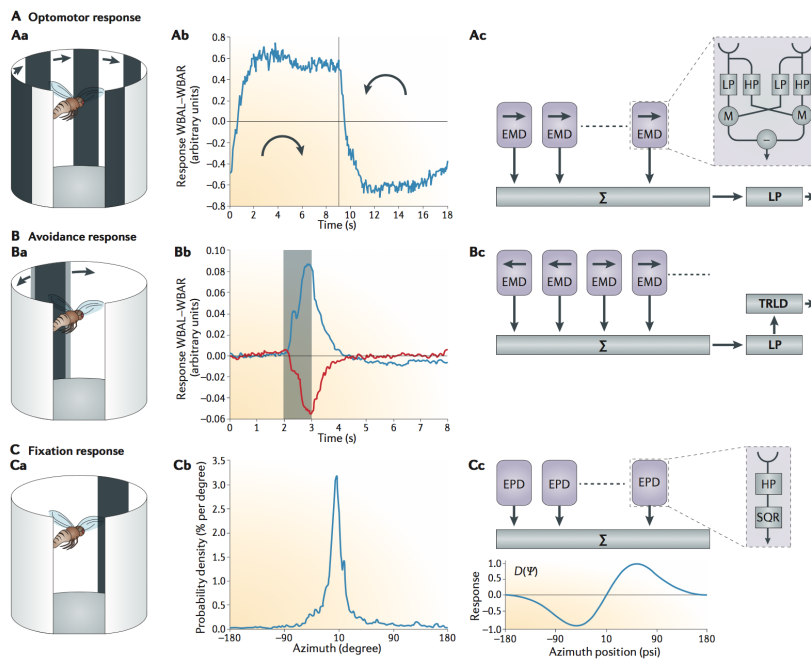


Figure 6. Visually Driven Behaviors (Aa) When a fly is suspended in the middle of a striped drum rotating around it, its turning tendency follows the direction of pattern movement. (Ab) During clockwise motion of the drum (first half), the fly tries to turn clockwise too. During anticlockwise drum rotation, the fly tries to turn in the opposite direction (the blue trace indicates the turning tendency of the fly). (Ac) Such a behaviour can be modelled by pooling the output signals of an array of elementary motion detectors (EMDs) and sending the pooled signal through a low-pass filter (LP). An EMD consists of two mirror-symmetrical subunits, with each containing an LP, a high-pass filter (HP) and a multiplier (M). In each subunit, the low- and high-pass filtered signals from adjacent photoreceptors are multiplied, and the output signals of the multipliers are then subtracted. (Ba) When confronted with an object positioned laterally in the fly's visual field that all of a sudden starts expanding, flies consistently turn away from it. (Bb) When the expanding object is to the left of the fly, they turn to the right (red trace), and when it is on the right, flies turn to the left (blue trace). (Bc) This response can be modelled like the optomotor response, except that in this case, EMDs need to be tuned to opposite directions of motion, with the split point at the pole of expansion. When the output signal of the large-field unit passes a certain threshold (TRLD), the response is executed. (Ca,b) When the fly is given control over the position of a single bar, it tends to keep the stripe in front of it most of the time. (Cc) The fixation response can be modelled by an array of elementary position detectors (EPDs) that are spatially pooled with a specific weight function $D(\psi)$. An EPD is realized as a temporal HP, followed by a squaring unit. For all responses, the turning tendency of the flies was calculated by optically determining the difference of their left and right wing beat amplitudes. Positive values thus represent a clockwise turning tendency of the fly. Figure and caption taken with permission from [Borst \(2014a\)](#).

3.3.3 Fixation Response

Recently, there has been significant progress in the advancement of our understanding of the fixation response and in particular the roles of T₄ and T₅. We have shown the T₄ and T₅ cells provide the output of local motion detectors onto LPTCs. A recent study showed that flies, in which synaptic transmission of both T₄ and T₅ is blocked, show absolutely no optomotor response, regardless of how strong the grating contrast is (Bahl et al., 2013). Interestingly, these flies are still able to fixate a black bar under closed-loop conditions, although at a reduced level. A closer look at the results and further experimentation revealed that flies in which T₄ and T₅ were blocked responded to a single bar appearing at various locations under open-loop conditions at the same magnitude as control flies (Bahl et al., 2013). These results imply the existence of a separate position circuit within the optic lobe, which runs parallel to the motion detection circuit and is responsible for landmark detection. This position circuit explains why T₄/T₅ block flies still exhibit a fixation response under closed loop conditions. An open question still remains: Why do these flies perform worse in fixation than control flies if the position system is still intact? Bahl et al. (2013) probed this by challenging the fly with three different stimuli: a bar moving through a slit from front to back, a bar moving through a slit from back to front, and homogeneous luminance modulation within the slit with the same time course as the bar motion. T₄/T₅ block flies respond to all three stimuli by turning toward the slit. This indicates that the flies “interpret” each stimulus identically, demonstrating that they are not only blind to large field motion but also to local motion. Control flies, on the other hand, respond differently to each of the stimuli. If the response to the non-moving luminance change is subtracted from each of the moving bar stimuli, a clear asymmetry can be seen, namely that the motion induced response for front to back motion is much stronger than the back to front motion component. Such an asymmetry of the motion response would support stripe fixation in front of the fly under closed loop conditions. These results taken together suggest that the position and motion pathways can indeed be separated at the neuronal level. The optomotor response is controlled exclusively by the motion circuitry, including T₄/T₅ and the fixation response is controlled by a combination of the position and motion circuits.

3.4 COMPARING MOTION DETECTION IN MICE AND *drosophila*

One of the most fascinating things about investigating the neural implementation of motion detection in flies is the ability to compare the results to across the animal kingdom. This allows us to draw conclusions about the possible implementations of mathematical computations in various biological systems.

The most striking commonality between the retina and fly optic lobe is the early splitting of the pathways into ON and OFF channels. In the vertebrate retina this splitting happens right at the photoreceptor-bipolar synapse, in contrast it is done one synapse later in the fly optic lobe. The lamina seems to be an intermediate layer with no correspondence in vertebrates. Interestingly, due to the ON characteristic of fly photoreceptor and the sign reversal at their output synapse, luminance is represented in the same way in both systems: that is, by a hyperpolarization of membrane potential of photoreceptors in the vertebrate retina as well as lamina monopolar cells in the fly optic lobe. Along with the ON-OFF splitting, the computation of motion direction is done separately in each pathway in both systems. Once the direction of motion is detected, the information from both ON and OFF pathways is fused at the very next synapse: in the fly optic lobe, T₄ and T₅ cells jointly synapse onto lobula plate tangential cells, creating a motion signal which is independent from either the moving brightness increments or decrements that formed it. The same is observed in the vertebrate retina, where starburst amacrine cells from both ON and OFF layers contact ON-OFF retinal ganglion cells. The next parallel between the vertebrate retina and insect optic lobe is the representation of motion information along four orthogonal directions. This is all the more amazing given that the primary receptor lattice has a hexagonal geometry in the insect eye, with a 60-degree angle between neighboring axes. While this arrangement is retained through all neuropil layers, T₄ and T₅ cells nevertheless come in four flavors with a 90-degree angle between their preferred axes, owing to a combination of the oblique h- and y-rows of the hexagonal lattice to establish horizontal motion directionality (Buchner, 1976). Finally, the optimal temporal frequency of both systems seems to be similar (around 1-2 Hz).

There are also some remarkable differences between the two systems. The first difference relates to the directional sampling. In the vertebrate retina, the range of directions along which primary motion information is extracted covers the continuum of all possible directions as represented by the radial dendrites of

Parallel Pathways

Cardinal Directions

*Directional
Sampling*

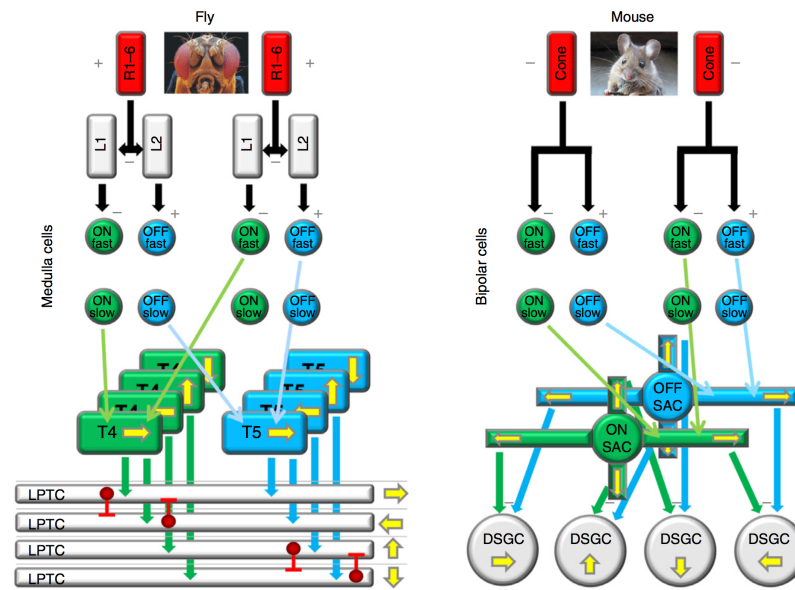


Figure 7. Fly and Mouse Motion Detection Neural Components. In the fly, photoreceptors R1-6 synapse onto lamina monopolar cells L1 and L2, with a sign-inverting synapse. L1 and L2 provide the entry to ON and OFF pathways. In the mouse, cone photoreceptors themselves split the signal onto ON and OFF bipolar cells. The first cells displaying direction selectivity are the T4 and T5 cells in the fly optic lobe and the ON and OFF starburst amacrine cells (SAC) in the mouse retina. Motion information from the two pathways becomes fused at the next synapse: on the dendrites of the lobula plate tangential cells (LPTC) in the fly and ON-OFF direction-selective ganglion cells (DSGC) in the mouse retina. Figure and caption taken with permission from [Borst and Helmstaedter \(2015\)](#).

starburst amacrine cells in both ON and OFF layers. This information is compressed onto four axes only in the next stage, from starburst amacrine onto ganglion cells, together with the fusion of ON and OFF pathways ([Yonehara et al., 2013](#)). In the insect optic lobe, motion information is extracted at the very first stage along these four cardinal directions. Accordingly, the directional tuning curves of fly motion vision appear narrower than those of mouse. This difference may be a result of direction selectivity being synaptically imposed on the postsynaptic neuron by an excitatory drive from presynaptic neurons aligned with the four cardinal directions (fly) versus the suppression of a range of non-preferred directions sampled at much smaller radial intervals (mouse). But why is the direction-selectivity circuit in the mouse implemented at the level of an inhibitory neuron and not directly at the input synapse to the direction-selective ganglion

cells? In contrast to fly, the mammalian retina contains many different types of direction selective output neurons with different preferred directions, such as ON-OFF JAM-B (Oyster and Barlow, 1967; Elstrott et al., 2008), ON JAM-B (Oyster and Barlow, 1967; Sun et al., 2006) and OFF JAM-B ganglion cells (Kim et al., 2008). By equipping the mouse retina with a ubiquitous and versatile direction-selective inhibitory neuron, postsynaptic ganglion cells of various response types can be made selective for an almost arbitrary range of motion directions by simply connecting to the appropriate range of starburst amacrine cell dendrites, without the need to re-implement the direction-selectivity circuit in each of these ganglion cell types. Examples of more ganglion cell types with prominent starburst amacrine contact are reported in refs. (Helmstaedter et al., 2013; Beier et al., 2013).

The next difference relates to the place where motion information provided by ON and OFF pathways is fused: in the vertebrate retina, these are again local cells, namely the direction-selective ganglion cells covering a few degrees of the visual field each. In the insect optic lobe, this fusion happens on the large dendrites of wide-field, motion-sensing tangential cells with a receptive field diameter of up to 180 degrees. No local, motion-sensing cells have been reported so far in the fly that are sensitive to both ON and OFF motion. Furthermore, lobula plate tangential cells exhibit motion opponency while this response feature is not found in retinal ganglion cells. This hints at motion opponency being a particular feature of wide-field motion-sensitive neurons, but not local ones; compare, for example, cortical neurons in area V1 and MT (Snowden et al., 1991). Finally, in the fly, the ON-OFF tangential cells seem to be the only direction-selective neurons found downstream, leading to the impression that, as soon as primary motion information is extracted, the separation of ON and OFF is no longer needed. In contrast, the mouse retina, in addition to ON-OFF ganglion cells, also houses direction-selective ganglion cells that are fed preferentially by either the ON or the OFF pathway (Kim et al., 2008; Amthor et al., 1989a,b; Wyatt and Daw, 1975). Some of these differences may relate to use of ON-OFF direction-selective signals for the perception of global motion in flies but, more likely, for object detection in mice. Conversely, large-field direction-selective neurons in mouse may serve the equivalent purpose of global motion detection, but seem to be separately selective for ON or OFF motion.

3.4.1 The First Signs of Direction Selectivity

In both mouse and fly visual system, ON and OFF signals are separated. What might the advantage of such splitting be? Motion results in a temporal correlation of similar events at two spatial locations: if a bright object passes two neighboring points in space, luminance first increases sequentially when the object's leading edge passes, and then decreases again when the object's trailing edge passes. A motion-sensitive post-synaptic neuron receiving input from these two locations should signal motion in each case, for the leading and the trailing edge. However, in the first case, it should become excited if both inputs increase their membrane potential, and in the second, it should be excited if both inputs decrease their membrane potential. There is no biophysical mechanism known so far that allows such an implementation of the sign rule of multiplication. If, however, the inputs are split into an ON and OFF channel, brightness increments and decrements are handled separately with a positive sign within each pathway, and then motion-sensitive neurons only face the task of correlating two positive input signals by whatever cellular mechanism. This seems to greatly alleviate the problem of implementing such a correlation biophysically.

Beside the nonlinear signal combination, the other key algorithmic step in motion detection is asymmetric temporal filtering, which creates a signal delay between the two inputs. The first question is where the delay is generated. Currently, three different scenarios seem plausible. First, the input signals could exhibit different release dynamics. Second, different dendritic receptors on the motion-computing neuron could give rise to intracellular signals with different dynamics. Third, input signal and postsynaptic receptor could result in signals of identical dynamics, with the delay generated intracellularly in the postsynaptic neuron by the specific geometry of the dendrite or inhomogeneous distribution of transmembrane conductances (Hauselt et al., 2007). The lines of evidence described above suggest that the signal delay is implemented via spatially separated innervation by two different cell types with different dynamics: cone bipolar cells type 2 versus 3a in the case of OFF direction selectivity in the mouse (Baden et al., 2013; Kim et al., 2014) and Tm3 versus Mi1 in the case of T4 ON direction selectivity in the fly (Takemura et al., 2013; Behnia et al., 2014). In the mouse, support for the first model is provided by evidence based on both calcium recording from axon terminals of retinal bipolar cells (Baden et al., 2013) and EM-based connectivity analysis (Kim et al., 2014). These hypotheses are far from set in stone. The

relationship between bipolar cell morphology and different response kinetics in bipolar cell terminals is based solely on the depth within the inner plexiform layer where the various kinetics types were measured (Kim et al., 2014). Therefore, a direct classification of bipolar cells dynamics is difficult, especially on the ON side, where, for example, three subtypes of type 5 bipolar cells largely co-stratify (Helmstaedter et al., 2013). Furthermore, recent evidence indicates that strong visual stimulation can alter the direction selectivity of ganglion cells (Rivlin-Etzion et al., 2012; Vlasits et al., 2014). This phenomenon may be attributed to changes in the synaptic dynamics presynaptic to the starburst amacrine cells due to either an experience-dependent mechanism or an exhaustive synaptic depletion. In addition, the evidence for spatially segregated innervation of starburst dendrite by bipolar cells with different dynamics is so far based on neurite contacts (Kim et al., 2014), not yet on identified synapses. The ideal experiment would aim to directly observe the temporal kinetics of identified bipolar cell type terminals when presenting a directional stimulus, followed by structural proof of the implied circuit. Another interesting question revolves around the ON channel. It seems like the distribution of response kinetics in bipolar cells are less distinct (Baden et al., 2013). This leaves several questions: is there a differential bipolar-to- starburst circuit implemented as well? If so, which are the contributing bipolar cell types? These questions need to be addressed by further studies. Here, it should also be kept in mind that both the specific geometry of starburst amacrine cell dendrites and the transmembrane conductance gradient could support direction selectivity themselves, without any delay in the input signals (Hausselet et al., 2007). This provides support for the third model of temporal filter implementation. It remains to be determined whether multiple mechanisms based on synaptic delays, postsynaptic effects and asymmetric dendritic geometries are implemented in parallel, and to what relative degrees they contribute to the functional direction-selective signals in the retina.

In the fly ON channel of motion computation, a half-detector of the Hassenstein-Reichardt type was proposed to be implemented via Mi1 and Tm3 cells synapsing onto T4 cells (Take-mura, 2014; Behnia et al., 2014). However, the spatial offset between the anatomical receptive field centers of Mi1 and Tm3 amounts to only about 20% of the interommatidial distance (Take-mura et al., 2013), thus significantly reducing the signal difference between the two potential inputs to the T4 cell. Additionally, the average offset per T4 neuron was found to have a high degree of variability and is only properly aligned for three of the

four cardinal directions. Oddities were also seen for the difference in temporal dynamics between Mi1 and Tm3 cells (Behnia et al., 2014). The small temporal delay, about 18 ms, exhibits a wide range of fluctuations and reproduces a temporal tuning curve consistent with experimental data from T4 cells (Maisak et al., 2013) only after subtraction of mirror-symmetrical subunits, a process generally thought to be implemented only on the postsynaptic tangential cells (Borst and Egelhaaf, 1990; Mauss et al., 2015). The situation is even less clear in T5 cells, which receive input from four types of interneurons, without any immediate correspondence to a simple motion-detection scheme (Shinomiya et al., 2014). In support of an alternative implementation of the delay via different receptor kinetics, mRNA sequencing reveals expression of slow, muscarinic and fast, nicotinic acetylcholine receptors in both T4 and T5 cells (Shinomiya et al., 2014). Furthermore, detailed anatomical analysis reveals distinct morphological features that could potentially support production of delays via tapered dendrites in T4 cells (Takemura et al., 2013). More experiments are needed to clarify the role of each of the input neurons for motion detection in T4 as well as T5 cells. The field continues to move rapidly forward and the emergence of new data such as Takemura et al., 2017 has thrown previous findings into new light. It is clear that further studies are needed to fully decipher motion computation in *Drosophila*.

BIBLIOGRAPHY

- Alderson, T.
1965. Chemically induced delayed germinal mutation in *Drosophila*. *Nature*, 207(993):164–167. (Cited on page 8.)
- Amthor, F. R., E. S. Takahashi, and C. W. Oyster
1989a. Morphologies of rabbit retinal ganglion cells with complex receptive fields. *Journal of comparative neurology*, 280(1):97–121. (Cited on page 59.)
- Amthor, F. R., E. S. Takahashi, and C. W. Oyster
1989b. Morphologies of rabbit retinal ganglion cells with concentric receptive fields. *Journal of Comparative Neurology*, 280(1):72–96. (Cited on page 59.)
- Autrum, H. J.
1950. Die Belichtungspotentiale und das Sehen der Insekten (Untersuchungen an *Calliphora* und *Dixippus*). *Zeitschrift für vergleichende Physiologie*, 32:176–227. (Cited on page 16.)
- Baden, T., P. Berens, M. Bethge, and T. Euler
2013. Spikes in mammalian bipolar cells support temporal layering of the inner retina. *Current Biology*, 23(1):48–52. (Cited on pages 60 and 61.)
- Bahl, A., G. Ammer, T. Schilling, and A. Borst
2013. Object tracking in motion-blind flies. *Nature Neuroscience*, 16(6):730–8. (Cited on pages 3 and 56.)
- Baird, G. S., D. a. Zacharias, and R. Y. Tsien
1999. Circular permutation and receptor insertion within green fluorescent proteins. *Proceedings of the National Academy of Sciences of the United States of America*, 96(20):11241–11246. (Cited on page 10.)
- Bausenwein, B. and K.-F. Fischbach
1992. Activity labeling patterns in the medulla of *Drosophila melanogaster* caused by motion stimuli. *Cell & Tissue Research*, 270(1):25–35. (Cited on pages 18, 19, and 21.)
- Behnia, R., D. A. Clark, A. G. Carter, T. R. Clandinin, and C. Desplan
2014. Processing properties of ON and OFF pathways for

Drosophila motion detection. *Nature*, 512:427–430. (Cited on pages 50, 60, and 61.)

Behnia, R. and C. Desplan

2015. Visual circuits in flies: beginning to see the whole picture. *Current Opinion in Neurobiology*, 34:125–132. (Cited on page 50.)

Beier, K. T., B. G. Borghuis, R. N. El-Danaf, A. D. Huberman, J. B. Demb, and C. L. Cepko

2013. Transsynaptic tracing with vesicular stomatitis virus reveals novel retinal circuitry. *Journal of Neuroscience*, 33(1):35–51. (Cited on page 59.)

Benzer, S.

1967. Behavioral mutants of *Drosophila* isolated by counter-current distribution. *Proceedings of the National Academy of Sciences of the United States of America*, 58(3):1112–1119. (Cited on page 8.)

Berndt, A., O. Yizhar, L. A. Gunaydin, P. Hegemann, and K. Deisseroth

2009. Bi-stable neural state switches. *Nature Neuroscience*, 12(2):229–234. (Cited on page 13.)

Berni, J., A. M. Muldal, and S. R. Pulver

2010. Using Neurogenetics and the Warmth-Gated Ion Channel TRPA₁ to Study the Neural Basis of Behavior in *Drosophila*. *Journal of Undergraduate Neuroscience Education*, 9(1):5–14. (Cited on page 13.)

Bischof, J., R. K. Maeda, M. Hediger, F. Karch, and K. Basler

2007. An optimized transgenesis system for *Drosophila* using germ-line-specific phiC31 integrases. *Proceedings of the National Academy of Sciences of the United States of America*, 104(9):3312–7. (Cited on page 9.)

Bloomington

2016. <http://flystocks.bio.indiana.edu/>.

Borst, A.

1986. Time Course of the Housellies' Landing Response. *Biological Cybernetics*, 383:379–383. (Cited on page 3.)

Borst, A.

2009a. *Drosophila's* view on insect vision. *Current Biology*, 19(1):R36–R47. (Cited on page 17.)

- Borst, A.
2009b. *Drosophila's* view on insect vision. *Current Biology*, 19(1):36–47. (Cited on page 12.)
- Borst, A.
2010. Neurophysiology: recording from neurons in action. *Current Biology*, 20(16):679–680. (Cited on page 5.)
- Borst, A.
2013. Neurobiology of Movement-Sensitive Behavior in Flies. In *New Visual Neurosciences*, J. S. Werner and C. L. M, eds. (Cited on page 6.)
- Borst, A.
2014a. Fly visual course control: behaviour, algorithms and circuits. *Nature Reviews Neuroscience*, 15(9):590–599. (Cited on pages 20, 54, and 55.)
- Borst, A.
2014b. Neural circuits for elementary motion detection. *Journal of neurogenetics*, 28(3-4):361–373. (Cited on page 5.)
- Borst, A. and M. Egelhaaf
1990. Direction selectivity of blowfly motion-sensitive neurons is computed in a two-stage process. *Proceedings of the National Academy of Sciences of the United States of America*, 87(23):9363–7. (Cited on page 61.)
- Borst, A. and J. Haag
2002. Neural networks in the cockpit of the fly. *Journal of Comparative Physiology*, 188(6):419–437. (Cited on page 18.)
- Borst, A., J. Haag, and D. F. Reiff
2010. Fly motion vision. *Annual Review of Neuroscience*, 33:49–70. (Cited on page 19.)
- Borst, A. and M. Helmstaedter
2015. Common circuit design in fly and mammalian motion vision. *Nature Neuroscience*, 18(8):1067–1076. (Cited on pages 4 and 58.)
- Boyden, E. S., F. Zhang, E. Bamberg, G. Nagel, and K. Deisseroth
2005. Millisecond-timescale, genetically targeted optical control of neural activity. *Nature Neuroscience*, 8(9):1263–1268. (Cited on page 13.)
- Braitenberg, V.
1967. Patterns of Projection in the Visual System of the Fly. *Experimental Brain Research*, 298:271–298. (Cited on page 16.)

- Brand, A. H. and N. Perrimon
1993. Targeted gene expression as a means of altering cell fates and generating dominant phenotypes. *Development (Cambridge, England)*, 118(2):401–415. (Cited on page 8.)
- Broca, P.
1888. *Mémoires sur le cerveau de l'homme et des primates*. Paris: C. Reinwald. (Cited on page 11.)
- Broussard, G. J., R. Liang, and L. Tian
2014. Monitoring activity in neural circuits with genetically encoded indicators. *Frontiers in Molecular Neuroscience*, 7:1–17. (Cited on pages 10 and 12.)
- Buchner, E.
1976. Elementary movement detectors in an insect visual system. *Biological Cybernetics*, 24(2):85–101. (Cited on pages 15 and 57.)
- Buchner, E., S. Buchner, and I. Bühlhoff
1984. Deoxyglucose mapping of nervous activity induced in *Drosophila* brain by visual movement - I. Wildtype. *Journal of Comparative Physiology A*, 155(4):471–483. (Cited on page 19.)
- Cajal, S. R. and D. Sánchez
1915. Contribución al conocimiento de los centros nerviosos de los insectos. *Trabajos del Laboratorio de Investigacionens biológicas*, 13:1–168. (Cited on page 15.)
- Chalfie, M., Y. Tu, W. W. Ward, G. Euskirchen, and D. Prasher
1994. Green fluorescent protein as a marker for gene expression. *Science*, 9(2):1258–62. (Cited on page 10.)
- Chen, T.-W., T. J. Wardill, Y. Sun, S. R. Pulver, S. L. Renninger, A. Baohan, E. R. Schreiter, R. a. Kerr, M. B. Orger, V. Jayaraman, L. L. Looger, K. Svoboda, and D. S. Kim
2013. Ultrasensitive fluorescent proteins for imaging neuronal activity. *Nature*, 499(7458):295–300. (Cited on page 10.)
- Chuhma, N., K. F. Tanaka, R. Hen, and S. Rayport
2011. Functional connectome of the striatal medium spiny neuron. *Journal of Neuroscience*, 31(4):1183–1192. (Cited on page 14.)
- De Vries, S. E. and T. R. Clandinin
2012. Loom-sensitive neurons link computation to action in the drosophila visual system. *Current Biology*, 22(5):353–362. (Cited on page 54.)

- Denk, W. and H. Horstmann
2004. Serial Block-Face Scanning Electron Microscopy to Reconstruct Three-Dimensional Tissue Nanostructure. *PLoS Biology*, 2(11):1900–1909. (Cited on page 7.)
- Denk, W., J. H. Strickler, and W. W. Webb
1990. Two-photon laser scanning fluorescence microscopy. *Science*, 248:73–76. (Cited on page 7.)
- Dickson, B. J.
2008. Wired for sex: the neurobiology of drosophila mating decisions. *Science*, 322(5903):904–909. (Cited on page 6.)
- Eichner, H. and A. Borst
2011. Hands-on parameter search for neural simulations by a MIDI-controller. *PloS one*, 6(10):e27013. (Cited on page 4.)
- Elstrott, J., A. Anishchenko, M. Greschner, A. Sher, A. M. Litke, E. Chichilnisky, and M. B. Feller
2008. Direction selectivity in the retina is established independent of visual experience and cholinergic retinal waves. *Neuron*, 58(4):499–506. (Cited on page 59.)
- Fenko, L., O. Yizhar, and K. Deisseroth
2011. The Development and Application of Optogenetics. *Annual Review of Neuroscience*, 34(1):389–412. (Cited on page 13.)
- Fischbach, K. F. and A. P. Dittrich
1989. The optic lobe of *Drosophila melanogaster*. I. A Golgi analysis of wild-type structure. *Cell & Tissue Research*. (Cited on pages 15, 17, 19, and 20.)
- Fish, M. P., A. C. Groth, M. P. Calos, and R. Nusse
2007. Creating transgenic *Drosophila* by microinjecting the site-specific phiC31 integrase mRNA and a transgene-containing donor plasmid. *Nature Protocols*, 2(10):2325–2331. (Cited on page 9.)
- Flight, M. H.
2013. Visual system: Mapping motion detection. *Nature Reviews Neuroscience*, 14. (Cited on page 24.)
- Franceschini, N., K. Kirschfeld, and B. Minke
1981. Fluorescence of photoreceptor cells observed in vivo. *Science*, 213(4513):1264–1267. (Cited on page 15.)
- Gilbert, C.
2013. Brain connectivity: Revealing the fly visual motion circuit. *Current Biology*, 23(18):R851–R853. (Cited on page 24.)

- Gollisch, T. and M. Meister
2010. Eye Smarter than Scientists Believed: Neural Computations in Circuits of the Retina. *Neuron*, 65(2):150–164. (Cited on page 2.)
- Gordon, M. D. and K. Scott
2009. Motor control in a *Drosophila* taste circuit. *Neuron*, 61(3):373–84. (Cited on page 14.)
- Grether, M. E., J. M. Abrams, J. Agapite, K. White, and H. Steller
1995. The head involution defective gene of *Drosophila melanogaster* functions in programmed cell death. *Genes and Development*, 9(14):1694–1708. (Cited on page 11.)
- Grienberger, C. and A. Konnerth
2012. Imaging Calcium in Neurons. *Neuron*, 73(5):862–885. (Cited on page 10.)
- Gunaydin, L. A., O. Yizhar, A. Berndt, V. S. Sohal, K. Deisseroth, and P. Hegemann
2010. Ultrafast optogenetic control. *Nature Neuroscience*, 13(3):387–392. (Cited on page 13.)
- Guo, Z. V., A. C. Hart, and S. Ramanathan
2009. Optical interrogation of neural circuits in *Caenorhabditis elegans*. *Nature Methods*, 6(12):891–6. (Cited on page 14.)
- Haag, J. and A. Borst
1998. Active Membrane Properties and Signal Encoding in Graded Potential Neurons. *Journal of Neuroscience*, 18(19):7972–7986. (Cited on page 18.)
- Haag, J. and A. Borst
2001. Recurrent network interactions underlying flow-field selectivity of visual interneurons. *Journal of Neuroscience*, 21(15):5685–92. (Cited on page 6.)
- Haag, J. and A. Borst
2004. Neural mechanism underlying complex receptive field properties of motion-sensitive interneurons. *Nature Neuroscience*, 7(6):628–34. (Cited on pages 5 and 18.)
- Haag, J., W. Denk, and A. Borst
2004. Fly motion vision is based on Reichardt detectors regardless of the signal-to-noise ratio. *Proceedings of the National Academy of Sciences of the USA*, 101(46):16333–8. (Cited on page 6.)

- Hadjikhani, N., a. K. Liu, a. M. Dale, P. Cavanagh, and R. B. Tootell
1998. Retinotopy and color sensitivity in human visual cortical area V8. *Nature Neuroscience*, 1(3):235–41. (Cited on page 2.)
- Haikala, V., M. Joesch, A. Borst, and A. S. Mauss
2013. Optogenetic control of fly optomotor responses. *Journal of Neuroscience*, 33(34):13927–34. (Cited on page 14.)
- Hamada, F. N., M. Rosenzweig, K. Kang, S. R. Pulver, A. Ghezzi, T. J. Jegla, and P. A. Garrity
2008. An internal thermal sensor controlling temperature preference in *Drosophila*. *Nature*, 454:217–220. (Cited on page 13.)
- Hardie, R.
1991. Whole-cell recordings of the light induced current in dissociated drosophila photoreceptors: evidence for feedback by calcium permeating the light-sensitive channels. *Proceedings of the Royal Society of London B: Biological Sciences*, 245(1314):203–210. (Cited on page 16.)
- Hardie, R. C.
1989. A histamine-activated chloride channel involved in neurotransmission at a photoreceptor synapse. *Nature*, 339(6227):704–706. (Cited on page 16.)
- Hardie, R. C. and P. Raghu
2001. Visual transduction in *Drosophila*. *Nature*, 413(6852):186–193. (Cited on pages 16 and 17.)
- Hassenstein, B.
1951. Ommatidienraster und Afferente Bewegungsintegration (Versuche an dem Rüsselkäfer *Chlorophanus viridis*). *Zeitschrift für vergleichende Physiologie*, 33:301–326. (Cited on page 3.)
- Hassenstein, B. and W. Reichardt
1956. Systemtheoretische Analyse der Zeit-, Reihenfolgen- und Vorzeichenauswertung bei der Bewegungsperzeption des Rüsselkäfers *Chlorophanus*. *Zeitschrift für Naturforschung*, 11:513–524. (Cited on page 3.)
- Hausen, K.
1976. Functional Characterization and Anatomical Identification of Motion Sensitive Neurons in the Lobula plate of the Blowfly *Calliphora erythrocephala*. *Zeitschrift für Naturforschung*, 31c:629–633. (Cited on pages 6, 18, and 19.)

- Hausselet, S. E., T. Euler, P. B. Detwiler, and W. Denk
2007. A dendrite-autonomous mechanism for direction selectivity in retinal starburst amacrine cells. *PLoS Biol*, 5(7):e185. (Cited on pages 60 and 61.)
- Heim, R., D. C. Prasher, and R. Tsien
1994. Wavelength mutations and posttranslational autooxidation of green fluorescent protein. *Proceedings of the National Academy of Sciences*, 91:12501 – 12504. (Cited on page 10.)
- Heisenberg, M., R. Wonneberger, and R. Wolf
1978. Optomotor-blindH31-a *Drosophila* mutant of the lobula plate giant neurons. *Journal of Comparative Physiology*, 124(4):287–296. (Cited on page 19.)
- Helmstaedter, M., K. L. Briggman, S. C. Turaga, V. Jain, H. S. Seung, and W. Denk
2013. Connectomic reconstruction of the inner plexiform layer in the mouse retina. *Nature*, 500(7461):168–74. (Cited on pages 7, 14, 59, and 61.)
- Hengstenberg, R., K. Hausen, and B. Hengstenberg
1982. The number and structure of giant vertical cells (VS) in the lobula plate of the blowfly *Calliphora erythrocephala*. *Journal of Comparative Physiology A*, 149:163–177. (Cited on page 18.)
- Hille, B.
2001. *Ion Channels of Excitable Membranes*, 3 edition. Sunderland, MA: Sinauer Associates Inc. (Cited on page 10.)
- Hodgkin, A. and A. Huxley
1952. A quantitative description of membrane current and its application to conduction and excitation in nerve. *Bulletin of Mathematical Biology*, 52(1-2):25–71. (Cited on page 6.)
- Hofbauer, A. and J. A. Campos-Ortega
1990. Proliferation pattern and early differentiation of the optic lobes in *drosophila melanogaster*. *Development Genes and Evolution*, 198(5):264–274. (Cited on pages 15, 16, and 17.)
- Hubel, D. H. and T. N. Wiesel
1968. Receptive Fields and Functional Architecture. *Journal of Physiology*, 195:215–243. (Cited on page 2.)
- Janelia, R. C.
2015. http://emanalysis.janelia.org/flyem_tables.php.
- Jenett, A., G. M. Rubin, T.-T. B. Ngo, D. Shepherd, C. Murphy, H. Dionne, B. D. Pfeiffer, A. Cavallaro, D. Hall, J. Jeter, N. Iyer,

- D. Fetter, J. H. Hausenfluck, H. Peng, E. T. Trautman, R. R. Svirskas, E. W. Myers, Z. R. Iwinski, Y. Aso, G. M. DePasquale, A. Enos, P. Hulamm, S. C. B. Lam, H.-H. Li, T. R. Lavery, F. Long, L. Qu, S. D. Murphy, K. Rokicki, T. Safford, K. Shaw, J. H. Simpson, A. Sowell, S. Tae, Y. Yu, and C. T. Zugates
2012. A GAL4-driver line resource for *Drosophila* neurobiology. *Cell Reports*, 2(4):991–1001. (Cited on page 9.)
- Joesch, M., J. Plett, A. Borst, and D. F. Reiff
2008. Response properties of motion-sensitive visual interneurons in the lobula plate of *Drosophila melanogaster*. *Current Biology*, 18(5):368–374. (Cited on pages 5, 6, 19, and 20.)
- Joesch, M., B. Schnell, S. V. Raghu, D. F. Reiff, and A. Borst
2010. ON and OFF pathways in *Drosophila* motion vision. *Nature*, 468(7321):300–304. (Cited on pages 12, 20, and 50.)
- Johns, D. C., R. Marx, R. E. Mains, B. O'Rourke, and E. Marbán
1999. Inducible genetic suppression of neuronal excitability. *Journal of Neuroscience*, 19(5):1691–1697. (Cited on page 11.)
- Kastner, S., P. De Weerd, and L. G. Ungerleider
2000. Texture segregation in the human visual cortex: A functional MRI study. *Journal of Neurophysiology*, 83:2453–2457. (Cited on page 2.)
- Kauer, I., A. Borst, and J. Haag
2015. Complementary motion tuning in frontal nerve motor neurons of the blowfly. *Journal of Comparative Physiology A*. (Cited on page 6.)
- Kim, I.-J., Y. Zhang, M. Yamagata, M. Meister, and J. R. Sanes
2008. Molecular identification of a retinal cell type that responds to upward motion. *Nature*, 452(7186):478–482. (Cited on page 59.)
- Kim, J. S., M. J. Greene, A. Zlateski, K. Lee, M. Richardson, S. C. Turaga, M. Purcaro, M. Balkam, A. Robinson, B. F. Behabadi, M. Campos, W. Denk, and H. S. Seung
2014. Space-time wiring specificity supports direction selectivity in the retina. *Nature*, 509(7500):331–6. (Cited on pages 7, 60, and 61.)
- Kitamoto, T.
2001. Conditional modification of behavior in *Drosophila* by targeted expression of a temperature-sensitive *shibire* allele in defined neurons. *Journal of Neurobiology*, 47(2):81–92. (Cited on page 12.)

- Kleinfeld, D., A. Bharioke, P. Blinder, D. D. Bock, K. L. Briggman, D. B. Chklovskii, W. Denk, M. Helmstaedter, J. P. Kaufhold, W.-C. A. Lee, H. S. Meyer, K. D. Micheva, M. Oberlaender, S. Prohaska, R. C. Reid, S. J. Smith, S. Takemura, P. S. Tsai, and B. Sakmann
2011. Large-scale automated histology in the pursuit of connectomes. *Journal of Neuroscience*, 31(45):16125–38. (Cited on page 14.)
- Knoll, M. and E. Ruska
1932. Das Elektronenmikroskop. *Zeitschrift für Physik*, 79(9-10):699. (Cited on page 7.)
- Lai, S.-L. and T. Lee
2006. Genetic mosaic with dual binary transcriptional systems in *Drosophila*. *Nature Neuroscience*, 9(5):703–709. (Cited on page 9.)
- Land, M. F.
1997. Visual acuity in insects. *Annual review of entomology*, 42(46):147–177. (Cited on page 15.)
- Land, M. F. and D.-E. Nilsson
2012. *Animal Eyes*, second edition. Oxford Animal Biology Series. (Cited on page 2.)
- Lee, T. and L. Luo
1999. Mosaic analysis with a repressible cell marker for studies of gene function in neuronal morphogenesis. *Neuron*, 22(3):451–61. (Cited on page 10.)
- Lichtman, J. W., H. Pfister, and N. Shavit
2014. The big data challenges of connectomics. *Nature Neuroscience*, 17(11):1448–1454. (Cited on page 14.)
- Lima, S. Q. and G. Miesenböck
2005. Remote control of behavior through genetically targeted photostimulation of neurons. *Cell*, 121:141–152. (Cited on page 13.)
- Lin, J. Y., P. M. Knutsen, A. Muller, D. Kleinfeld, and R. Y. Tsien
2013. ReaChR: a red-shifted variant of channelrhodopsin enables deep transcranial optogenetic excitation. *Nature Neuroscience*, 16(10):1499–508. (Cited on page 13.)
- Lindsley, D. L. and G. G. Zimm
1992. *The New Redbook. The Genome of Drosophila melanogaster*. Academic Press. (Cited on page 9.)

- Luan, H., N. C. Peabody, C. R. Vinson, and B. H. White
2006. Refined Spatial Manipulation of Neuronal Function by Combinatorial Restriction of Transgene Expression. *Neuron*, 52(3):425–436. (Cited on page 9.)
- Luo, L., E. M. Callaway, and K. Svoboda
2008. Genetic Dissection of Neural Circuits. *Neuron*, 57(5):634–660. (Cited on page 8.)
- Maisak, M. S., J. Haag, G. Ammer, E. Serbe, M. Meier, A. Leonhardt, T. Schilling, A. Bahl, G. M. Rubin, A. Nern, B. J. Dickson, D. F. Reiff, E. Hopp, and A. Borst
2013. A directional tuning map of *Drosophila* elementary motion detectors. *Nature*, 500(7461):212–6. (Cited on pages 23 and 61.)
- Mank, M., D. F. Reiff, N. Heim, M. W. Friedrich, A. Borst, and O. Griesbeck
2006. A FRET-based calcium biosensor with fast signal kinetics and high fluorescence change. *Biophysical Journal*, 90(5):1790–6. (Cited on page 10.)
- Mank, M., A. F. Santos, S. Drenberger, T. D. Mrsic-Flogel, S. B. Hofer, V. Stein, T. Hendel, D. F. Reiff, C. Levelt, A. Borst, T. Bonhoeffer, M. Hübener, and O. Griesbeck
2008. A genetically encoded calcium indicator for chronic in vivo two-photon imaging. *Nature Methods*, 5(9):805–811. (Cited on page 10.)
- Masland, R. H.
2001. Neuronal diversity in the retina. *Current Opinion in Neurobiology*, 11(4):431–436. (Cited on page 2.)
- Masland, R. H.
2013. Accurate maps of visual circuitry. *Nature*, 500:4–5. (Cited on page 24.)
- Mauss, A., K. Pankova, A. Arenz, A. Nern, G. Rubin, and A. Borst
2015. Neural Circuit to Integrate Opposing Motions in the Visual Field. *Cell*, 162(2):351–362. (Cited on page 61.)
- Mauss, A. S., M. Meier, E. Serbe, and A. Borst
2014. Optogenetic and pharmacologic dissection of feedforward inhibition in *Drosophila* motion vision. *Journal of Neuroscience*, 34(6):2254–2263. (Cited on page 53.)

- Meier, M., E. Serbe, M. S. Maisak, J. Haag, B. J. Dickson, and A. Borst
2014. Neural circuit components of the drosophila off motion vision pathway. *Current Biology*, 24(4):385–392. (Cited on pages 35, 50, and 53.)
- Miyawaki, A., J. Llopis, R. Heim, J. M. McCaffery, J. a. Adams, M. Ikura, and R. Y. Tsien
1997. Fluorescent indicators for Ca^{2+} based on green fluorescent proteins and calmodulin. *Nature*, 388:882–887. (Cited on page 10.)
- Moffat, K. G., J. H. Gould, H. K. Smith, and C. J. O’Kane
1992. Inducible cell ablation in *Drosophila* by cold-sensitive ricin A chain. *Development (Cambridge, England)*, 114(3):681–687. (Cited on page 11.)
- Morgan, T. H.
1910. Sex limited inheritance in *Drosophila*. *Science*, 32(812):120–122. (Cited on page 5.)
- Muller, H. J.
1928. The production of mutations by X-Rays. *Proceedings of the National Academy of Sciences*, 14:714–726. (Cited on page 8.)
- Nagel, G., M. Brauner, J. F. Liewald, N. Adeishvili, E. Bamberg, and A. Gottschalk
2005. Light Activation of Channelrhodopsin-2 in Excitable Cells of *Caenorhabditis elegans* Triggers Rapid Behavioral Responses. *Current Biology*, 15(24):2279–2284. (Cited on page 13.)
- Ohkura, M., M. Matsuzaki, H. Kasai, K. Imoto, and J. Nakai
2005. Genetically encoded bright Ca^{2+} probe applicable for dynamic Ca^{2+} imaging of dendritic spines. *Analytical Chemistry*, 77(18):5861–5869. (Cited on page 10.)
- Oyster, C. W. and H. B. Barlow
1967. Direction-selective units in rabbit retina: distribution of preferred directions. *Science*, 155(3764):841–842. (Cited on page 59.)
- Pulver, S. R., S. L. Pashkovski, N. J. Hornstein, P. a. Garrity, and L. C. Griffith
2009. Temporal dynamics of neuronal activation by Channelrhodopsin-2 and TRPA1 determine behavioral output in *Drosophila* larvae. *Journal of Neurophysiology*, 101(6):3075–3088. (Cited on page 13.)

- Quian Quiroga, R., L. Reddy, G. Kreiman, C. Koch, and I. Fried
2005. Invariant visual representation by single neurons in the human brain. *Nature*, 435(7045):1102–1107. (Cited on page 2.)
- Rajashekhar, K. P. and V. R. Shamprasad
2004. Golgi analysis of tangential neurons in the lobula plate of *Drosophila melanogaster*. *Journal of Biosciences*, 29(1):93–104. (Cited on page 20.)
- Reichardt, W. and H. Wenking
1969a. Optical detection and fixation of objects by fixed flying flies. *Die Naturwissenschaften*, 56(8):424. (Cited on page 3.)
- Reichardt, W. and H. Wenking
1969b. Optical detection and fixation of objects by fixed flying flies. *Die Naturwissenschaften*, 56(8):424. (Cited on page 3.)
- Reiff, D. F. and A. Borst
2008. Advances in studying neural circuit function with genetic probes for calcium. *Cell Science Reviews*, 5(2). (Cited on page 11.)
- Reiff, D. F., J. Plett, M. Mank, O. Griesbeck, and A. Borst
2010. Visualizing retinotopic half-wave rectified input to the motion detection circuitry of *Drosophila*. *Nature Neuroscience*, 13(8):973–8. (Cited on page 11.)
- Riehle, A. and N. Franceschini
1984. Motion detection in flies: parametric control over on-off pathways. *Experimental Brain Research*, 54(2):390–394. (Cited on page 4.)
- Rivera-Alba, M., S. N. Vitaladevuni, Y. Mishchenko, Y. Mishchenko, Z. Lu, S.-Y. Takemura, L. Scheffer, I. A. Meinertzhagen, D. B. Chklovskii, and G. G. de Polavieja
2011. Wiring economy and volume exclusion determine neuronal placement in the *Drosophila* brain. *Current Biology*, 21(23):2000–5. (Cited on page 17.)
- Rivlin-Etzion, M., W. Wei, and M. B. Feller
2012. Visual stimulation reverses the directional preference of direction-selective retinal ganglion cells. *Neuron*, 76(3):518–525. (Cited on page 61.)
- Rubin, G. M. and a. C. Spradling
1982. Genetic transformation of *Drosophila* with transposable element vectors. *Science*, 218(4570):348–353. (Cited on page 8.)

- Sakmann, B. and E. Neher
1984. Patch Clamp Techniques Ionic Channels in Excitable Membranes. *Annual Reviews Physiology*, 46:455–472. (Cited on page 6.)
- Schnaitmann, C., C. Garbers, T. Wachtler, and H. Tanimoto
2013. Color discrimination with broadband photoreceptors. *Current biology : CB*, 23(23):2375–82. (Cited on page 15.)
- Schnell, B., M. Joesch, F. Forstner, S. V. Raghu, H. Otsuna, K. Ito, A. Borst, and D. F. Reiff
2010. Processing of horizontal optic flow in three visual interneurons of the drosophila brain. *Journal of neurophysiology*, 103(3):1646–1657. (Cited on pages 5, 19, and 20.)
- Schnell, B., S. V. Raghu, A. Nern, and A. Borst
2012. Columnar cells necessary for motion responses of wide-field visual interneurons in *Drosophila*. *Journal of comparative physiology. A, Neuroethology, sensory, neural, and behavioral physiology*, 198(5):389–95. (Cited on page 53.)
- Schobert, B. and J. K. Lanyi
1982. Halorhodopsin is a light-driven chloride pump. *Journal of Biological Chemistry*, 257(17):10306–10313. (Cited on page 14.)
- Shaw, S. R.
1989. The retina-lamina pathway in insects, particularly diptera, viewed from an evolutionary perspective. In *Facets of vision*, Pp. 186–212. Springer. (Cited on page 16.)
- Shimomura, O., F. H. Johnson, and Y. Saiga
1962. Extraction, purification and properties of aequorin, a bioluminescent protein from the luminous hydromedusa, *Aequorea*. *Journal of Cellular and Comparative Physiology*, 59(165):223–239. (Cited on page 10.)
- Shinomiya, K., T. Karuppudurai, T.-Y. Lin, Z. Lu, C.-H. Lee, and I. A. Meinertzhagen
2014. Candidate neural substrates for off-edge motion detection in drosophila. *Current Biology*, 24(10):1062–1070. (Cited on pages 18, 21, 50, 51, and 61.)
- Simpson, J. H.
2009. *Chapter 3 Mapping and Manipulating Neural Circuits in the Fly Brain*, volume 65, 1 edition. Elsevier Inc. (Cited on page 6.)

- Snowden, R. J., S. Treue, R. G. Erickson, and R. A. Andersen
1991. The response of area mt and v1 neurons to transparent motion. *Journal of Neuroscience*, 11(9):2768–2785. (Cited on page 59.)
- Strausfeld, N. J. and J. K. Lee
1991. Neuronal basis for parallel visual processing in the fly. *Visual Neuroscience*, 7:13–33. (Cited on page 6.)
- Strother, J. A., A. Nern, and M. B. Reiser
2014. Direct observation of on and off pathways in the *Drosophila* visual system. *Current Biology*, 24(9):976–983. (Cited on pages 50 and 53.)
- Sun, W., Q. Deng, W. R. Levick, and S. He
2006. On direction-selective ganglion cells in the mouse retina. *The Journal of physiology*, 576(1):197–202. (Cited on page 59.)
- Suster, M. L., L. Seugnet, M. Bate, and M. B. Sokolowski
2004. Refining GAL4-driven transgene expression in *Drosophila* with a GAL80 enhancer-trap. *Genesis*, 39:240–245. (Cited on page 10.)
- Svoboda, K. and R. Yasuda
2006. Principles of two-photon excitation microscopy and its applications to neuroscience. *Neuron*, 50(6):823–839. (Cited on page 7.)
- Sweeney, S. T., K. Broadie, J. Keane, H. Niemann, and C. J. O’Kane
1995. Targeted expression of tetanus toxin light chain in *Drosophila* specifically eliminates synaptic transmission and causes behavioral defects. *Neuron*, 14(2):341–351. (Cited on page 11.)
- Takemura, S.-y.
2014. Connectome of the fly visual circuitry. *Microscopy*, 64:37–44. (Cited on pages 49 and 61.)
- Takemura, S.-y., A. Bharioke, Z. Lu, A. Nern, S. Vitaladevuni, P. K. Rivlin, W. T. Katz, D. J. Olbris, S. M. Plaza, P. Winston, T. Zhao, J. A. Horne, R. D. Fetter, S. Takemura, K. Blazek, L.-A. Chang, O. Ogundeyi, M. a. Saunders, V. Shapiro, C. Sigmund, G. M. Rubin, L. K. Scheffer, I. A. Meinertzhagen, and D. B. Chklovskii
2013. A visual motion detection circuit suggested by *Drosophila* connectomics. *Nature*, 500(7461):175–81. (Cited on pages 7, 21, 60, and 61.)

- Takemura, S.-y., T. Karuppudurai, C.-Y. Ting, Z. Lu, C.-H. Lee, and I. A. Meinertzhagen
2011. Cholinergic circuits integrate neighboring visual signals in a *Drosophila* motion detection pathway. *Current Biology*, 21(24):2077–2084. (Cited on pages 18 and 21.)
- Takemura, S.-y., A. Nern, D. B. Chklovskii, L. K. Scheffer, G. M. Rubin, and I. A. Meinertzhagen
2017. The comprehensive connectome of a neural substrate for motion detection in drosophila. *eLife*, 6:e24394. (Cited on pages 49, 52, and 61.)
- Vlasits, A. L., R. Bos, R. D. Morrie, C. Fortuny, J. G. Flannery, M. B. Feller, and M. Rivlin-Etzion
2014. Visual stimulation switches the polarity of excitatory input to starburst amacrine cells. *Neuron*, 83(5):1172–1184. (Cited on page 61.)
- Wardill, T. J., O. List, X. Li, S. Dongre, M. McCulloch, C.-Y. Ting, C. J. Kane, S. Tang, C.-H. Lee, R. C. Hardie, et al.
2012. Multiple spectral inputs improve motion discrimination in the drosophila visual system. *Science*, 336(6083):925–931. (Cited on page 16.)
- Wernet, M. F., M. W. Perry, and C. Desplan
2015. The evolutionary diversity of insect retinal mosaics: common design principles and emerging molecular logic. *Trends in Genetics*, 31(6):316 – 328. (Cited on page 17.)
- Wertz, A., A. Borst, and J. Haag
2008. Nonlinear integration of binocular optic flow by DNOVS2, a descending neuron of the fly. *Journal of Neuroscience*, 28(12):3131–40. (Cited on page 19.)
- White, J., E. Southgate, J. Thomson, and F. Brenner
1986. The structure of the nervous system of the nematode *Caenorhabditis elegans*. *Philosophical transactions of the Royal Society of London. Series B, Biological sciences*, 314:1–340. (Cited on page 7.)
- Wilson, R. I., G. C. Turner, and G. Laurent
2004. Transformation of Olfactory Representations in the *Drosophila* Antennal Lobe. *Science*, 303:366–371. (Cited on page 6.)
- Wu, M., A. Nern, W. R. Williamson, M. M. Morimoto, M. B. Reiser, G. M. Card, and G. M. Rubin
2016. Visual projection neurons in the drosophila lobula link feature detection to distinct behavioral programs. *eLife*, 5:e21022. (Cited on page 54.)

- Wyatt, H. J. and N. W. Daw
1975. Directionally sensitive ganglion cells in the rabbit retina: specificity for stimulus direction, size, and speed. *Journal of Neurophysiology*, 38(3):613–626. (Cited on page 59.)
- Yonehara, K., K. Farrow, A. Ghanem, D. Hillier, K. Balint, M. Teixeira, J. Jüttner, M. Noda, R. L. Neve, K.-K. Conzelmann, and B. Roska
2013. The first stage of cardinal direction selectivity is localized to the dendrites of retinal ganglion cells. *Neuron*, 79(6):1078–85. (Cited on page 58.)
- Yonehara, K. and B. Roska
2013. Motion detection: neuronal circuit meets theory. *Cell*, 154(6):1188–9. (Cited on page 24.)
- Zhang, F., L.-P. Wang, M. Brauner, J. F. Liewald, K. Kay, N. Watzke, P. G. Wood, E. Bamberg, G. Nagel, A. Gottschalk, and K. Deisseroth
2007. Multimodal fast optical interrogation of neural circuitry. *Nature*, 446(7136):633–639. (Cited on page 14.)
- Zipfel, W. R., R. M. Williams, and W. W. Webb
2003. Nonlinear magic: multiphoton microscopy in the biosciences. *Nature biotechnology*, 21(11):1369–1377. (Cited on page 7.)

LIST OF FIGURES

Figure 1	Hassenstein-Reichardt Motion Detector	4
Figure 2	<i>Drosophila</i> genetics	12
Figure 3	<i>Drosophila</i> Retina	17
Figure 4	The fly visual system	20
Figure 5	Motion Circuitry	52
Figure 6	Visually Driven Behaviors	55
Figure 7	Fly and Mouse Motion Detection Neural Components	58

ACKNOWLEDGEMENTS

First of all I would like to thank Axel Borst for being a very helpful, understanding, and inspiring supervisor throughout my time in his lab. He provided me with the fruitful combination of scientific guidance and experimental freedom that ensured successful academic results but also a very enjoyable working atmosphere. I could develop my own strategies, pursue ideas off the beaten track but also count on support in times of doubt. The cooperative and amicable environment in our lab made every day a positive and formative experience.

I would also like to thank Liesl. She continues to be an unwavering source of support and motivation in my life. Without her this thesis would have never been completed. Beyond this she inspires me to be both a better person and father by setting and inspiring example and continually raising the bar.

Thank you to the entire Borst lab for a wonderful experience.

Matthew Maisak

Summary

Accomplished neuroscientist with expertise in neural imaging techniques, modeling, and data analysis. Five years experience in synthesizing multi-source data and quickly identifying strategic implications and insights for all stakeholders. Strong track record of leading international projects in complex, fast-paced matrix environments. Extensive experience communicating difficult concepts and strategies to audiences of all levels.

Consulting Experience

Roche Diagnostics, Management Start-Up

Mannheim, Germany

IN-HOUSE CONSULTANT

Jan 2015 - Jun 2016

- Global Labeling Strategy: Led an international team in the conceptualization of a global labeling strategy for the Roche core business areas. Worked with stakeholders to identify areas of improvement and strategy implementation. Harmonized processes globally leading to increased data management capabilities and 500k year over year savings.
- Partner Management: Led the development of a business excellence process for supporting external manufacturing efforts for the professional diagnostics division. Developed and implemented a partner management strategy and organization leading to a 10% decrease in the management costs of our partnerships.

Professional Experience

Max Plank Institute of Neurobiology, Dept. Circuits-Computation-Models

Munich, Germany

DOCTORAL RESEARCHER

2010-2015

- Developed in vivo 2-photon imaging under visual stimulation, including customized microscopic hardware, data acquisition software and graphical user interfaces for online and offline image processing, signal extraction, and advanced data analysis.
- Conceptualized and conducted experiments to investigate the neuronal implementation of a mathematical model in the motion sensitive visual system.
- Successfully coordinated and led a team of five scientists in supporting experiments for my work resulting in a publication in Nature

St. Louis University, Dept. of Physics

St. Louis, MO, USA

TEACHING ASSISTANT

2009 - 2010

- Led two experimental labs twice a week
- Conception and presentation of accompanying lectures
- Identified and tutored struggling students

St. Louis University, Dept. of Biology

St. Louis, MO, USA

PRECEPTOR

2009 - 2010

- Prepared and taught semester-long cellular biology discussion for three sections of 30 undergraduate
- Tutored Students in Preparation for Exams

Education

Yale School of Medicine

New Haven, CT, USA

MD CANDIDATE

2017- Present

- MCAT: 519 (97th percentile)

Ludwig Maximilians Universität

Munich, Germany

PHD IN NEUROSCIENCE

2010 - 2018

- Functional imaging of the neural components of Drosophila motion detection
- Young Scientist of the Year Award

St. Louis University

St. Louis, MO, USA

BACHELOR'S BIOLOGY

2006-2010

- Ignation Scholar (4 years)
- GPA: 3.89/4.0

Leadership & Extracurricular

Yale University

New Haven, CT, USA

MENTOR

2017-Present

- Mentored two undergraduate students in the medical school application process
- Revised medical school applications for mentees

Haven Free Clinic

New Haven, CT, USA

VOLUNTEER

2017

- Volunteered in a primary care clinic for under-served populations
- Performed routine health screenings and eye exams

Digitalizing Roche Forum

Mannheim, Germany

ORGANIZER

2016

- Organized the action committee for presenting the machine learning algorithms used in molecule advancement at Roche
- Helped present Data Science work flow to senior management

Global Medical Affairs Summit: Roche Diagnostics

Basel, Switzerland

PARTICIPANT

2015

- Global summit of medical affairs and market access topics at Roche Diagnostics

International Conference on Invertebrate Vision

Bäckeskog, Sweden

SPEAKER: OPTICAL RECORDING OF DIRECTION SELECTIVE NEURONS IN THE VISUAL SYSTEM OF *Drosophila*

2013

- Presented my doctoral work to 300 leaders in the field of insect vision

Projects Abroad

Kathmandu, Nepal

VOLUNTEER

2007

- Observed orthopedic surgeries and went on daily rotations
- Taught English to In-Patients

Honors & Awards

2013 **Young Scientist of the Year Award**, Max Planck Institute of Neurobiology

2006-2010 **Dean's List**, St. Louis University

Skills

Scripting MATLAB (advanced), R (basic)

Office MS Office (advanced in Word, Excel, Power Point, Outlook), L^AT_EX (basic)

Trainings Leading People @ Roche, PMP Project Management 1&2, Leading in a Matrix, Intercultural Work, Conflict Management, Economics for Scientists

Languages English [Native], German [Fluent]

Other Wilderness First Responder, PADI Advanced Open Water SCUBA

Eidesstattliche Versicherung/Affidavit

Hiermit versichere ich an Eides statt, dass ich die vorliegende Dissertation "**Functional Imaging of the neural components of *Drosophila* motion detection**" selbständig angefertigt habe, mich außer der angegebenen keiner weiteren Hilfsmittel bedient und alle Erkenntnisse, die aus dem Schrifttum ganz oder annähernd übernommen sind, als solche kenntlich gemacht und nach ihrer Herkunft unter Bezeichnung der Fundstelle einzeln nachgewiesen habe.

I hereby confirm that the dissertation "**Functional Imaging of the neural components of *Drosophila* motion detection**" is the result of my own work and that I have only used sources or materials listed and specified in the dissertation.

.....
New York, den 06.10.2019
New York, 06.10.2019

.....
Unterschrift
Signature
Matthew Maisak

List of publications and author contributions

- **Maisak MS**¹, Haag J¹, Ammer G, Serbe E, Meier M, Leonhardt A, Schilling T, Bahl A, Rubin GM, Nern A, Dickson BJ, Reiff DF, Hopp E and Borst A. (2013) A Directional Tuning Map of *Drosophila* Elementary Motion Detectors. *Nature* 500: 212-216.
 - **M.S.M.** and J.H. jointly performed and, together with A.Bo., evaluated all calcium imaging experiments. G.A., E.S. and M.M. recorded from tangential cells. A.L., T.S. and A.Ba. performed the behavioral experiments. G.M.R., B.J.D. and A.N. generated the driver lines and characterized their expression pattern. D.F.R. performed preliminary imaging experiments. E.H. helped with programming and developed the PMT shielding for the two-photon microscope. A.Bo. designed the study and wrote the manuscript with the help of all authors.
- Meier M¹, Serbe E¹, **Maisak MS**, Haag J, Dickson BJ and Borst A. (2014) Neural Circuit Components of the *Drosophila* OFF Motion Vision Pathway. *Current Biology* 24: 385-392.
 - M.M, E.S. and A.B. designed the study. M.M. and E.S. performed electrophysiological recordings. M.M., E.S., **M.S.M.**, and J.H. performed calcium imaging experiments. B.J.D. provided unpublished Gal4-lines. M.M., E.S. and A.B. wrote the paper with help of the other authors.

.....
Matthew Maisak Prof. Dr. Alexander Borst
Supervisor

¹ equal contribution